NONDESTRUCTIVE TEST TECHNIQUE DEVELOPMENT BASED ON THE QUANTITATIVE PREDICTION OF BOND ADHESIVE STRENGTH

J. R. Zurbrick

For the Period

1969 July 21 to 1970 July 20

AVSD-0331-70-RR

ADVANCED RESEARCH PROJECTS AGENCY
PROGRAM
ON
NONDESTRUCTIVE TESTING

ARPA Order No. 1247
Program Code No. 9D10

Contract No. N00156-69-C-0913
Naval Air Engineering Center
Aero Materials Department
Warminster, Pennsylvania 18974

Prepared by

AVCO GOVERNMENT PRODUCTS GROUP
SYSTEMS DIVISION
201 LOWELL STREET
WILMINGTON, MASSACHUSETTS 01887

NONDESTRUCTIVE TEST TECHNIQUE DEVELOPMENT BASED ON THE QUANTITATIVE PREDICTION OF BONI ADHESIVE STRENGTH

J. R. Zurbrick

For the Period

1969 July 21 to 1970 July 20

AVSD-0331-70-RR

ADVANCED RESEARCH PROJECTS AGENCY
PROGRAM
ON
NONDESTRUCTIVE TESTING

ARPA Order No. 1247
Program Code No. 9D10

Contract No. N00156-69-C-0913
Naval Air Engineering Center
Aero Materials Department
Warminster, Pennsylvania 18974

Prepared by

AVCO GOVERNMENT PRODUCTS GROUP
SYSTEMS DIVISION
201 LOWELL STREET
WILMINGTON, MASSACHUSETTS 01887

FOREWORD

This report was prepared by Avco Corporation, Systems Division, Lowell, Massachusetts, under sponsorship of the Advanced Research Projects Agency (ARPA), as part of its program on Nondestructive Testing, managed by Dr. O. Conrad Trulson, Deputy Director for Materials Sciences. The work was administered by the Naval Air Engineering Center (NAEC), under Contract No. N00156-69-C-0913, with Mr. Forrest S. Williams serving as Technical Manager.

The annual technical report covers the period from 1969 July 21 to 1970 July 20, in the continuing three-year program at Avco/SD. Mr. E. A. Proudfoot was Project Manager and Mr. J. R. Zurbrick was Principal Investigator. Mr. Zurbrick gratefully acknowledges the generous assistance of Mr. T. M. Ludwig in the Surface Condition Study, Mr. A. M. Chetson in the NDT Technique Feasibility Studies, Mr. E. A. Proudfoot in the experimental data analysis, and Mr. D. R. Smith in the careful preparation of adhesive bond test specimens, all of the Materials Applications Department. Appreciation for management assistance and guidance is extended to Mr. Carlton H. Hastings, Chief of the Nondestructive Test and Evaluation Section.

ABSTRACT

The second annual period of research and development at Avco Systems Division into Nondestructive Tests for the Evaluation of Bonded Materials, sponsored by the Advanced Research Projects Agency, has continued the course of direction established by the first year's studies, namely development of NDT techniques for characterizing metallic substrate surfaces. Results of a Surface Condition Study on 6061-T6 Aluminum alloy butt tensile, core shear, and single lap shear specimens of various roughnesses, bonded with an Epon 828/DETA formulation have supported the creation of a practical equation for predicting bond adhesive strength (Zurbrick). Major controlling variables, i.e. substrate surface free energy, contact angle, and bondline thickness are all potentially measurable nondestructively. A strong correlation between white light specular reflection values and values of aluminum substrate surface free energies calculated from experimental data was obtained, encouraging extensive investigation of this NDT technique. Exo-electron emission, ultrasonic gas-phase transmission, and electric field reflectometry techniques were also evaluated in continuing feasibility studies.

CONTENTS

ILLUSTRATIONS

TABLES

I. INTRODUCTION

The practical application of adhesive bonded structures in military hardware designs over the past decade created a need for means to assure bond quality. Nondestructive instrumentation and techniques were correspondingly developed to detect bond/unbond in most situations and predict bond cohesive strength in certain restricted cases, mainly honeycomb sandwich structures. Confidence in adhesive bonding for primary load bearing structural components has grown to the point where current and anticipated designs present a critical need for nondestructive means to predict adhesive bond strength in production floor and field service applications.

Review during the first year of the subject contract of the problem as a whole, and subsequent subdivision into the contributing parts revealed that currently available tests and controls for materials and processing are seldom applied in practice to the extent necessary for proper control (Reference 1).

Discussions with experienced adhesives engineers revealed service failures attributable to lack of testing/controls in nearly every category listed in an idealized bonding sequence. Obviously the reason for exclusion of many tests and control steps was economic in nature. Highly reliable adhesive bonds cannot be assured when any critical control or test is eliminated.

The most critical area for NDT research and development was concluded to be that of substrate surface preparation prior to bonding. Today, adherend surfaces are not specifically controlled, but are accepted on the basis of controls applied to the processes by which they are produced. As a consequence, an extensive Surface Condition Study was conducted to learn the influences of surface roughness, contact angle, and mechanical means of preparation on adhesive bond strength.

By combining, in one person, the multi-disciplines and experiences of adhesive formulation, adhesive bonding, science of adhesion, polymer chemistry, physics of material-energy interactions, and nondestructive testing, a fresh concentration of creative interest could be applied to this basic study, in order that a unifying theory for bond strength prediction could be sought.

Although it is presumptive for the nondestructive testing discipline to assume the responsibilities of some other discipline, necessity requires that some sort of working foundation be created. This begins with carefully selected semantics and definitions which satisfy the particular viewpoint of NDT without violating the established definitions of other disciplines. Simply enough this is the interdisciplinary "escape" mechanism for technological advancement.

In order to develop nondestructive tests responsive to surface characteristics we first identified those characteristics which in turn are important to adhesive bonding. The science of adhesion offered a few solid clues, but not a firm and complete foundation. Adhesive bonding technology offered many empirical rules and an almost equal number of exceptions.

Much of the science of adhesion literature deals with the properties of free surfaces with extrapolations into resultant interfaces. More detailed searching led us rapidly into the physical chemistry and thermodynamics of free surfaces where lubrication, surfactants, friction phenomena, and catalysis enter the picture. The surprising result of these investigations has been the predominance of the "work of adhesion" term and the wide use of surface free energies as derived from contact angle measurements to explain various observed phenomena in each area of industrial specialty. More important, perhaps, is the observation that a common bibliography is referenced by the various investigators. All this implies a highly in-bred theoretical foundation to surface properties, from which there seems to be, at best, only a weak predictive capability for complex practical materials systems.

Thus a basic requisite to developing nondestructive test techniques for measuring the adhesive-bond-strength-influencing properties of the substrate surface, is the identification and quantization of those surface properties. Once that milestone has been gained, the NDT technique development is relatively straight forward, through a systematic study of applicable energy forms, and careful correlation and analysis of nondestructive and destructive test data.

II. SUMMARY

The current year's program (1969 July 21 - 1970 July 20) included three separate investigations:

- .Surface Condition Study
- .Bond Strength Predictive Capability Study
- .NDT Technique Feasibility Studies

The Surface Condition Study encompassed 13 different surface conditions on 6061-T6 aluminum substrates. Butt tensile, core shear, and lap shear specimens were bonded from the carefully-evaluated substrates using an Epon 828/DETA formulation. The surfaces were characterized by contact angle and profilometer measurements. Bond strengths and bondline thicknesses were obtained from the destructive test specimens.

The Bond Strength Predictive Capability Study was coordinated closely with the Surface Condition Study so that experimental data could be analyzed in terms of accepted adhesion theories. A new equation (Zurbrick) for predicting bond strength was developed in which all the controlling variables could potentially be measured nondestructively; substrate surface free energy, contact angle, and bondline thickness:

$$\text{BOND STRENGTH} = \frac{\gamma_S - \gamma_S \cos\theta}{(\frac{1}{2})(k_o)(\text{Bondline thickness})(175127)}$$

where: γ_S = substrate surface free energy, ergs/cm^2
γ_L = liquid (adhesive or distilled water) surface free energy, ergs/cm^2 (a constant)
θ = contact angle, degrees
k_o = effective strain coefficient (a constant)

This equation allowed the calculation of substrate surface free energies (γ_S) from experimental data, supplying values useful in cross correlations with nondestructive test data.

The NDT Technique Feasibility Studies included the following:

- .Exo-electron emission
- .Ultrasonic gas-phase transmission
- .Electric field reflectometry
- .Light specular reflectance

Of these, light reflectance and electric field reflectometry at 1 KHz exhibited the most promise. A strong correlation between white light relative reflectance and substrate surface free energy was obtained, encouraging further, more intensive development.

Conclusions and Recommendations

The following was concluded:

1. A practical equation for predicting bond adhesive strength from nondestructively measurable quantities has been developed.

2. A strong preliminary correlation has been found to exist between aluminum substrate surface free energy, calculated from experimental data, and white light specular reflectance.

3. Substrate surface free energy is influenced by the mechanical means used to generate the surface.

The following is recommended:

1. Conduct a development study centered around the Zurbrick equation for predicting bond adhesive strength using the four major structural substrate metals, aluminum, stainless steel, titanium and brass, and appropriate structural adhesives.

2. Coordinate the development of nondestructive test techniques for characterizing substrate surfaces with the bond strength study so that meaningful correlations may be derived between calculated surface free energies and NDT response values.

3. Place strong developmental emphasis on light reflectance techniques for measuring surface free energies.

4. Continue electric field reflectometry feasibility studies, particularly at low frequencies.

5. Continue ultrasonic gas phase transmission technique feasibility studies to determine sources of higher harmonic frequencies emanating from the substrate surface.

III. PROGRAM PLAN

A. Scope

The preliminary long-term goal of this program is to significantly advance technological capabilities to control the adhesive bonding process and thereby, the resultant adhesive bonds.

A particular viewpoint of this program is that adhesive bonding technology for the most part centers itself in the theoretical and empirical world of polymer chemistry and adhesive systems formulation. The substrate to which the adhesive is applied is a more peripheral consideration. In structural, primary load-bearing bonds, preparation of the substrate surfaces to enhance compatability with the adhesive is necessary, causing the adhesive-oriented technologist to focus some attention in that area.

That attention, however, is frustrated directly by an encounter with a surprisingly distant technical discipline, the science of adhesion. The theoretical basis of the science of adhesion centers upon the substrate surface and its properties. The adhesive is a more peripheral consideration. When necessary, the adhesive is adjusted to enhance its compatability with the solid surface being studied. Obviously these two viewpoints are directly opposed, and in philosophical, if not economic, conflict; Figure 1.

In this program we recognize the conflict but prefer not to choose one viewpoint over the other. Polymer chemistry, adhesive formulation and associated arts carry, for economic reasons, the greatest persuasive weight. Yet those exploring the theoretical science of adhesion have quantized important basic relationships, although the opposed viewpoints have greatly restricted practical application of these relationships.

Attention in the currently-funded program was focused on characterization of the adherend surface prior to bonding, which had been identified earlier as an area of adhesive bonding technology that remains largely undefined. Three separate investigations have been performed.

1. Surface Condition Study
2. Bond Strength Predictive Capability Study
3. NDT Technique Feasibility Studies

Program plans were formulated for each, with special emphasis on their supporting interrelationships.

B. Surface Condition Study

1. Purpose: To study the effects of surface roughness and character on bond strength, with special emphasis on proper surface characterization so that important variables may be identified, as a guide in selection of NDT methods and techniques.

2. Primary Materials Designations

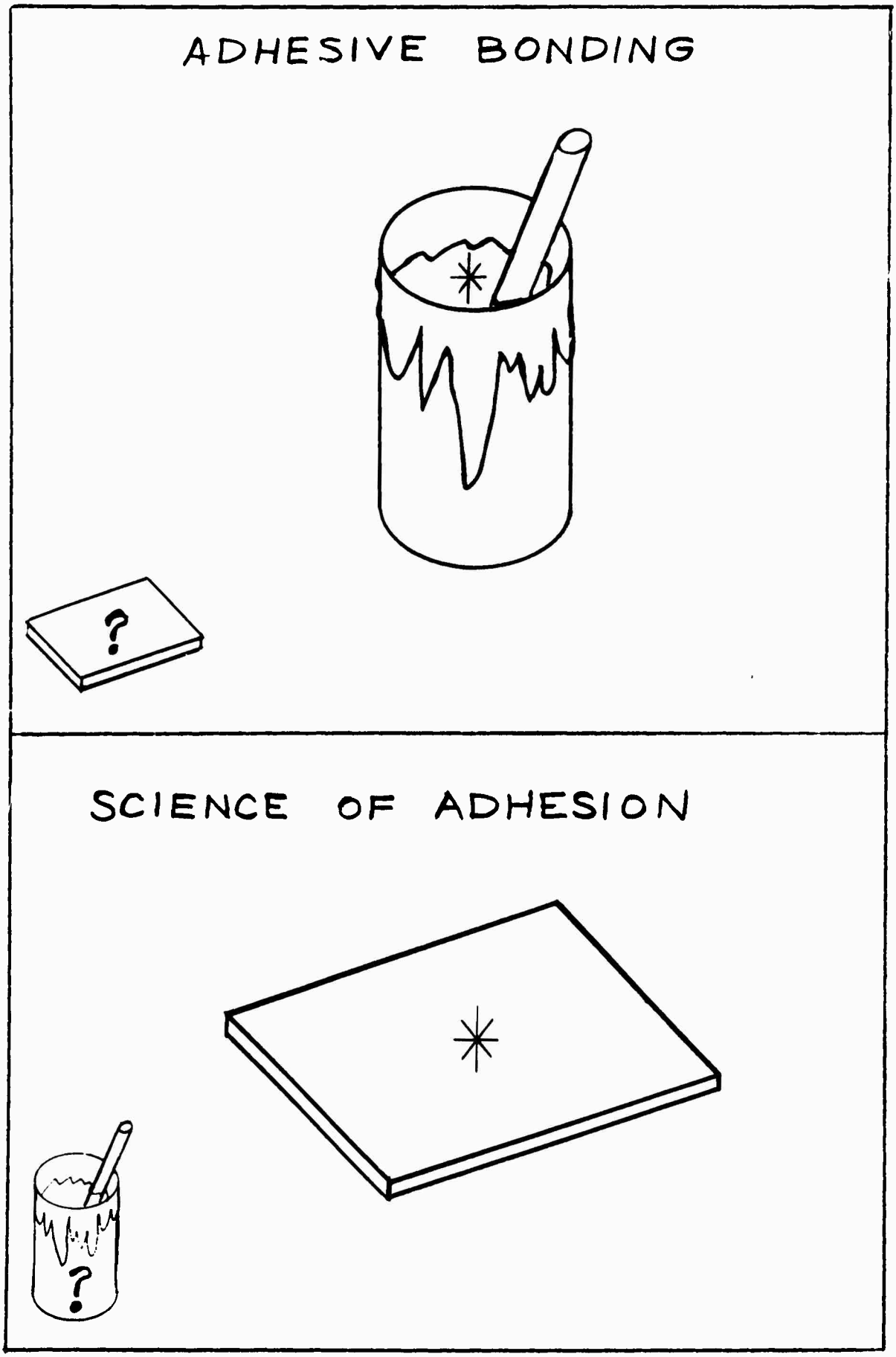

FIGURE 1. SEPARATE MATERIALS EMPHASES OF TWO SCIENTIFIC DISCIPLINES HAS SLOWED TECHNOLOGICAL ADVANCEMENT

2.1 Substrates

Aluminum alloy 6061-T6, will be used throughout this study. The majority of structural bonds in the field are produced with at least one aluminum substrate. Lengths of stock equalling 960 inches of 0.750 dia. rod, and 800 sq. inches of 0.064 ±.005 sheet stock are required.

2.2 Adhesive

Epon 828 in combination with diethylenetriamine will be used

3. Tests for Bond Strengths

3.1 Core Shear

3.1.1. Test Procedure ME-103, Avco ATD

3.1.2 Specimen design TS-418 with special surface finishes, Avco ATD.

3.1.3 Substrate size: 0.750 dia. X .375 long, 2 req'd each test specimen.

3.1.4. Bond-line thickness 0.006"

3.1.5 Bond area: 0.750 dia.

3.1.6 Bonded specimen overall length: 0.756"

3.2 Butt Tensile

3.2.1. Test procedure ME-108, Avco ATD

3.2.2. Specimen design ANC-452, Avco ATD with special surface finishes

3.2.3. Substrate size: 0.750 dia. X 2.0 long. 2 required for each test specimen.

3.2.4. Bond-line thickness 0.006"

3.2.5. Bond area: 0.750 dia.

3.2.6. Bonded specimen overall length: 4.006"

3.3 Lap Shear

3.3.1. Test procedure MM-A-132 and ASTMD-1002

3.3.2. Specimen design TS-420 with special surface finishes

3.3.3. Substrate size: 1.0 X 4.0 X 0.064 ±.005 thickness; 2 required for each test specimen.

3.3.4. Bond-line thickness 0.006"

3.3.5. Bond area: 1.0" X 0.50"

3.3.6. Bonded specimen overall length 7.5"

4. Surface Roughness Preparation

4.1 Machine produced finishes

4.1.1. Use metal-cutting techniques, such as lathe turning and fly-cutting, to produce the required range of surface finishes.

4.1.2. Roughness for each specimen type

a. Butt tensile

1. 150 RMS microinches
2. 110 " "
3. 80 " "
4. 20 " "

b. Lap shear

1. 150 RMS microinches
2. 110 " "
3. 80 " "
4. 40 " "

c. Core shear

1. 150 RMS microinches
2. 110 " "

4.1.3. Quantity for each specimen type-produce 10 surfaces (2 per bonded test specimen) for each roughness level. (100 surfaces total)

4.1.4. Finished area

a. Core shear - 3/4" dia., one end
b. Butt tensile - 3/4" dia., one end
c. Lap shear - 1" X 4", one face

4.2 Lapped Finish

4.2.1. Use lapping technique to a convenient, smooth finish on the as-blanked surface.

a. Butt tensile as-blanked = 32 RMS microinches
b. Core shear as-blanked = 32 RMS microinches
c. Lap shear as-blanked = Rolled stock surface

4.2.2. Roughness for each specimen type

a. Butt tensile

1. 40 RMS microinches
2. 10 " "
3. 7 " "
4. 5 " "

b. Core shear

1. 20 RMS microinches
2. 10 " "
3. 7 " "
4. 5 " "

c. Lap shear

1. 80 RMS microinches
2. 40 RMS microinches
3. 20 RMS microinches
4. 10 RMS microinches
5. 7 RMS microinches
6. 5 RMS microinches

4.2.3. Quantity for each specimen type-produce 10 surfaces (2 per bonded test specimen) for each roughness level except the 10 RMS level. Produce 50 surfaces for the 10 RMS level. (270 surfaces total)

4.2.4. Finished Area

a. Core shear - 3/4" dia., one end
b. Butt tensile - 3/4" dia., one end
c. Lap shear - 1" wide X 1" long, one face

4.3 Grit Blast Finish

4.3.1. Use dry grit - blasting technique to produce four types of surfaces as controlled by variation in grit size and blast pressure.

4.3.2. Roughness for each specimen type

a. Characteristic of 140 silica grit at 20# pressure
b. " " 140 silica grit at 80# "
c. " " 80-100 alum. oxide grit at 20# pressure.
d. " " 80-100 alum. grit at 80# pressure

4.3.3. Quantity for each specimen type-produce 10 grit-blasted surfaces for each of the four conditions. Use remaining 40 lapped surfaces (10 RMS) for each specimen type (120 surfaces total).

4.3.4. Finished Area

a. Core shear - 3/4" dia. one end
b. Butt tensile - 3/4" dia., one end
c. Lap shear - 1" X 1", one face

4.4 Polished Finish

4.4.1. Use hand and/or lathe polishing techniques to produce the required finishes on the as-blanked surfaces for each specimen type.

4.4.2. Roughness for each specimen type

a. Butt tensile

1. Mirror finish

b. Lap shear

1. Mirror finish

c. Core shear

1. Mirror finish

4.4.3. Quantity for each specimen type - produce 10 surface (2 per bonded test specimen). (30 surfaces total)

4.4.4. Finished Area

a. Core shear - 3/4" dia., one end
b. Butt tensile - 3/4" dia., one end
c. Lap shear - 1" X 1", one face

5. Surface Evaluation

5.1 Roughness profile and appearance

5.1.1. One representative surface of each roughness level, for each finish technique, for each specimen type will be examined (40 surfaces total).

5.1.2. Oblique lighted photomicrographs at appropriate power for each representative surface prior to etching.

5.1.3. Recording profilometer data for each representative surface prior to etching.

5.1.4. Oblique lighted photomicrograph at appropriate power for each representative surface after etching/cleaning.

5.1.5. Recording profilometer data for each representative surface after cleaning/etching.

5.1.6. Phase tests so that time between etching and bonding is less than 2 hours (4 hours max.).

5.2 Surface energy determination

5.2.1. Use same 40 representative surfaces for this study.

5.2.2. Measure contact angle (Langmuir technique) using distilled water for each representative surface.

a. Advancing θ
b. Receding θ

5.2.3. Phase tests so that time between etching and bonding is less than 2 hours. (4 hours max.)

6. Preparation for Bonding

6.1 Cleaning

6.1.1. Vapor or solvent degrease

6.1.2. Alkaline water solution clean

6.1.3. Rinse in water

6.2 Etching/Controlled Oxidation

6.2.1. Immerse in sulfuric acid-sodium dichromate solution

6.2.2. Rinse in distilled water (water break-free check)

6.2.3. Air or oven dry

6.3 Close process control required

6.4 Replication - three specimens per situation

7. Adhesive Bonding

7.1 Substrate Alignment

7.1.1. Core shear - V-blocks

7.1.2. Butt tensile - V-blocks

7.1.3. Lap shear - jig

7.2 Adhesive Preparation

7.2.1. Portion weights; resin/hardener

7.2.2. Mixing time and conditions

7.2.3. Time from mixing to application

7.2.4. Time from substrate cleaning to bonding

7.2.5. Bond to fixed bond-line thickness

7.3 Cure Conditions

7.3.1. Initial cure temperature, pressure and time. (environment and humidity).

7.3.2. Post-cure (if any) temperature, pressure and time. (environment and humidity).

7.4 Close process control required

7.4.1. Duplicate resin mixture batches.

7.4.2. Avoid over-age, excessive pot life in the resin batch.

8. Nondestructive Test Evaluation

8.1 Defect Detection

8.1.1. Film radiography

8.1.2. Ultrasonic pulse echo

9. Destructive Test Evaluation

9.1 Core Shear

9.2 Butt Tensile

9.3 Lap Shear

10. Correlation and Analysis

10.1 Correlations

10.1.1. Bond strength vs roughness

10.1.2. Bond strength vs. contact angle or surface free energy.

10.1.3. Investigate Bond strength, roughness, and contact angle correlations with NDT data

10.2 Analysis - analyze fits and compare with theory

11. Conclusions and Recommendations

11.1 Conclusions - Draw from results and observations

11.2 Recommendations - among others, select an appropriate finish to be used in subsequent studies under this contractual program.

C. Prediction of Bond Strength

1. Purpose: To study the known relationships between substrate surface variables and adhesive material variables which are thought to influence bond strength, within the context of practical bonded joint designs, so that a theoretical and analytical basis may be created for predicting bond strength from nondestructive test values.

2. Definition of Surfaces and Interfaces

The first step is to develop a conceptional definition of substrate surfaces, liquid surfaces and substrate/adhesive interfaces which encompasses the known interactions in physics between them and the many energy forms, as well as the wetting, absorption, and chemical bonding phenomena particular to adhesive bonding, lubrication, and catalysis. The needs and viewpoint of nondestructive evaluation requires definitions which emphasize material-energy interactions. In this case a bridge is to be built between the adhesive bonding and science of adhesion disciplines, to connect their distant viewpoints into a central, unified theoretical foundation.

3. The second step is to use the NDT-oriented definitions as a reference point for equating the engineering values of load, dimension, stress, strain, and modulus to the physical and chemical energies and dimensions at the atomic and molecular level. The concept here is that actions observed on a gross scale come as a result of atomic scale actions brought together in a complex summation process characteristic of the material involved.

4. The third step is to separate characteristic variables and parameters which may be measured on a gross scale by nondestructive means. The development of nondestructive test techniques becomes, therefore, relatively straightforward when such a foundation is provided. The nondestructive test data may then be analyzed in a multifunctional, multivariable set of equations which approximate the most important internal summation processes, to produce a set of characterizing values for any given adhesive bond situation.

D. NDT Technique Feasibility

1. Purpose: To determine, for a given form of energy, if the interaction of that energy with the surface of a substrate material produces characteristic changes in the energy which relate to adhesive-bond-influencing conditions of that surface.

2. In general, acoustic energy over the practical range of frequencies and electromagnetic energy over the full range of frequencies can be considered for the nondestructive evaluation of substrate surfaces. In both cases applicability is somewhat controlled, and limited, by the practical means currently used to generate and detect the energy, just as this same situation subdivides the spectrum into "bands", i.e. visible light, infrared, microwaves, sonic, ultrasonic, x-ray, etc. Applicability is further limited by certain laws of physics which relate wavelength to scattering, diffraction, and interference phenomena. We can further narrow the selection of energy forms from the vantage point of past experience, where the influence of external variables associated with test technique play an important part. By this selection process, four forms of energy were chosen for feasibility studies in terms of specific techniques:

a. exo-electron emission
b. ultrasonic gas phase transmission
c. electric field reflectometry
d. light reflectance

The feasibility studies contained five steps:

1. Analysis of theoretical basis for applicability to practical nondestructive test situations.

2. Assembly of equipment for preliminary tests to perform the essential material energy interaction and observe the form of instrument response.

3. Develop and adjust a rudimentary technique so that the desired response is separated from external variables.

4. Perform a series of tests on specimens known to contain a range of values for a given surface condition variable of interest.

5. Crossplot instrument response versus the variable of interest and observe for evidence of correlation.

The ability to obtain an identifiable instrument response associated with changes in surface condition constituted proof of feasibility. A correlation between instrument response and a known single variable provided positive direction for further, enthusiastic development. The lack of correlation suggested only that some part of the test technique was not adequately controlled or exact conditions used were unfavorable. Further development of techniques and conditions and data analysis methods is required in these cases. Such further development was beyond the scope of the current year's program.

IV. SURFACE CONDITION STUDY

The information gained from substrate and specimen preparations was grouped for each specimen type; butt tensile, core shear, and lap shear. One representative surface, code 3A, for each of 13 different surface conditions within each group, was thoroughly characterized both in the as prepared condition and immediately following sulfuric acid sodium dichromate etch just prior to adhesive bonding. All substrates were measured for bond-line thicknesses. Nondestructive test and destructive test data for the bonded specimens were summarized.

A. Surface Finishes

A total of 390 substrate surfaces were prepared as indicated in Table I. This was sufficient to provide five specimens at two substrates per specimen for each surface condition and type of specimen. Of these, three specimens per surface condition were bonded and tested.

Photomicrographic, surface roughness. and contact angle data are presented in Appendix I in grouped fashion for the most beneficial comparisons.

The photomicrographs were taken with a Burke and James "Rembrandt" model camera using an Agfa solinar lens (focal length = 5 cm., f = 3.5) The film used was Polaroid type 52, 4" X 5".

A Taylor-Hobson Tallysurf Recording Profilometer, Model 3, provided the Center-line-average (CLA) and strip chart profile data. Interpretation of the strip charts is aided by Table II. All data is in units of microinches.

Contact angle measurements were performed on the Langmuir-style device pictured in Figure 2. The surface tc be measured was brought into the plane of the table. A few small drops of distilled water were placed on the surface to form one highly-domed drop. While sighting along the juncture of the droplet and the surface via a surface mirror attached to the protractor, the protractor was adjusted until the axis of the arm was aligned exactly with the three-phase point. This operation was found to be most important to obtaining accuracy and reproducibility. The observed light-extinction angle was read from the protractor.

For highly polished, pure-element surfaces, a single contact angle is reported in the literature. In less-perfect cases advancing and receding contact angles are reported. Investigation of the hydrodynamic and gravitational forces involved in the cited measurements, as they relate to the distinctly rough surfaces being studied under this contract, revealed that many important forces act to modify the basic surface-free-energy attractions. Our own early observations revealed other parameters which affect the light extinction point determination, such as droplet shape and "lay" of the surface texture.

A satisfactory technique for performing the contact angle measurements, in consideration of both the theoretical and practical aspects, was developed. By adding water to an existing droplet in small increments the droplet was brought to its maximum contact angle, beyond which, the droplet would "jump" outward to a lower contact angle. Conversely, by removing small increments

TABLE I

SURFACE ROUGHNESS PREPARATION

Nominal Roughness	Butt Tensile	Core Shear	Lap Shear
1 rms $\times$ in.	Paper lapped	Paper lapped	Paper lapped
5 rms	Paper lapped	Paper lapped	Paper lapped
7 rms	Paper lapped	Paper lapped	Paper lapped
10 rms	Paper lapped	Paper lapped	Paper lapped
20 rms	Turned	Paper sanded	Paper sanded
40 rms	Paper sanded	Paper sanded	Turned
80 rms	Turned	Paper sanded	Turned
110 rms	Turned	Turned	Turned
150 rms	Turned	Turned	Turned
Fine grit low pressure	140 Mesh silica 20 psi	140 Mesh silica 20 psi	140 Mesh silica 20 psi
Fine grit high pressure	140 Mesh silica 80 psi	140 Mesh silica 80 psi	140 Mesh silica 80 psi
Coarse grit low pressure	80-100 Mesh Al_2O_3 20 psi	80-100 Mesh Al_2O_3 20 psi	80-100 Mesh Al_2O_3 20 psi
Coarse grit high pressure	80-100 Mesh Al_2O_3 80 psi	80-100 Mesh Al_2O_3 80 psi	80-100 Mesh Al_2O_3 80 psi

TABLE II

STANDARD RANGE AND MAGNIFICATION FACTORS

SCALE MAGNA-FICATION Switch Position	Magnification	Full Scale Chart 2 ins. or 5 cms.		Each Small Division Represents		Full Scale C.L.A. Index	
		Micro-inches	Microns	Micro-inches	Microns	Micro-inches	Microns
1	1,000	2,000	50	100	2.5	200	5.0
2	2,000	1,000	25	50	1.25	100	2.5
3	5,000	400	10	20	0.5	40	1.0
4	10,000	200	5	10	0.25	20	0.5
5	20,000	100	2.5	5	0.125	10	0.25
6	50,000	40	1	2	0.05	4	0.1

1 Micro-inch =.000001 in. 1 Micron = 0.001 mm. = 40 micro-inches

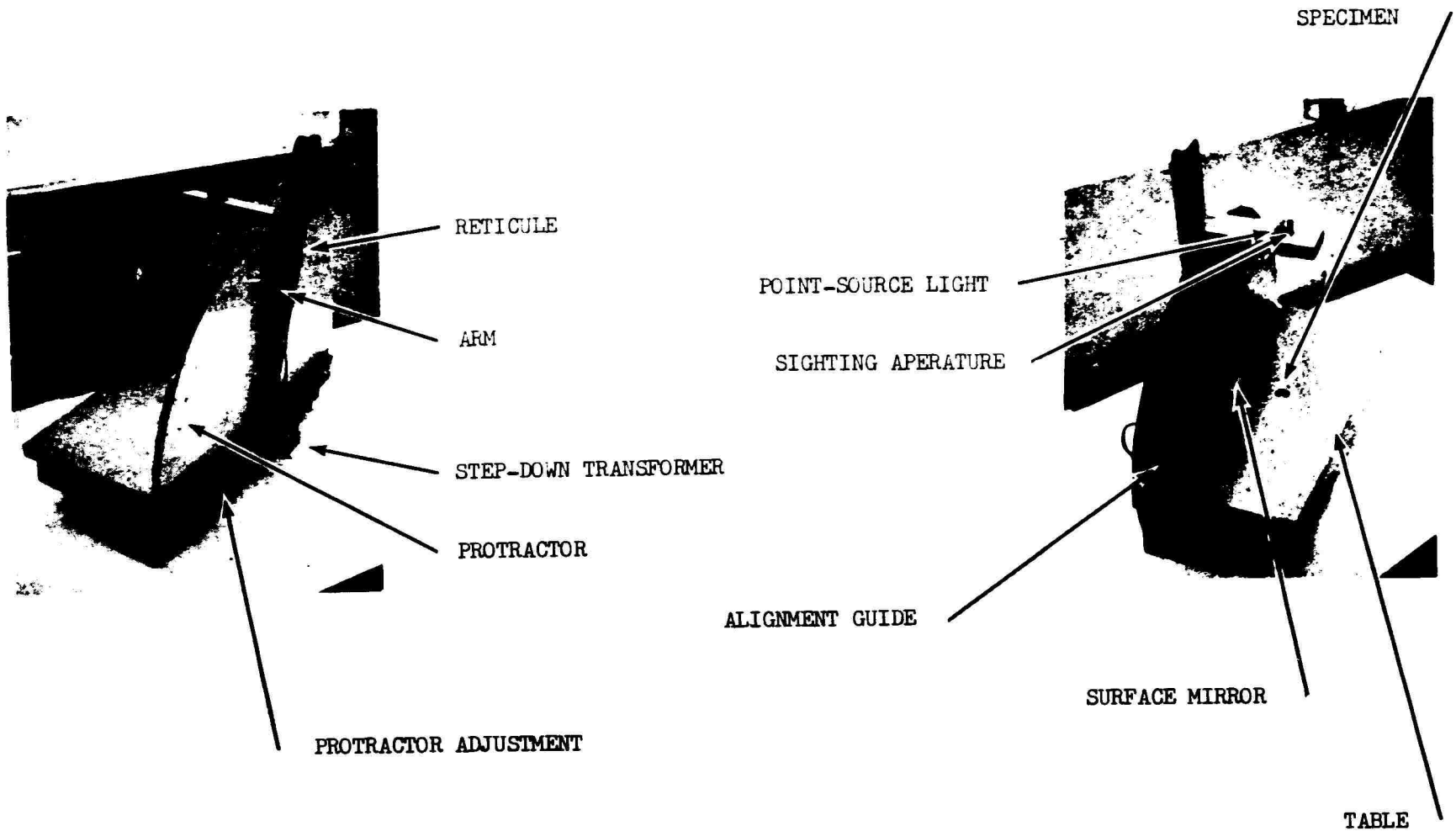

FIGURE 2. CONTACT-ANGLE MEASURING DEVICE DEVELOPED AT AVCO FOR SURFACE CHARACTERIZATION SPECIMENS (AFTER LANGMUIR)

of water from an existing droplet, a minimum contact angle could be obtained, just prior to the droplet retracting in a "jump" motion. In all cases the test surfaces were horizontal. The results were found to be reproducible and properly related to surface energetics. The data is reported in a group of three values, θ maximum, θ minimum, and the angular difference between them, $\Delta\theta$.

B. Preparation for Bonding

The schedule for bond preparation, etched surface evaluation, and adhesive bonding was carefully arranged to benefit both data-taking and bonding. Three hours after etching had been completed, the curing agent was added to the adhesive resin mixture, with the bonds being completed within 30 minutes from the start of that mixing. Twelve specimens were prepared each day for two days, with fifteen specimens being prepared the third day, for a given type of specimen. Three such series covered the butt tensile, core shear, and lap shear specimen types.

The substrate cleaning and etching was conducted according to Avco RAD Specification G100004-4, "Immersion Cleaning and Etching of Aluminum and Aluminum Alloy, Process for" except that manual solvent wiping with methylethyl ketone (MEK) replaced the recommended vapor degreasing. Distilled water was used for the final rinse.

C. Adhesive Bonding

The adhesive formula for each of nine batches was:

Epoxy resin	Epon 828	50.00 grams
Viscosity adjuster	Cab-o-sil	1.25 grams
Total prepared resin		51.25 grams
Hardener	DETA	5.00 grams
Total mixture		56.25 grams

The epoxy resin and fumed silica were mixed together in two master batches, each consisting of 750.00 grams of resin and 18.75 grams of Cab-o-sil. Prior to mixing, the Cab-o-sil was dried for four hours at 230°F. After mixing the batches were placed under full vacuum for at least 10 minutes at room temperature to remove air and volatiles. The master batches were stored at room temperature. A day's batch of prepared resin and hardener was mixed by hand for two minutes and then spread thin to maximize evolution of reaction exotherm heat. This procedure minimized mixture aging over the 30-minute application period. Curing in all cases was conducted at room temperature (72° ±4) for a minimum of 24 hours in order to avoid thermal expansion variability.

TABLE III

BOND LINE THICKNESS, MILS

Surface Finish Nominal	Butt Tensile			Core Shear			Lap Shear		
	1A	2A	3A	1A	2A	3A	1A	2A	3A
1 rms	5.5	3.8	4.9	5.7	4.8	4.2	2.1	3.9	2.7
5 rms	4.4	4.2	4.4	5.5	6.3	4.6	2.6	1.0	3.2
7 rms	10.0	4.7	6.7	5.2	4.9	3.9	5.0	2.0	1.3+
10 rms	7.1	6.6	4.2	5.1	3.6	5.0	1.2	2.3	3.5
20 rms	7.6	6.5	5.5	6.3	9.7	7.4	3.9	3.1	1.9
40 rms	6.1	6.5	5.2	8.8	8.2	7.9	4.5	4.6	3.6
80 rms	4.7	6.4	6.7	7.4	5.5	5.2	7.2	6.1	4.4
110 rms	8.3	7.5	8.1	5.6	5.2	8.2	3.6	5.9	6.4
150 rms	7.7	4.9	6.0	6.0	7.5	6.4	5.0	2.7	2.8
FGLP	6.1	5.6	4.5	8.1	6.6	5.8	3.7	4.4	3.9
FGHP	6.6	5.8	5.5	5.5	4.6	4.9	3.7	3.0	4.8
CGLP	7.3	6.0	4.6	6.0	7.3	5.7	2.2	1.3	2.7
CGHP	4.4	2.7	5.3	3.9	5.4	4.0	3.0	5.2	5.3

The cylindrical substrates were aligned and cured in Vee-blocks using substrate length measurements to set the 0.006 inch bond-line thickness. The lap-shear specimens, however, required a special set-up procedure. Because differing surface finishes were machined, lapped, fly-cut on the specimen surfaces, more or less material was removed from some specimens, yielding specimens which varied in the thickness by 3-4 mils from the original blanking stock.

All specimens were dry fitted, shimming individual specimens with plastic (mylar) film such that a 1 mil feeler guage blade could not be inserted between the mating halves at the point to be bonded.

Previous experiments with the bonding system (adhesive) used in this program permitted bonds of approximately 6 mil thickness to be obtained on lap shear specimens when a "dead weight" of 100 grams per sq. in. was applied to the buttered halves. The weight-adhesive viscosity combination allowed the substrates to seek that equilibrium which, in previous experiments, yielded an approximately 6 mil thick bond line. Individual lap shear substrates were pre fitted in a bonding fixture specifically designed to maintain the alignment and overlap required. Bonding fixtures were made to bond six individual lap shear specimens simultaneously. One substrate of each of six specimens was placed onto the fixture and spring loaded. The second or mating substrate was placed on the fixture and a straight edge was placed across the 0.50 in. overlap area of all six specimens. Mylar and/or polyethylene film shim stock was added as necessary under the lower individual substrates so that less than one mil clearance was noted between the suspended straight edge and any singular substrate (in the overlap area). It should be noted that the fixtures were initially designed for mating 0.064 in. nominal thickness substrates yielding an approximate 5 mil parallel bond line. Following surface preparation the adhesive was prepared and spread into a thin film. Each substrate was wet with adhesive, covering the sample width and approximately 0.625 in. of the bonding edge. Samples were permitted to set at room temperature about 20 minutes to permit application of adhesive to all samples, allow excess air to escape and ensure a more uniform consistency viscosity-wise (adhesive). Specimens were then assembled and a 100 gram per square inch (overlap area) load was applied by means of a pre weighed bar. Room temperature cure of 24 hours was effected before specimens were removed from the fixtures. Resulting bondline thicknesses are given in Table III.

D. Nondestructive Test Evaluation

a. Radiography

A few butt tensile specimens were radiographed at an oblique angle. A sensitivity of 2-1T with an aluminum penetrameter (0.015" thk, 0.008" dia. hole) was obtained. A polyethylene film step wedge (0.005" and 0.010" thick) was constructed and placed across the bond area. The polyethylene film could not be adequately discriminated in the radiographs. Similar lack of ability to radiographically observe bubbles in the bond line was experienced with the lap shear and core shear specimens.

Radiographic conditions:

Using a Philips-Norelco 50-150 KV X-ray tube with a 2.5 mm focal spot operated at 100 KV, 10 Ma for 1 minute and a focus to film distance of 48 inches, representative radiographs were obtained on Eastman Kodak type "M" film. Films were hand processed (developed) for 8 minutes at 68°F. The tube was positioned at an angle of 30° off the perpendicular such that the area of interest was projected onto the film for the butt tensile specimens.

b. Ultrasonic Pulse-echo

The centering holes and load-pin holes in the butt tensile specimens made it impossible to obtain unambiguous bond/unbond indications.

The lap shear specimens were all inspected for bond/unbond, and no unbonds were detected. Reference bond/unbond specimens were prepared from two pairs of substrates using coupling agent to represent the bonded case.

Equipment used:

Branson Sonary, Model 51C

A.I. 5.0 MHz/.312 dia. type SFZ transducer

Delay 5	Damping 9½
Range 6	C Gain A
Reject 1 o'clock	Extended Range 3 o'clock

The core shear specimens were all inspected for bond/unbond, and no unbonds were detected. Reference bond/unbond specimens were prepared from two pairs of substrates using coupling agent for the bonded case.

Equipment used:

Branson Sonoray, Model 51C

AI 5.0 MHz/.312 dia. SFZ transducer

Delay 5	Damping 10
Range 6½	C Gain A
Reject 1 o'clock	Extended Range 3 o'clock

E. Destructive Test Evaluation

Results of destructive tests are presented in Table IV. The specimens were all pulled at room temperature, 75° ±2°F and 50% RH, on the Instron universal testing machine. Crosshead speed was adjusted to provide an applied stress rate of 600 to 700 psi per minute.

F. Data correlation and analysis

All of the data, notes, and photographs obtaining during the Surface Condition Study were assembled according to specimen type and nominal surface roughness. The cosine values of all contact angles were obtained from trigonometric tables and added to the data lists. These lists served as the primary data source for crossplot trials.

TABLE IV

ADHESIVE BOND ULTIMATE STRENGTH, PSI

Surface Finish Nominal	Butt Tensile			Core Shear			Lap Shear		
	1A	2A	3A	1A	2A	3A	1A	2A	3A
1 rms	3900	3750	3200	3140	4500	460	1360	1320	910
5 rms	5770	4780	5540	1280	1470	2870	1260	1390	910
7 rms	3600	3920	5190	1610	1590	4530	1240	1320	1140
10 rms	4100	5040	2660	2310	3600	3610	1160	1280	1080
20 rms	5580	6930	4750	2800	4370	1000	990	1200	1120
40 rms	4070	3920	4240	2440	2940	3040	1000	1000	822
80 rms	5300	4210	5100	2320	4710	1250	1130	1060	830
110 rms	4450	4080	3630	3280	2000	590	940	970	760
150 rms	5750	5510	5320	1610	2470	1800	860	1120	770
FGLI	7590	5210	7300	4440	4160	1400	975	940	975
FGHP	6930	7160	5510	1540	5150	4260	1050	1040	1060
CGLP	5110	6720	4710	5250	4770	4730	925	1230	1180
CGHP	6110	5760	6770	5480	5270	5070	1230	965	1130

The first reaction to the lists was one of frustration. The values gave the initial impression of complete and unrelated randomness. (Such is not unusual in adhesive bonding studies.) A few simple relations among three or perhaps four specimens were observed through casual inspection of the data, but these were promptly reversed by another set of specimens. Based on this, however, a number of computer analyses were run using linear equation solutions for three unknowns, from data of three selected specimens. The equation format for this multifunctional, multivariable study was generally:

$$\text{Bond Strength} = (C_1)(1+\cos\theta)+(C_2)(\text{CLA})+C_3\left(\frac{1}{\text{thickness}}\right) \qquad (1)$$

The experimental values were simulaneously solved together to provide empirical values for the linear constants, C_1, C_2, and C_3. The format in equation (1) satisfied the general conclusions drawn in the adhesive bonding literature.

The general conclusion from the linear-equation trials was that the cos 0 term seemed to dominate the data, that inverse bondline thickness modified the relationship, and that CLA was of no consequence. The lack of correlation in CLA was expected (Reference 2). The other two observations satisfied the findings and conclusions most frequently found in the literature and most generally agreed to by adhesive bonding technologists (Reference 3).

The data analysis effort was shifted to direct concentration on the cos 0 interrelationships to seek out the primary single function involving bond strength. No direct relationship could be found between any of the four contact angle values (as prepared cos 0 max and cos 0 min; after-etch cos 0 max and cos 0 min) and bond strength. The idea of historical influence was studied through these relationships:

$$\cos\theta_{max}\ \text{Ratio} = \frac{(1+\cos\theta_{max})_E-(1+\cos\theta_{max})_M}{(1+\cos\theta_{max})_E} \qquad (2)$$

$$\cos\theta_{min}\ \text{Ratio} = \frac{(1+\cos\theta_{min})_E-(1+\cos\theta_{min})_M}{(1+\cos\theta_{min})_E} \qquad (3)$$

where: subscripts, M = as prepared; E = after etch.

It was generally observed that the surfaces prepared with the smoother finishes were roughened by etching, and that those prepared with the rougher finishes were smoothed by etching. There appeared, through the ratios of equations (2) and (3), an impression that initial surface preparation did influence bond strength, even though considerable changes due to etching had taken place. No direct correlation of this, however, could be obtained.

Attention was then turned to bondline thickness as a function of bond strength. No direct correlation was observed. The misalignment of substrates was taken into consideration by observing the thickness variation of each bondline as well as its average thickness. Again, no support for a direct correlation to bond strength was forthcoming.

These experiences turned the attention to the bond strength values themselves. The questions were asked,"how exactly were the values obtained for each type of specimen;

what was considered in calculating bond strength (breaking load divided by ideal bonding area); and what measurement errors were inherent?" The answers, mostly speculative, shed no real light on the meaningfulness of the reported bond strength values.

One firm relationship did grow out of this study. It was observed that a brittle fracture pattern was exhibited by each of the butt tensile and core shear specimens, figures 3 and 4. An analogous pattern was somewhat evident in the lap shear specimens, figure 5.

The failure mechanism appeared to be as follows:

a. Initiation of failure at the interface between cured adhesive and one of the substrates. ("adhesive failure")

b. Brittle failure by rapid wavefront propagation radially away from the initiation site. Failure was "cohesive" in the cured adhesive.

c. Breakup of the shock wavefront and subsequent dissipation of energy by scattering.

d. Final separation of the bonded joint by non-brittle, viscoelastic flow, somewhat anologous to the peeling mechanism.

Most important, however, was this observation:

The bond strength was inversely proportional to the area of the interfacial separation at the initiation site.

That observation fits very well with brittle fracture strengths versus initiation site sizes observed for high strength metals and structural ceramics.

Perhaps more important was the conclusion that bond adhesive strength is directly controlled by the interfacial bond condition, rather than bulk adhesive or bulk substrate properties.

Reinspection of the entire listed data, in the light of the above-stated conclusions, provided the foundation for creative inspiration on the part of the author. What if the Thomas Young relationship held throughout the adhesive bonding process with regard to the quantum mechanical bond between cured adhesive and metallic substrate; would the surface energy state of the adhesive/substrate interface be directly related to bond strength? Through careful derivation and appropriate data analysis the answer was found to be "yes".

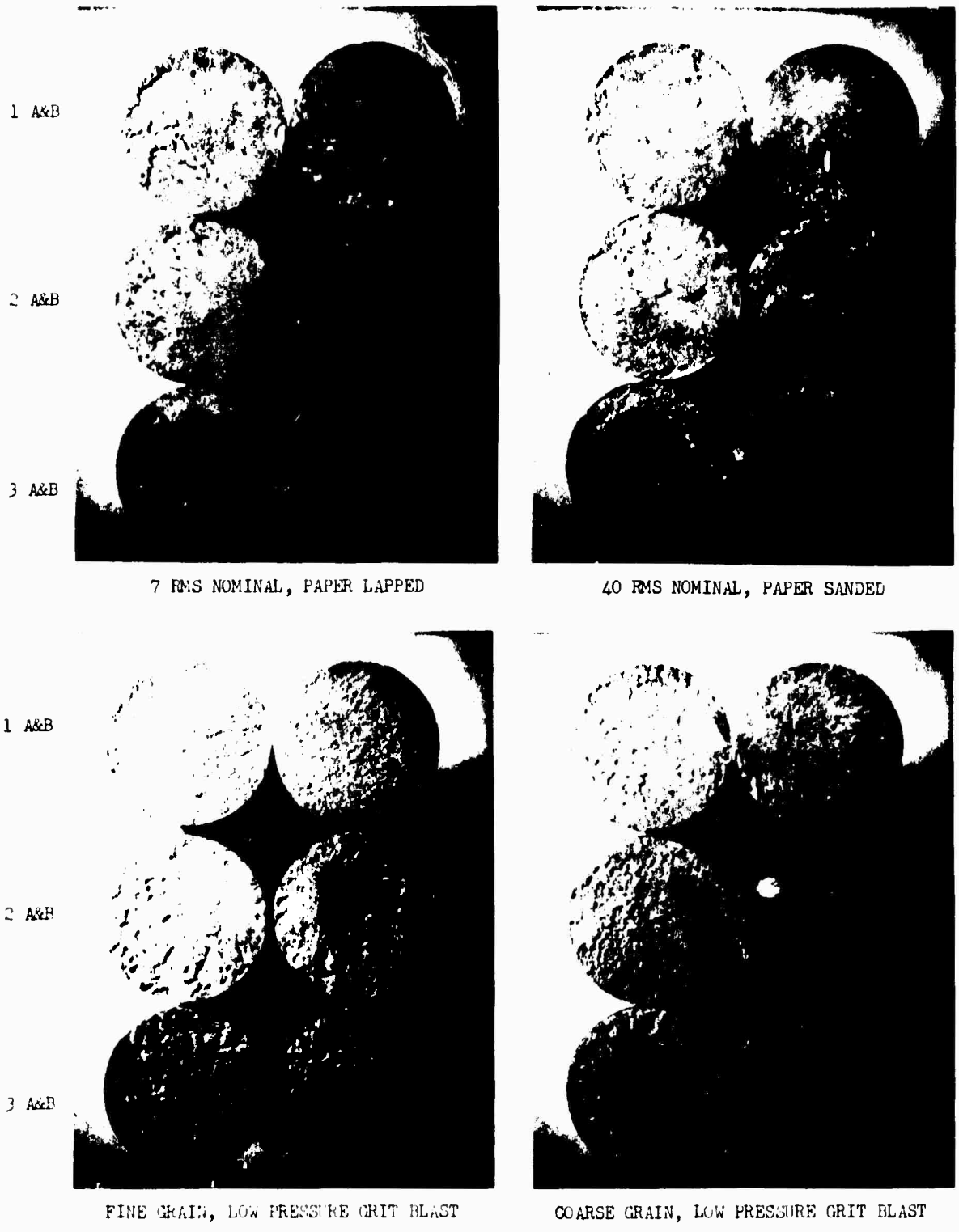

FIGURE 3. BOND FRACTURE SURFACES OF SELECTED BUTT TENSILE SPECIMENS

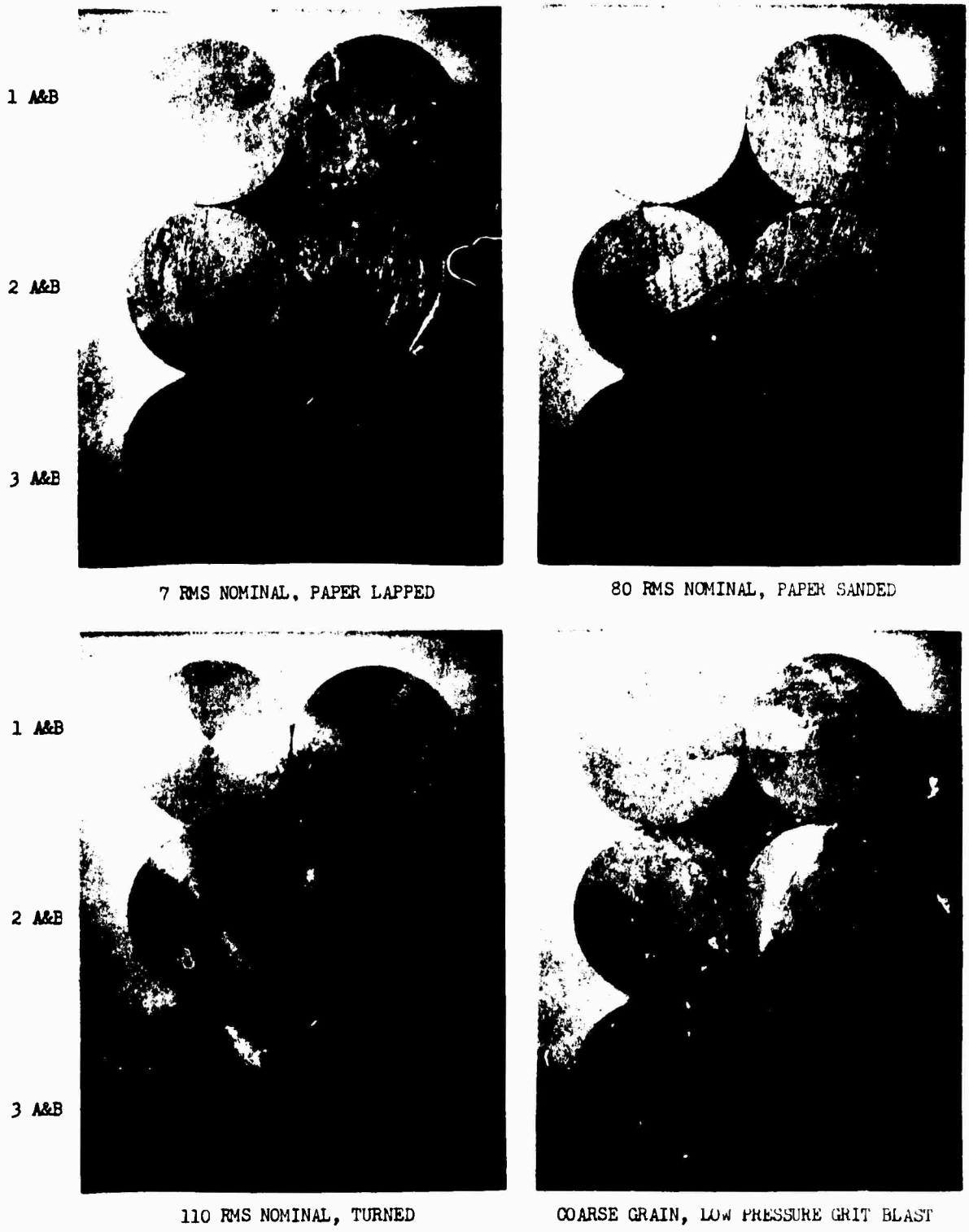

FIGURE 4. BOND FRACTURE SURFACES OF SELECTED CORE SHEAR SPECIMENS

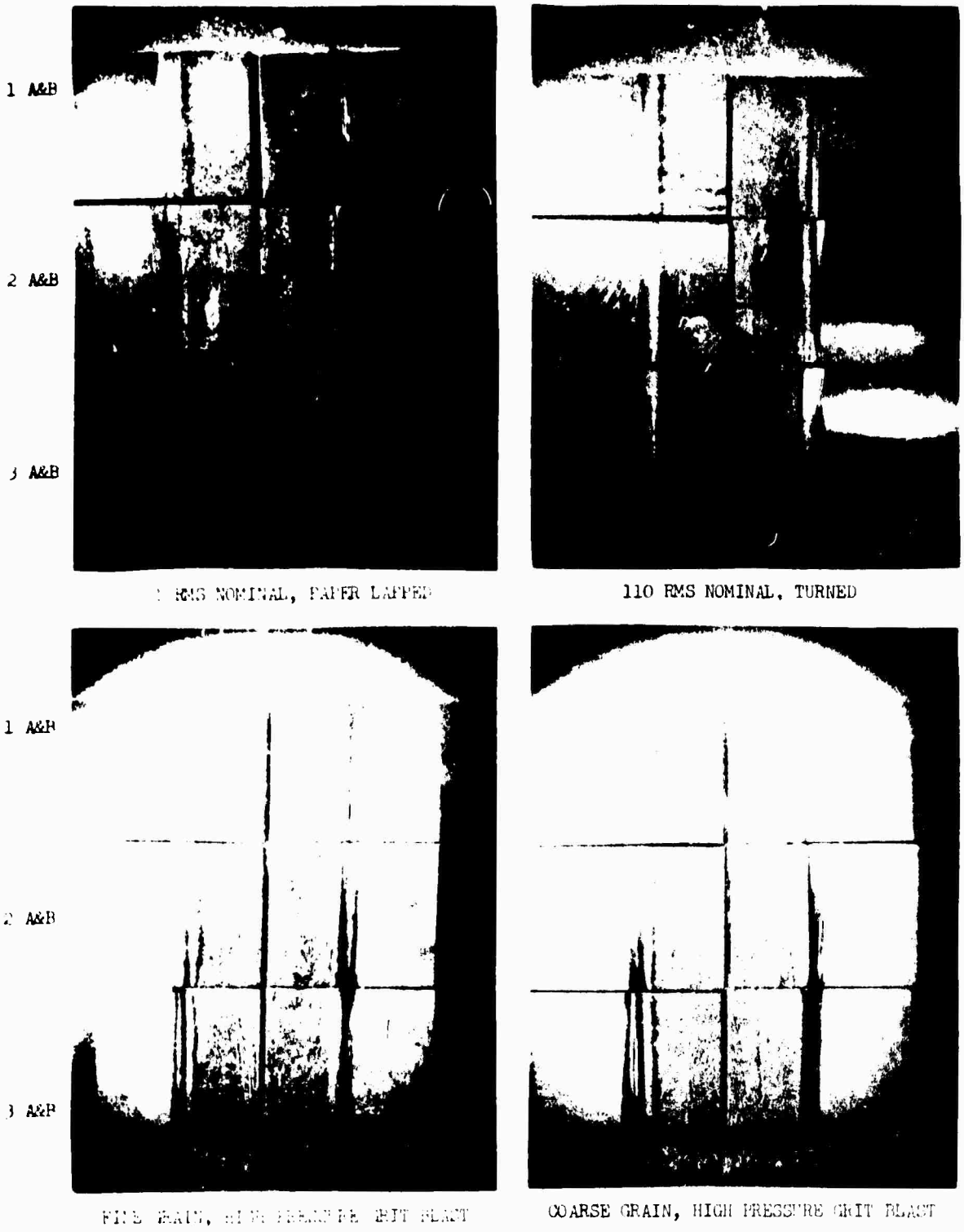

FIGURE 5. BOND FRACTURE SURFACES OF SELECTED LAP SHEAR SPECIMENS

V. PREDICTION OF BOND ADHESIVE STRENGTH

The ability to mathematically predict adhesive bond strength for practical adhesive bonds is a long-sought-after goal (References 4 and 5). Countless approaches have been tried over the decades with essentially no success whatever. The Science of Adhesion has fallen into a circular path of re-referencing the re-referenced works of the past. My discussion in this section takes advantage of what has already been learned, yet it leads off in a <u>new</u> direction, ir hopes of breaking the vicious circle. Adhesive bond strength <u>can</u> be accurately predicted, and in an amazingly straightforward manner.

All paths in the science of adhesion lead back to the Thomas Young equation (1805) which described the equilibrium between the stationary drop of a liquid and the surface of a solid:

$$\gamma_S - \gamma_{LS} - \gamma_L \cos\theta = 0 \qquad (4)$$

where: γ_S = solid surface energy (in vacuum)
γ_L = liquid surface free enery (in vacuum)
γ_{LS}= solid-liquid interface surface free energy
θ = contact angle at three phase point

The physical picture of this "contact angle" relationship is shown in Figure 6 Modifications of this basic relationship have been presented and studied by Dupre', Zisman, Wenzel et al., the main reason being the obvious physical inability to measure γ_{LS}. Their approaches have eliminated γ_{LS} and concentrated on analyzing in terms of γ_L and cos θ. But take a second look at γ_{LS}. Is this perhaps a case of "throwing the baby out with the bath water?" It certainly is, as we shall see.

A. <u>Defining a Surface</u>

Having observed that the various literature definitions for a "surface" are either too idealized, observationally vague, or mathematically restricted, we have sought to define a surface which has the capability to perform the material-energy interactions already cataloged in the sciences of physics and chemistry. This view prepares the way for selection of energy forms useful to the nondestructive characterization of surfaces. The highly idealized surface is usually defined in terms of a straight line; a boundary separating two phases. The bonding phenomenon takes place at or across the boundary. The boundary is considered to have finite thickness or no thickness at all. Much of this visualization has been created in an effort to prepare a simple mathematical model (Reference 6). Other simplicities include the idea of a forward-going chemical bonding reaction or thermodynamic energy transfer. When practical experiments are planned to study the correspondence of nature and theory, surfaces approximating straight-line boundaries (plane, smooth surfaces) are typically prepared (Reference 7). Close observations of these

$$\gamma_S = \gamma_{LS} + \gamma_L \cos\theta$$

THOMAS YOUNG EQUATION (1805)

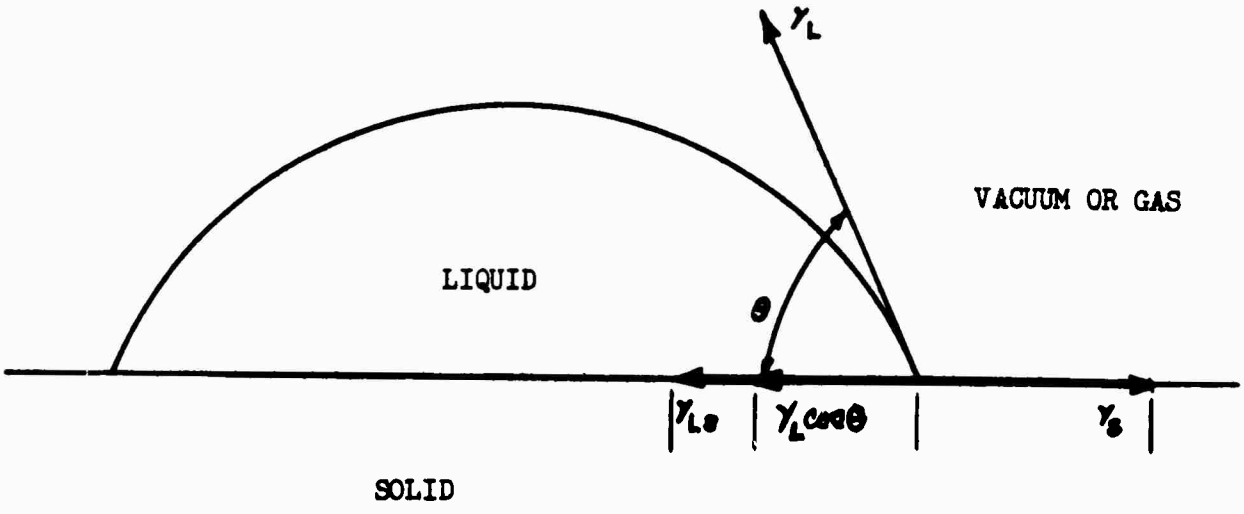

FIGURE 6. FORCE EQUILIBRIUM CONDITION AT THREE-PHASE POINT FOR A LIQUID DROPLET ON A SOLID SURFACE

surfaces via light optics, electron optics, x-ray diffraction and such, serve to create many more questions than the few answered.

The idealized approach has done little to satisfy the need for understanding the factors controlling practical adhesive bonding. In fact, the "surface" has never been sufficiently defined or characterized in the practical sense. Our own studies have revealed many subtle parametric variables which appear to have significant influences on bonding. Since it can be safely assumed that all the variables may occur together and that no one variable may be isolated for study, we are obligated to approach any practical effort toward defining a surface in terms of a fairly complex multifunctional, multivariable system. The effectiveness and practicality of this approach in nondestructive testing has been proved. (Reference 8).

B. Quantum Mechanical Definition

The quantum mechanical pictures of the lone atom and the extensions into chemical bonds between atoms focus on the electron. The energy and spacial distributions of the electron have been theoretically identified and quantized in terms of vibrational frequencies and potential energies of inter-mass associations and found to correspond directly with experimental evidence. The ability of electromagnetic energy, heat energy, and mechanical energy to modify or "jump" these electron energy states and spacial distributions is intrinsically woven into the whole quantum mechanical concept. (Reference 9).

The fact that a "surface" between gas and solid, or an "interface" between cured adhesive and substrate will be different from the bulk of either phase is to be expected from quantum mechanics theory. From the energy aspect alone, the surface/interface must be in a higher state of excitement (contain more stored energy) than the bulk by virtue of molecular orbitals between dissimilar atoms. Exactly how these energies are distributed is not yet understood. The existing general view of chemical bonding and surface boundary observed interactions provide sufficient basis for a suitable definition.

A surface is defined here as, "A region between two different phases which exists in an excited, high-energy state relative to the energy states normally associated with each of the bulk phases, where dimensional aspects are quasi-stable but energy aspects are highly mobile."

Note the last few words. Not only is the surface region excited energy-wise, but a large quantity of stored energy may be readily moved from place-to-place through the application of a small force applied from outside the surface region. The defined concept of "surface" is pictured in Figure 7, where the shading is intended to give the impression of variation and mobility.

The contributions of the excited, mobile surface energy state to adhesive bonding are familiar. Metallic surfaces in air exhibit characteristic light reflection, polarization, diffraction, diffusion, and color. These are strictly interactions of electromagnetic energy with surface energetics. The Faraday effect (rotation of polarization plane of light reflected from a polished electromagnet pole piece during magnetization) is an example of changes in material-energy inter-

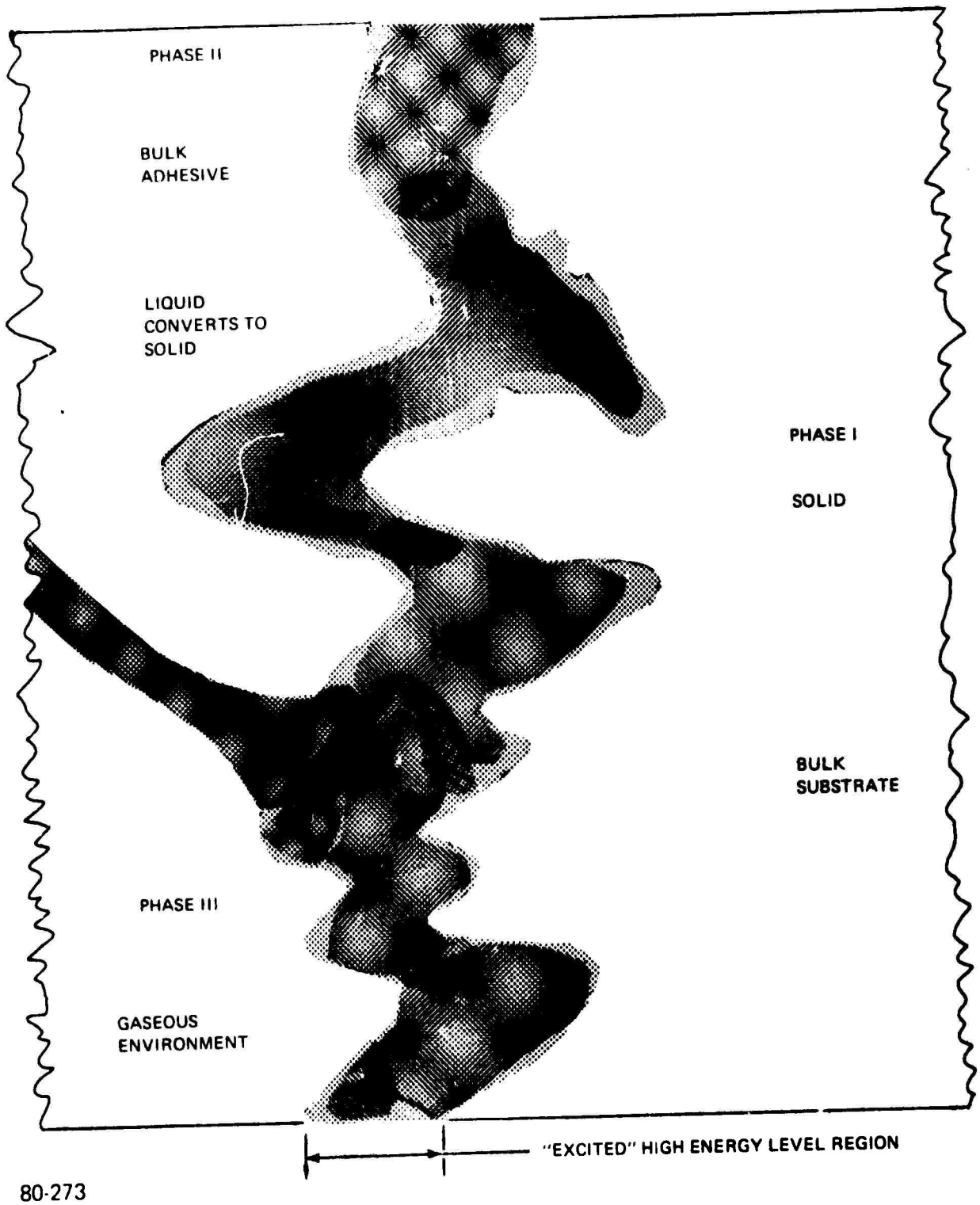

FIGURE 7. CONCEPT OF "SURFACE" IN TERMS OF QUANTUM MECHANICAL ENERGY STATES

actions wrought simply by applying an external force which shifts the energy distribution of the surface. Yet no observable dimensional change takes place.

The transient phenomenon of "wetting" attests to the energy mobility available in a surface. The new chemical bonds, and completely new set of surface (interface) energetics created as a result of wetting establishes the primary strength of the bond.

Curing or other chemical and physical changes which occur to "set" the adhesive apply external forces to the interface, shifting and modifying energy distributions there. Chemical attack along the interface, such as is experienced with adsorbed water, can greatly modify and shift interfacial bonding energies. Although these surface/interface phenomena will modify the primary strength value of an adhesive bond, ultimate bond strength in pounds load per square inch of area is a value derived from bulk material dimensions and properties. Hence, the exact contributions of bulk properties and dimensions, interfacial energetics, and externally (referenced to the interface) applied forces must be properly accounted for in any effort to correlate ultimate bond strength with nondestructive test response information. (Reference 10).

The nondestructive characterization of substrate surfaces prior to adhesive bonding is the specific goal of the current and future research and development programs. Based on quantum mechanical considerations it becomes evident that "wave energy" rather than "particle energy" is most useful to nondestructive testing of surfaces. Wave energy interactions depend most on surface electron energy state and mobility, while particle energy interactions depend most of the dimensional aspects of particulate mass location, that is, atomic-atomic distances, lattice structures, and molecular roughness. In all cases adhesive bonding is controlled by surface electron energy state.

Two general "wave energies" are used in nondestructive testing; mechanical (acoustics) and electromagnetic. Frequency characterizes the wave energy in terms of its ability to transfer energy per quantum and contain intelligible information (communicative data). A most important consideration here is that mechanical and electromagnetic energies are directly linked in a triad of force fields, gravitational/electric/magnetic existing in relatively stationary matter and in propagating quanta of energy. It is evident, then, that nondestructive measurements taken where the mechanical field, or the electrical field or the magnetic field dominately interacts with the test device, the informative data obtained has direct ties to the remaining two force fields. Because of this it is possible to obtain valuable material-energy-interaction data from test devices employing different single-field interactions and positively link their results to describe a multifunctional, multivariable material character, such as for substrate surfaces.

The approach taken here is that γ_{LS}, the surface free energy of the adhesive/substrate interface, is in fact the <u>true value of bond strength</u>. Stated slightly differently, γ_{LS} is the energy that must be added to the bond interface to form a given area of new substrate surface and an equal area of new adhesive surface. Is this the mechanism of observed adhesive bond failure?

Yes; and the concept is simplified if we assume that γ_{LS} changes in direct proportion to γ_L as the adhesive changes from liquid to solid through chemical reaction, solvent evaporation, coalescence, etc. This we do not actually know at present, but it is a reasonable assumption that will be borne out.

Quantum mechanics of chemical bonding support the idea that the action of wetting is the formation of substrate/adhesive chemical bonds, each bond exact in the frequency and molecular electron orbitals associated with the bond. The energy required to break one such bond is a fixed value, the total energy being the sum of energy for all bonds broken. Thus the adhesive bond strength is related directly to the number of chemical bonds formed during wetting. Existing bond energies and lengths (bonding, antibonding orbitals) will be modified somewhat by the physical/chemical changes in the bulk adhesive associated with "setting" (liquid to solid transformation) but for "proper" joints this should be minimal. (Bikerman's picture of the "weak boundary layer" is the case of a drastic modification, with time, of these bonds, even to the breaking of some. Although an important aspect, we will consider only the most frequent case where no wetting-assembled bonds are broken or severely changed, or no new bonds are added with time). The Thomas Young equation (4), therefore, contains all the necessary primary variables and fixes their relationship.

Equation (4) can be written as a simple force balance along a line:

$$\gamma_S = \gamma_{LS} + \gamma_L \cos \theta \qquad (5)$$

Rearrangement gives:

$$\gamma_{LS} = \gamma_L - \gamma_L \cos \theta \qquad (6)$$

a form which best serves this derivation. It says, essentially, adhesive bond strength is directly related to substrate surface free energy <u>less</u> the contact angle cosine component of adhesive surface free energy. For the purposes of analysis each of the four variables can be considered independent of each other except as related in equation (6). Note that γ_L will be a constant of value particular to the liquid of interest, i.e, an adhesive formulation, distilled water. With γ_S and cos θ as the independent variables, we see the following general set of relationships:

γ_{SL}	γ_S	γ_L	cos θ
Low-Low	Low	CONSTANT	Low
Med-Low	Med		
High-Low	High		
Low-Med	Low		Med
Med-Med	Med		
High-Med	High		
Low-High	Low		High
Med-High	Med		
High-High	High		

Because we expect a wide range of values for both γ_S and cos θ, (low, med, high) the resultant values of γ_{LS} can vary even more widely, and without definite apparent pattern. The randomness of adhesive bond strength data is well-known, and often cursed, by the concerned technologists in this field. The recent data produced under the subject contract is a case in point. Now we can begin the exact derivation.

Bond strength values obtained through tests on specimens represent the energy stored in the total loaded bond test specimen volume, both substrates and adhesive, at the moment of fracture initiation. This may be seen as follows:

$$\text{Bond strength} = \frac{\text{load at moment of fracture}}{\text{cross sectional area of bonded joint}} = \frac{L}{A}$$

$$\text{Bond strength} = \frac{\text{pounds force}}{\text{square inch}} = \text{psi} \qquad (7)$$

But: $1\ \text{lb/in}^2 = 68948\ \text{ergs/cm}^3 = 68948\ \frac{\text{dynes}}{\text{cm}^2}$

ergs = unit of energy; dynes = unit of force; 1 dyne-cm = 1 erg

Thus one psi represents the storage of some energy in the volume of material being loaded.

We can then proceed one step further:

For a given substrate material and configuration, which is held essentially constant, the important variable is the adhesive volume; bond strength is then directly related to the energy stored in the adhesive volume at the moment of fracture initiation.

And continuing:

At the moment of fracture, all of the stored energy is used to create the fracture surfaces.

Returning to the definition of surface free energy we see the obvious analog.

$$\underset{\text{(psi)}}{\text{bond strength}} \propto \underset{(\text{ergs/cm}^2)}{\gamma_{LS}} \qquad (8)$$

The new surfaces created essentially equal the cross-sectional area A, of the bonded joint configuration. For a given joint configuration that area is a constant, for all practical purposes.

It may readily be seen that the thickness dimension of the bondline is the energy storage primary variable.

But energy is stored by straining or displacing a thickness (or lateral or torsional) dimension to a new value, so that total displacement is the number value required for this derivation. Such displacements are extremely small in practical testing situations and are usually not measured. We can obtain empirical values from test data as will be seen later.

Using the linear relationship: (9)

Total displacement = (strain)(bondline thickness)

strain = change in dimension/unit dimension

and assuming that strain, k_o, is a constant for a given adhesive, substrate materials and specimen configuration, we can write:

$$\Delta d = (k_o)(d) \qquad (10)$$

For a general system:

$$\text{energy available for fracture surface} = A\int_{d_{min}}^{d_{max}} \sigma \, d(d)$$

where σ = stress
d = thickness dimension, apparent
A = joint area

Where the stress-strain relationship is linear over the full loading experience:

$$\text{energy} = \tfrac{1}{2}(\sigma_{max})(\Delta d)(A) \qquad (11)$$

combining equation (11) with (10) we obtain:

$$\text{energy} = (\tfrac{1}{2})(\text{ultimate bond strength})(k_o)(d)(A) \qquad (12)$$

where psi and inch dimensions are involved:

energy = (lb)(inch)

To convert these units to those familiar in the science of adhesion:

$$\frac{\text{energy}}{A} = \frac{1}{2}\,(\text{ultimate bond strength})(k_o)(d) \qquad (13)$$

lb/inch

1 lb/in = (1 lb/sq in)(1 inch)

$$1 \text{ lb/in} = (68948 \text{ dynes/cm}^2)(1 \text{ inch})\left(\frac{2.54 \text{ cm}}{\text{inch}}\right)$$

1 lb/in = 175127 dynes/cm or ergs/cm^2

Putting it all together gives us.

$$\gamma_{LS} = \left(\tfrac{1}{2}\right)(\text{ULT Bond Strength})(d)(175127)(k_o) \qquad (14)$$

(ergs/cm^2) (psi) (inch) $\frac{\text{ergs/cm}^2}{\text{lb/in}}$

We now have a good first approximation of the relationship between interfacial surface free energy and bond strength.

Going back to Thomas Young's relationship

$$\gamma_{SL} = \gamma_S - \gamma_L \cos\theta \qquad (6)$$

and substituting

$$\left(\tfrac{1}{2}\right)(UBS)(k_o)(d)(175127) = \gamma_S - \gamma_L \cos\theta \qquad (15)$$

$$UBS = \frac{\gamma_S - \gamma_L \cos\theta}{\left(\frac{1}{2}\right)(k_o)(d)(175127)} \qquad (16)$$

This equation provides the means to predict bond strength if we can non-destructively measure: d, bondline thickness
θ, contact angle
γ_S, substrate surface free energy

when:
1. γ_L is known
2. k_o is a known and constant
3. integral for stress-strain curve is known

Note that bond strength is inversely proportional to bondline thickness, which has been reported in the literature on numerous occasions.

In order to evaluate k_o and predict individual γ_S values from specimen test data we use equation (16) in this rearrangement:

$$\gamma_S - \gamma_L \cos\theta + (\quad)(UBS)(k_o)(d)(175127) \tag{17}$$

and for k_o

$$k_o = \frac{\gamma_S - \gamma_L \cos\theta}{(\quad)(UBS)(d)(175127)} \tag{18}$$

Using these values for a butt tensile specimen configuration:

γ_S = 200 ergs/cm^2 (estimated)

γ_L = 72.8 ergs/cm^2 (distilled water)

θ = 5°

cos θ = 0.996

UBS = 5000 psi

d = 0.006 inch

calculated k_o = 0.000047^6, $\approx$ 0.00005

apparent displacement = $(5X10^{-5})(0.006 \text{ inch}) = 0.3X10^{-6}$ inch

= 0.3 μinches

Using a γ_S value of 200 ergs/cm^2 and values from the data for butt tensile, core shear, and lap shear specimens listed, these apparent values of strain were obtained:

butt tensile	k_o	= 0.500 x 10^{-4}
core shear	k_o	= 0.833 x 10^{-4}
lap shear	k_o	= 4.000 x 10^{-4}

The exact calculations for γ_{LS} and γ_S using the experimental data are given in Tables I, II, and III in Appendix B. The summarized data in Tables V, VI, VII, and VIII shows the relationship between method of surface generation and substrate surface free energy, as prepared and after etch. These results have verified the analytical approach and provide the incentive to develop and refine it further.

TABLE V

SPECIMEN TYPE: BUTT TENSILE

CALCULATED SURFACE FREE ENERGIES

NOMINAL ROUGHNESS RMS inch	γ_{LS} AVERAGE ergs/cm^2	γ_S MAX (M) ergs/cm^2	γ_S MAX (E) ergs/cm^2	γ_S MIN (M) ergs/cm^2	γ_S MIN (E) ergs/cm^2	PREPARATION PROCESS
1	75	98	126	143	147	Paper lapped
5	102	115	161	168	174	Paper lapped
7	130	140	174	201	200	Paper lapped
10	107	116	150	179	179	Paper lapped
20	166	191	225	237	237	Turned
40	106	138	174	178	178	Paper sanded
80	126	140	179	197	198	Turned
110	141	153	203	211	214	Turned
150	151	159	201	215	222	Turned
FGLP	158	199	210	227	230	Grit Blast
FGHP	171	213	210	240	244	Grit Blast
CGLP	145	163	187	215	216	Grit Blast
CGHP	114	129	170	185	186	Grit Blast

TABLE VI

SPECIMEN TYPE: CORE SHEAR

CALCULATED SURFACE FREE ENERGIES

NOMINAL ROUGHNESS RMS inch	γ_{LS} AVERAGE ergs/cm^2	γ_S MAX (M) ergs/cm^2	γ_S MAX (E) ergs/cm^2	γ_S MIN (M) ergs/cm^2	γ_S MIN (E) ergs/cm^2	PREPARATION PROCESS
1	101	103	167	153	173	Paper lapped
5	72	92	142	142	144	Paper lapped
7	82	94	151	152	155	Paper lapped
10	104	127	168	174	176	Paper lapped
20	164	185	228	235	236	Paper sanded
40	169	187	235	240	242	Paper sanded
80	121	136	183	192	193	Paper sanded
110	82	103	143	150	154	Turned
150	97	118	154	167	169	Turned
FGLP	174	219	246	245	247	Grit Blast
FGHP	129	178	202	199	202	Grit Blast
CGLP	227	262	299	296	300	Grit Blast
CGHP	170	188	243	243	243	Grit Blast

TABLE VII

SPECIMEN TYPE: LAP SHEAR

CALCULATED SURFACE FREE ENERGIES

NOMINAL ROUGHNESS RMS inch	γ_{LS} AVERAGE ergs/cm^2	γ_S MAX (M) ergs/cm^2	γ_S MAX (E) ergs/cm^2	γ_S MIN (M) ergs/cm^2	γ_S MIN (E) ergs/cm^2	PREPARATION PROCESS
1	122	152	147	190	193	Paper lapped
5	88	92	109	147	157	Paper lapped
7	121	146	153	191	193	Paper lapped
10	95	129	109	164	166	Paper lapped
20	113	139	148	182	183	Paper sanded
40	141	160	208	211	213	Turned
80	213	246	254	279	284	Turned
110	163	192	233	228	236	Turned
150	111	125	116	178	180	Turned
FGLP	135	173	155	206	204	Grit Blast
FGHP	141	198	174	212	212	Grit Blast
CGLP	80	90	151	149	152	Grit Blast
CGHP	172	180	174	238	234	Grit Blast

TABLE VIII

GROUPED AVERAGES
OF
CALCULATED SURFACE FREE ENERGIES

METHOD OF SURFACE PREPARATION	PAPER LAPPED	PAPER SANDED	TURNED	GRIT BLAST
γ_S FOR MAXIMUM CONTACT ANGLE AS PREPARED	117.0	148.8	150.7	182.7
γ_S FOR MAXIMUM CONTACT ANGLE AFTER ETCH	146.4	179.1	184.4	201.8
γ_S FOR MINIMUM CONTACT ANGLE AS PREPARED	167.0	194.1	199.2	221.3
γ_S FOR MINIMUM CONTACT ANGLE AFTER ETCH	171.4	194.9	202.5	222.5
AVERAGE INTERFACE SURFACE FREE ENERGY γ_{LS}	99.9	123.4	130.8	151.3

VI. NDT TECHNIQUE FEASIBILITY STUDIES

The concept of a surface as a dynamic, rather than a static, energy relationship offers particular advantage when it comes to selection of nondestructive means for characterizing the surface. Quantitative nondestructive testing uses a well-characterized form of mechanical or electromagnetic energy which, as a result of encounter with a material, is changed in its character. The difference between input and output constitutes the unit of information pertaining to the condition of the material segment interrogated by the [illegible]. At Avco SD this "material-energy interaction", approach has been successfully applied to bulk materials. For the special case of surfaces and interfaces, this same approach is fully applicable. In fact, the increased energy state of the surface over that of the bulk performs some amazing changes in the character of incident energy, as attested by Snell's law of reflection and refraction and vibrational mode conversion and polarization, in magneto-optics and acoustics.

At best, the problem of selecting energy forms and test equipment to begin development of NDT techniques for surface characterization, is difficult. As a guide, the following rules were laid down:

1. Use a quantitatively characterizable energy form, mechanical or electromagnetic.

2. Select frequencies which provide interactions in the surface region rather than in the bulk of the material.

3. Match transmit and receive transducers to the physical measurement situation.

4. Avoid direct mechanical contact with the surface so as to maintain cleanliness.

5. Keep in mind the need for rapid scan and other factors necessary for economical, practical test procedures.

6. Aim toward utilization of computerized data processing techniques.

A. Exo - Electron Emission

1. Theoretical Basis

Numerous observers (References 11, 12, and 13) have measured the emission of electrons from free surfaces (usually solid) as a result of stimulation by some sort of energy input to the surface. The forms of energy have included electromagnetic, mechanical and acoustical, chemical, thermal, and charged particle impingement. The escape of electrons carries away energy from the bulk in the form of a heat of evaporation, usually called "work function," $\emptyset$. Uhlig (Reference 14) in his discussions on corrosion processes in metals, notes that low work function favors electron emission, one factor which encourages the formation of chemisorbed films. Extension of this to adhesive bonding would suggest that a surface producing a high electron output would favor wetting and spreading, and conversely, a low output would favor non-wetting.

The chemisorption of nonmetallic entities on a clean metallic surface is discussed by Langmuir (Reference 15), who has shown that the change in work function takes the form:

$$\Delta\phi \quad 4\pi n\mu$$

where: $\Delta\phi$ - change in work function
n - number of absorbed atoms
μ - dipole moment of negative charge to metal surface

The surface reaches its greatest change in work function when the maximum number of atoms are absorbed, which corresponds to a continuous monolayer. Zisman (Reference 16) and many others have demonstrated the ability of a polymeric continuous molecular monolayer to entirely change surface character from that of a metal (high surface free energy) to that of the bulk polymer (low surface free energy).

The above line of reasoning suggests the following:

a. A surface which, when appropriately stimulated, produces a high level of electron emission...

1) will favor wetting and spreading

2) will not be contaminated with an organic monolayer or any significant portion thereof.

3) may be oxidized by means of a controlled process, but not adversely modified by extended exposure to the ambient environment.

b. A surface which, when appropriately stimulated, produces a low level of electron emission...

1) will be contaminated with respect to the special needs of adhesive bonding.

2) will not favor wetting.

If these relationships can be quantized to characterize a surface segment in terms of its readiness for application of adhesive, perhaps to indicate the cause of non-acceptance, that is if there is a close correlation between work function and surface free energy, than a powerful nondestructive test method would be at hand.

2. Experimental Basis

Work conducted by Dr. George Martin and associates at North American Rockwell (Reference 17), in the interest of nondestructively detecting fatigue damage, provided an excellent starting point for developing a means to detect exo-electrons suitable to surface characterization in adhesive bonding.

Martin describes the practical design considerations necessary to produce an electron energy spectrometer. The detector designed and fabricated at N-R consisted of a cylindrical electrostatic mirror and a Channeltron electron multiplier, Figure 8. The analyzer electronics and voltage requirements are also diagrammed. The electron energy spectrometer offers the most versatile means of producing quantitative electron-output-count data by allowing selection of the electron energy parameter. It may well be found that certain narrow bands of electron energy are specific to the surface character which controls wetting, spreading, and adhesion.

Following the discussions of Zashkvara et al (Reference 18) Sar-el (Reference 19), and Hafner et al. (Reference 20), Martin describes the design functions for the cylindrical electrostatic mirror, as modified to embody guard ring potentials to provide a more uniform radial gradient field. These relationships have been organized for clarity as follows:

Zashkvara and Sar-el explored the focusing characteristics of the cylindrical electrostatic mirror and showed that when the mean path of an electron entering the gradient field inclines at an angle θ_o of 42° 18.5' from the cylindrical axis, focal length is a minimum, and axial focusing is second order, which allows for fine selection of electron energy by varying field potential. Under such conditions and assuming a point source, base resolution, R^o, becomes simply

$$\frac{\Delta E}{E_o} = R^o = 21T^3$$

where:
- ΔE = energy dispersion around E_o
- E_o = base-line energy to be detected
- T = percent solid angle transmission, according to the relationship $T = (\sin \theta_o)\alpha$ where $\sin 42^\circ 18.5 = 0.673$

The dispersion angle, α, is controlled by inner cylinder slot and axial aperature dimensions, Figure 9 and is kept to a practical minimum to minimize detection bandwidth. Refocusing occurs at distance L_o, for an inner cylinder radius of r_1:

$$L_o = 6.12\ r_1$$

Electron maximum trajectory, r_m, is

$$r_m = 1.8\ r_1$$

Electron particle kinetic energy, E_o, is

$$E_o = \frac{1.3\ e\ V}{\ln\left(\frac{r_2}{r_1}\right)}$$

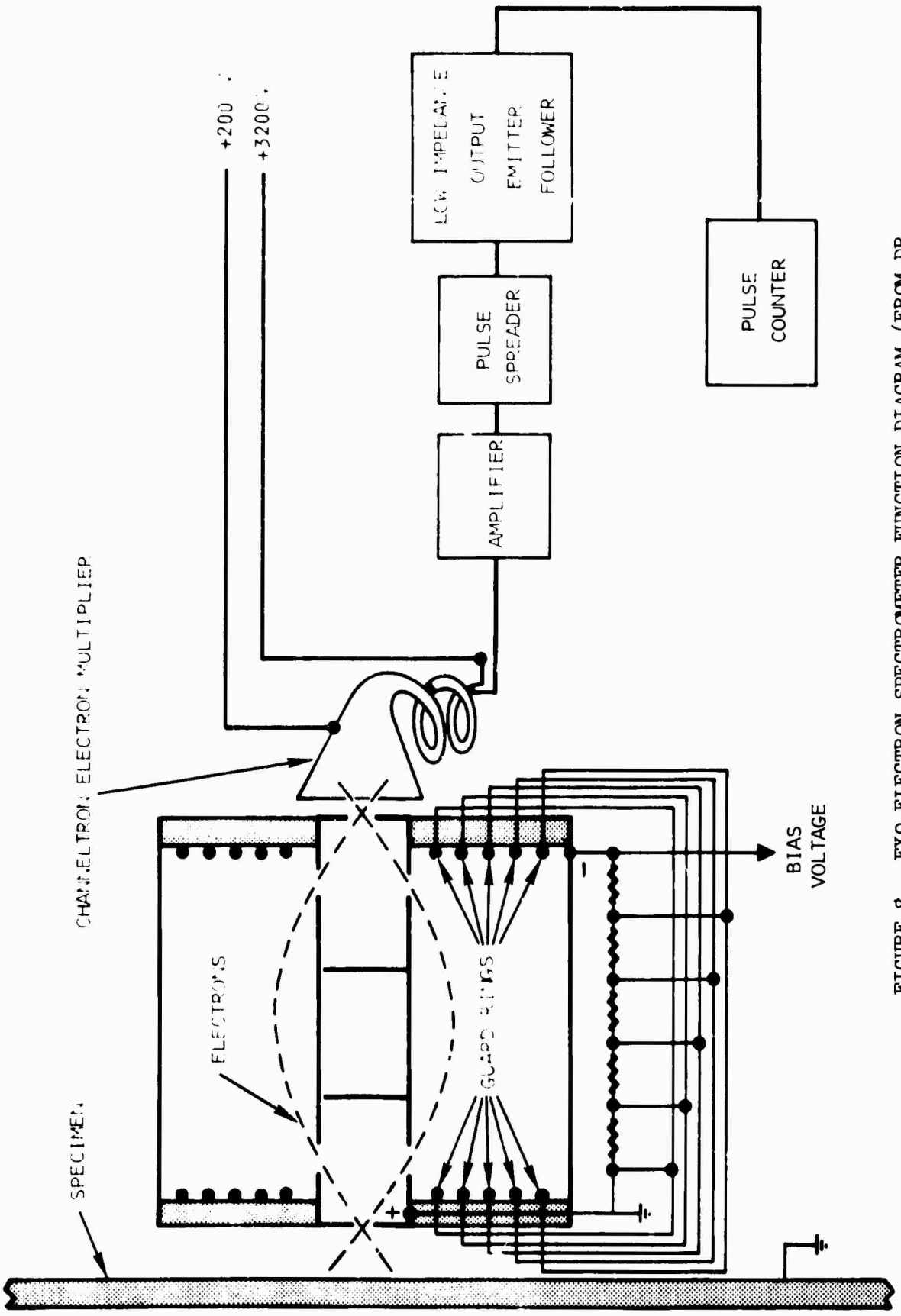

FIGURE 8. EXO-ELECTRON SPECTROMETER FUNCTION DIAGRAM (FROM DR. G. MARTIN, NORTH AMERICAN-ROCKWELL)

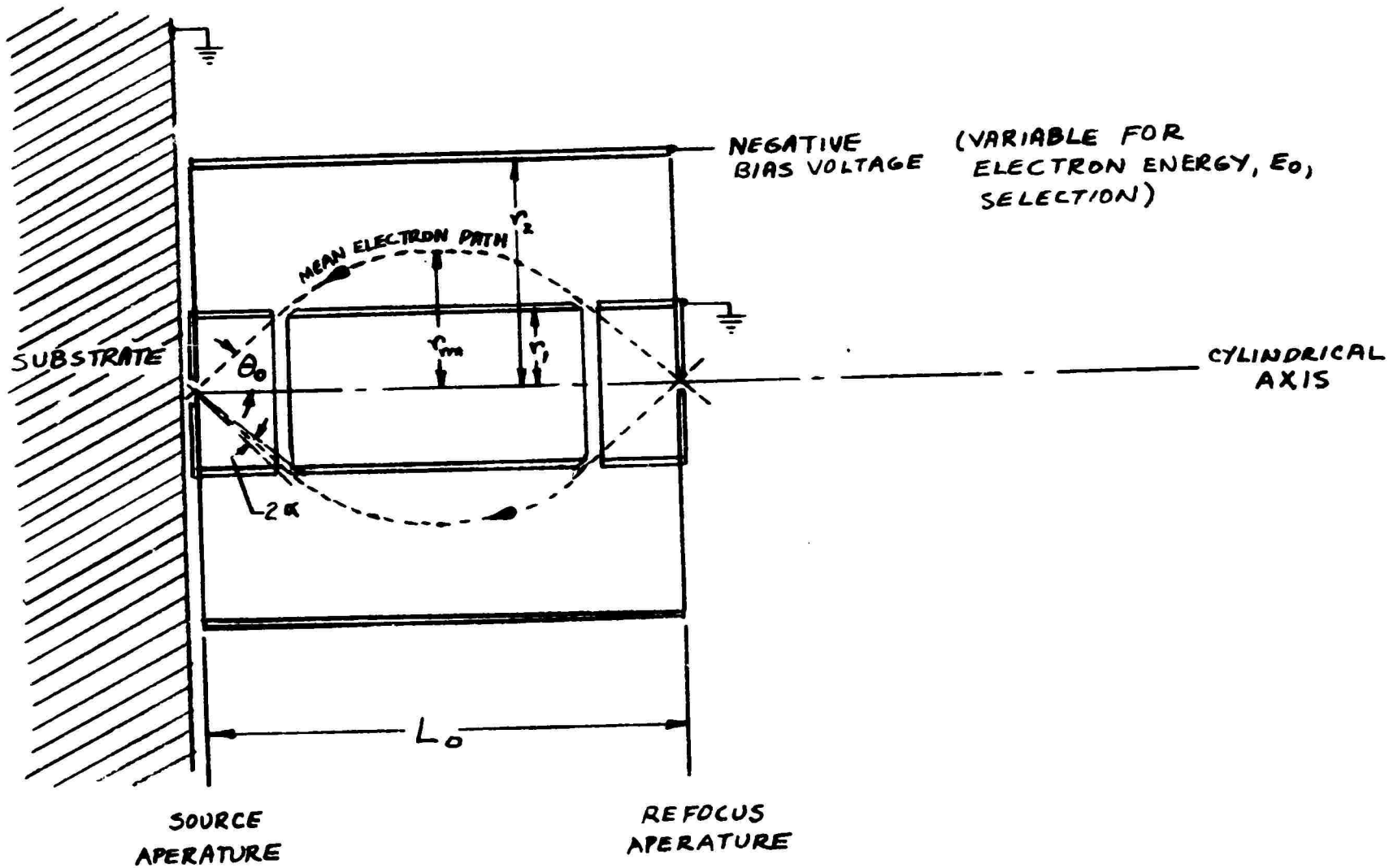

FIGURE 9. PRIMARY DESIGN DIMENSIONS FOR THE CYLINDRICAL ELECTRO-STATIC MIRROR

where: e = particle charge, electron-volts

V = potential between inner and outer cylinder, volts

r_2 = radius of outer cylinder

The design is then accomplished by selecting entrance and exit aperature diameter, slot width, and inner cylinder diameter. Geometrical considerations to provide θ_0 = 42° 18.5' and suitable 2 in turn set physical dimensions in terms of L_0. Knowing r_m, a convenient value for r_2 may be selected.

The appropriate range of applied high-voltage, V, sets the range of particle base-line voltage E_0, that may be counted. From this and α, resolution and percent transmission may be calculated. We would anticipate a series of repetitive calculations through these relationships to arrive at a design well-balanced for our particular needs.

Martin and associates recognized the need for guard rings at the ends of the cylindrical field to maintain radial gradients in the region of electron orbits.

Using the potential between concentric, infinite cylinders:

$$\varphi_2 - \varphi_1 = A \ln\left(\frac{r_2}{r_1}\right)$$

where: φ_2 = potential of outer cylinder, volts

φ_1 = potential of inner cylinder, volts

r_2 = radius of outer cylinder

r_1 = radius of inner cylinder

A = proportionality constant

For a given value of applied, V, which is to be divided into convenient equal voltage steps by n guard rings, then each voltage step is:

$$V_s = \frac{V}{(n+1)}$$

For a given basic cylinder design:

$$\ln\left(\frac{r_2}{r_1}\right) = \frac{V}{A} = \text{parametric constant}$$

or for a given step:

$$\ln\left(\frac{r_m}{r_1}\right) = \frac{m}{(n+1)} \cdot \frac{V}{A}$$

where: m is the integral number of steps counting from the inner cylinder giving:

$$r_m = r_1 \exp\left[\frac{m}{n+1} \cdot \frac{V}{A}\right]$$

3.Feasibility Analysis

High vacuum ($P < 10^{-7}$ torr) environments pose a significant drawback to practical application of the exo-electron emission method for non-destructive testing on other than a laboratory basis. Part of the problem lies in the fact that organic contaminants, particularly those of low molecular weight, will outgas during pull-down, greatly increasing the time necessary to reach desired vacuum levels. At the same time, however, evaporation of the contaminate and other adsorbed gases changes the actual character of the surface being characterized.

Recent measurements have been conducted at 1 atm in air using field-effect transitors, flat-plate collectors and electron acceleration schemes in order to satisfy practical nondestructive testing needs (Reference 21). While solving one problem, it was apparent that electron emission, electron transport and gas ionization considerations created a new set of variables and altered the basic emission theory. Current work by others is being closely followed, with the view toward initiating feasibility studies for surface characterization in the future based on the most promising techniques developed.

B. Ultrasonic Gas-Phase Transmission

1. Theoretical Basis

Following the concept of deBroglies' "pilot waves" associated with total-internal light reflection, the analogous "pilot waves" in ultrasonic acoustics serve as the basis for the "ultrasonic gas-phase transmission method." It is known in acoustics that a solid-gas interface (surface) presents a huge acoustic impedance (ρV) mismatch, resulting in total internal reflection of the acoustic wave (or pulse) in the solid. This serves as the basis for pulse-echo measurements in nondestructive testing. The "total" reflection is for all practical purposes total energy return, yet a small but significant amount of the acoustic energy is actually transmitted through the surface into the gas phase as pilot waves or wave fronts. That amount, and its frequency/phase/amplitude character, must depend upon the energy state (excitement) of the surface. Thus, by measuring the gas-phase transmitted acoustic energy, information concerning the state of the surface will be obtained.

2. Experimental Basis

The equipment and system used in the feasibility study are presented in Figure 10. A holding fixture was prepared for a fixed transmitting transducer (Automation Industries Type 57A3641, 2" dia, 1.0 MHz) and an adjustable receiving transducer (Budd Co. Model 4CWC, 1/2" dia, 1.0 MHz). The fixture and transmitter were placed in a tub of water such that the water surface reached approximately half way up a core shear specimen. The water bath provided consistent coupling between transmitter and specimen so that test reproducibility and effects of specimen rotation could be studied. The specimen rested on a cork pad over an 11/16" diameter aperature. Specimen surface to receiver distance was 7/16 inch. Photographs of the analyzer traces were obtained for comparison and frequency data reduction, Figure 11.

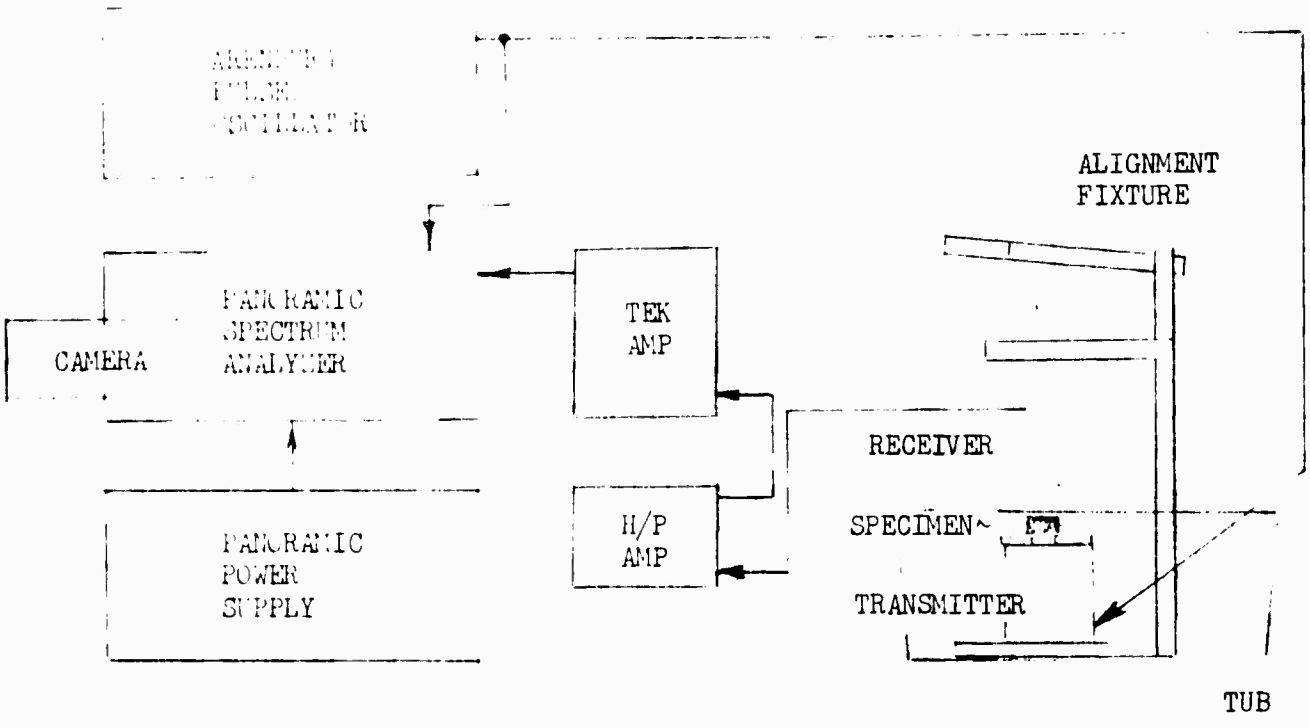

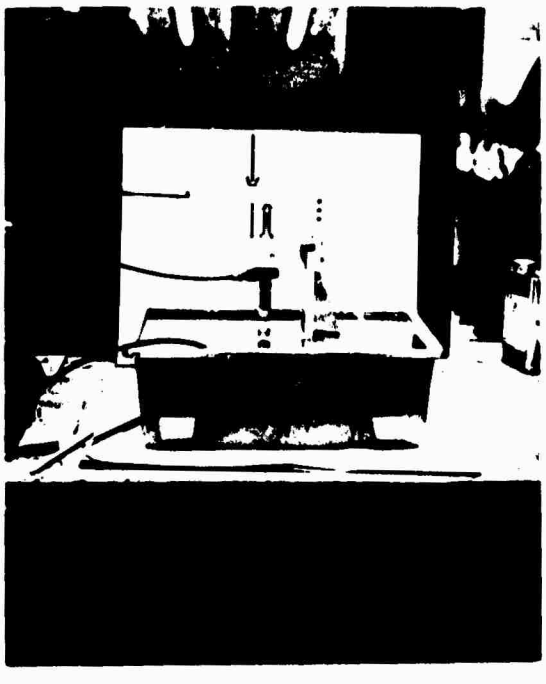

FIGURE 10. GAS-PHASE ULTRASONIC TRANSMISSION METHOD FEASIBILITY STUDY EQUIPMENT AND SYSTEM

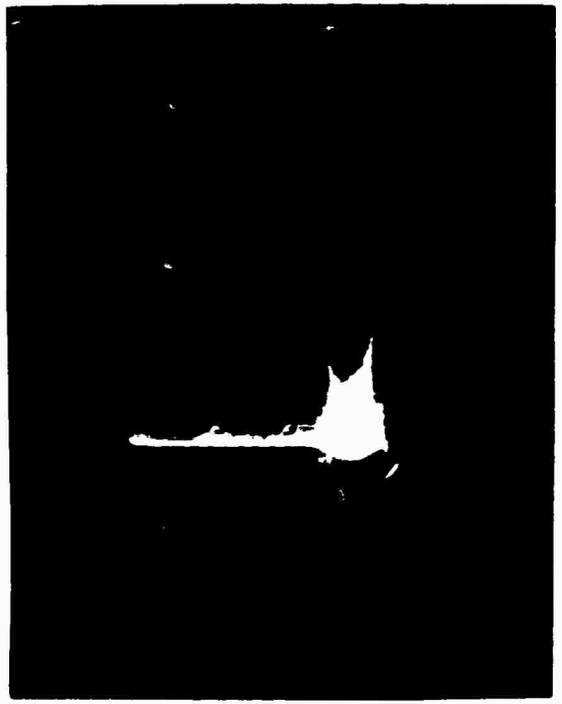

1.39 1.30 1.21 MHz

.018 MHz/Div.

(a) No specimen inserted. Signal emitted from surface of water.

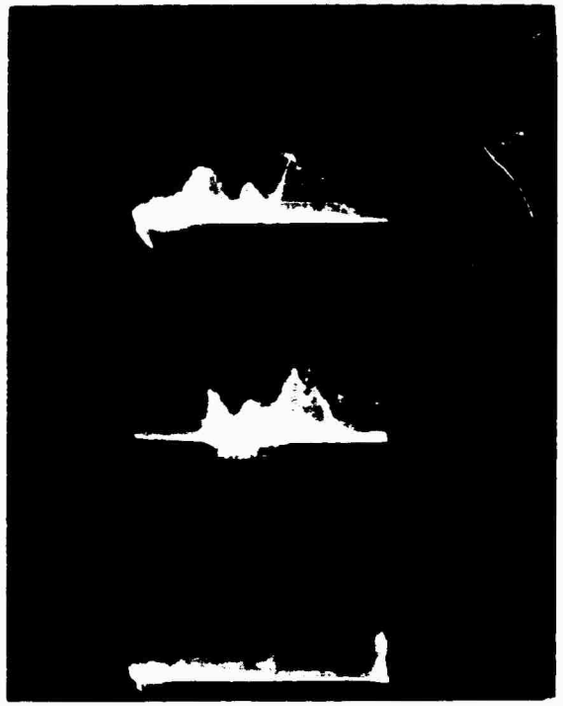

1.39 1.30 1.21 MHz

.018 MHz/Div.

(b) Core shear specimen CS-5 inserted into acoustic field. Signal emitted from clean surface.

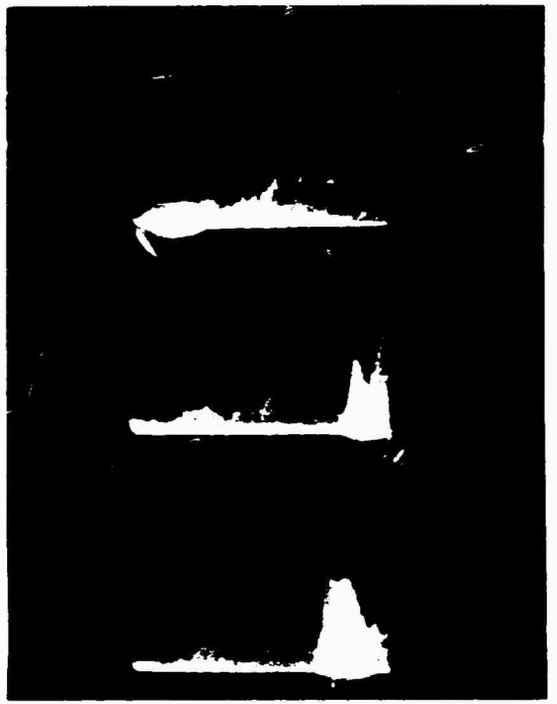

1.39 1.30 1.21 MHz

.018 MHz/Div.

(c) Core shear specimen 110 CS-3B, after destructive testing, inserted into acoustic field. Signal emitted from surface covered with thin fracture layer of adhesive.

FIGURE 11. FREQUENCY-DOMAIN RESPONSES FOR 6061-T6 ALUMINUM CORE SHEAR SPECIMENS

3. Feasibility Analysis

Results have shown that characteristic acoustic waves are emitted by substrate surfaces and that these may be readily detected and analyzed. Frequency domain analysis has revealed that new frequencies (1.275, 1.325, 1.350 MHz) arise as a result of specimen (core shear) insertion into the acoustic field. Additional frequencies, especially the higher harmonics, arise at low amplitudes corresponding to variations in surface energetic character. Test conditions were sufficiently stable to provide reproducible response signatures. This work encourages development of techniques directed toward isolating the surface-energy-characteristic frequencies for correlations with calculated surface free energy values.

C. Electric Field Reflectometry

1. Theoretical Basis

Just as we characterize surface-reflected light in terms of its intensity, color (frequency) polarization plane angle, etc. to describe the character of a surface (i.e. mirror, paint-job, velvet, frost), the reflections of electromagnetic energy at other frequencies will carry information related to surface energetics. By using single-frequency (coherent) energy forms, proper characterizations of incident and reflected energy may be readily accomplished. Selection of the frequency provides the means for isolating individual surface material-energy interaction relationships specifically related to adhesive bonding.

In electric field reflectometry a source of oscillating electromagnetic energy "illuminates" the substrate surface and is reflected by the surface. A small portion of the reflected energy is modified during this encounter according to the surface energy character and angle of incidence.

Voltage measurement in the electric field vector (as opposed to current measurement in the magnetic field vector) provides the energy-characterizing signal, which may be electrically processed to extract the surface-related changes.

Low frequencies, on the order of a few kilohertz, provide the near-field interactions associated with plate capacitors, approximately electrostatic conditions and attendant formulas. Microwave frequencies, in the low gigahertz region, provide interactions associated with travelling waves and standing waves in free space.

The wavelengths associated with these frequencies are orders of magnitude greater than light wavelengths, such that a rough surface does not create the "optical illusion" diffraction effects usually perceived by the casual observer in looking at such surfaces. The specific means of separating the large first order interactions from the small second and third-order interactions of interest is the primary goal in both the early feasibility studies and later technique developments.

2. Experimental Basis

By way of a starting point with existing equipment, electric field reflectometric measurements were conducted at 9.8 GHz (microwaves) and 1 KHz (low frequency capacitance) Figures 12 and 13. The open-ended microwave system provided a mixed voltage signal related to both phase and amplitude of the reflected standing wave. Local position of the substrate surface had a large effect on the phase relationship and a smaller effect on amplitude. Surface influences were found to be so buried in the signal as to be unobservable. In the simple, bulk-signal system of Figure 12, there was no provision for separating signal components. A second technique, the "magic tee" microwave balancing bridge, Figure 14, was investigated. Here the adjustable short balanced or "nulled out" the bulk standing wave load from the substrate, so that small deviations associated with surface character could be separated from the core shear specimen insertion signal. On the magic tee technique also, the detected voltage signal mixes phase and amplitude information. The ability to separate phase shift and amplitude in true impedance-bridge balance, although not attempted in these studies, usually aids the observation of second and third-order interactions.

In the low frequency reflectometric studies the separate contributions of phase and amplitude were read as values of probe capacitance and relative dissipation factor from the automatic capacitance bridge. A 1/4 inch square, "polarized" probe having a nominal depth of field of .032" was positioned near, but not touching, the substrate surface. Data indicated that a surface-response was being obtained, although reproducibility was marginal. A 1/2 inch diameter, "unpolarized" probe having a nominal depth of field of 0.100" was brought down on a 0.00025 inch thick film of Mylar placed on the substrate surface. The values of capacitance obtained in these studies was highly reproducible, indicating the following relationship to variation in surface energetics.

Substrate	C_P picofarad	γ_S ergs/cm^2	Roughness CLA μinch
Probe empty	0.28	--	--
CS-5	1.53	92	4.1
CS-20	1.48	185	23.0
CS-CGLP	1.73	262	25.0

3. Feasibility Analysis

To the extent that investigations were conducted with microwave electric field reflectometry, no positive results were obtained. Suitable specimen fixturing, a balanced bridge measuring system, and a goniometer arrangement for brewster's angle studies would be necessary for continued technique evaluation.

The low-frequency electric field reflectometric measurements did provide initial positive results. Although correspondance to surface energy state was shown, a direct correlation with surface free energy was not obtained. It was concluded that more than one variable contributed to the capacitance values, and that further study was necessary to separate them.

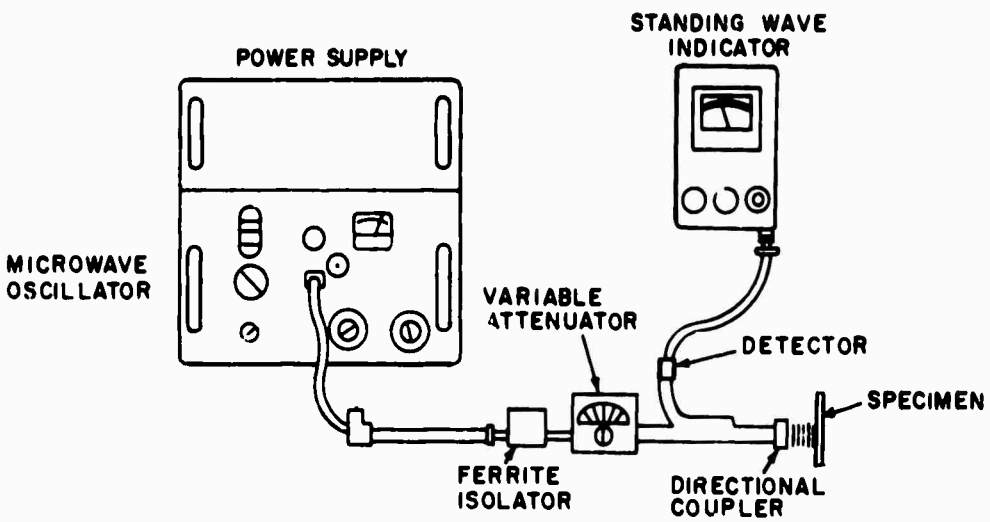

FIGURE 12. MICROWAVE REFLECTOMETRY - 9.8 GHZ

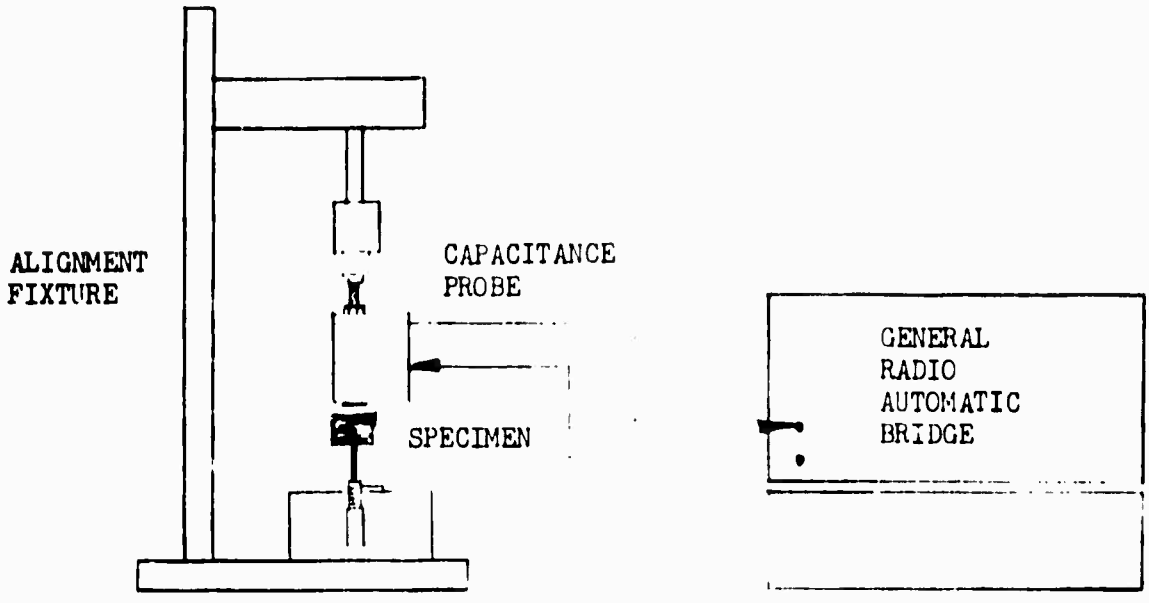

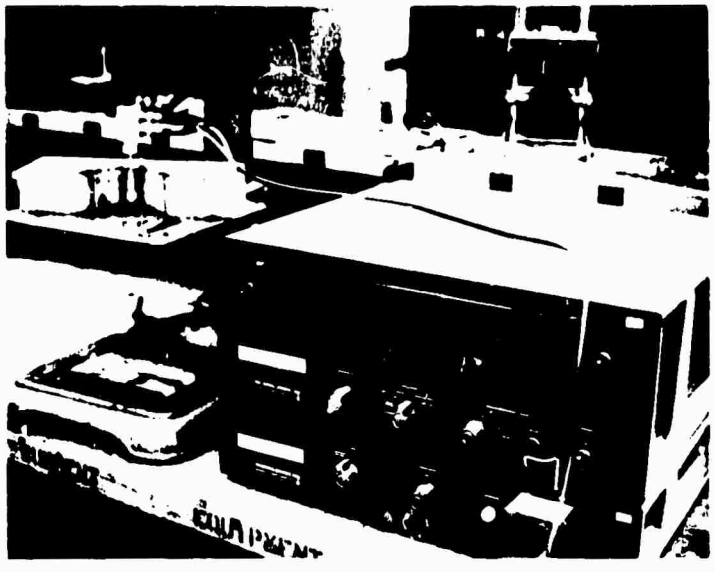

FIGURE 13. ELECTRIC FIELD REFLECTOMETRY METHOD FEASIBILITY STUDY EQUIPMENT AND SYSTEM (1.0 KHZ)

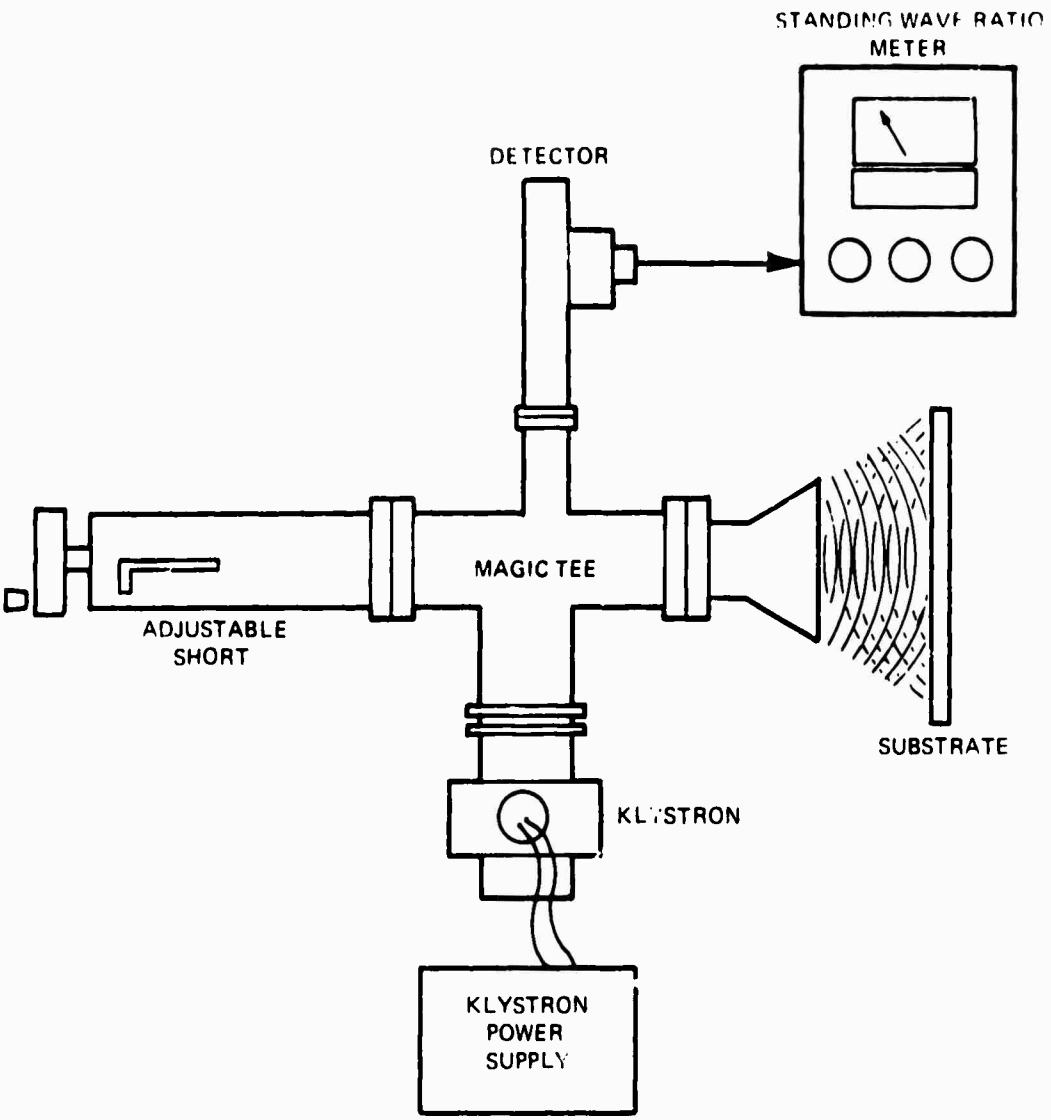

FIGURE 14. MAGIC TEE MICROWAVE BRIDGE TECHNIQUE - 9.8 GHZ

The design and fabrication of a capacitance probe especially suited for these studies is recommended.

D. Light Reflectance

1. Theoretical Basis

Although much scientific experience in the past has demonstrated little relationship between light reflection from a surface and adhesive-bond-influencing surface energetics, it is known in adhesive bonding that by viewing a metallic surface "from the proper angle near a light source," an experienced observer can derive some information as to relative cleanliness. Various instruments are available which provide distinct values for light reflectance, but quantitative values of surface energy, such as the values of substrate surface free energy (γ_S) calculated under the subject program, have not been available. Ignoring the possible diffraction influences associated with rough surfaces, for the moment, and relying on adhesive bonding experience, it was apparent that light reflectance could feasibly correlate with as-prepared surface free energy. Conditions of test were dictated by available test facilities rather than from theoretical considerations.

2. Experimental Basis

The entire group of remaining core shear specimens, which included 13 different prepared surfaces, was evaluated for white light reflectance at an incident angle of 45° and a detector angle of 45°. Light reflection, diffusion, and diffraction contributed to the single relative reflectance value. The diffraction effects due to the "lay" of the surface were averaged by taking 8 readings at 45° polar angle intervals. A Photovolt Photoelectric Glossmeter Model 610, using a search unit Type 660-M, provided the relative reflectance data, Figure 15. The 660-M search unit, recommended for metallic surfaces, measures specular reflection from the surface. Light from the bulb is collimated and brought at a 45° incident angle to the test surface. Reflected light at 45° is focused through an aperature for clean-up and presented to the self-generating, barrier type photocell. A compensating photocell observes the light source intensity. The measurement unit is a voltage wheatstone bridge with controls which allow zero suppression and range expansion. A sensitive galvanometer indicates bridge unbalance on a 0-100 scale.

A preliminary correlation between incandescent light reflectance and substrate surface free energy is shown in Figure 16. Analysis of the correlation indicates there are two separate and parallel relationships, suggesting that a distinct parameter having two discreet values has affected the light reflectance values. This parameter has not yet been identified.

3. Feasibility Analysis

The feasibility of using light energy to nondestructively measure aluminum substrate surface free energy has been proved. Such results encourage further work to refine the relationship and isolate influencing parameters for aluminum and other substrates. Test technique variables needing to be studied include angle of incidence, monochromatic, non-coherent sources;

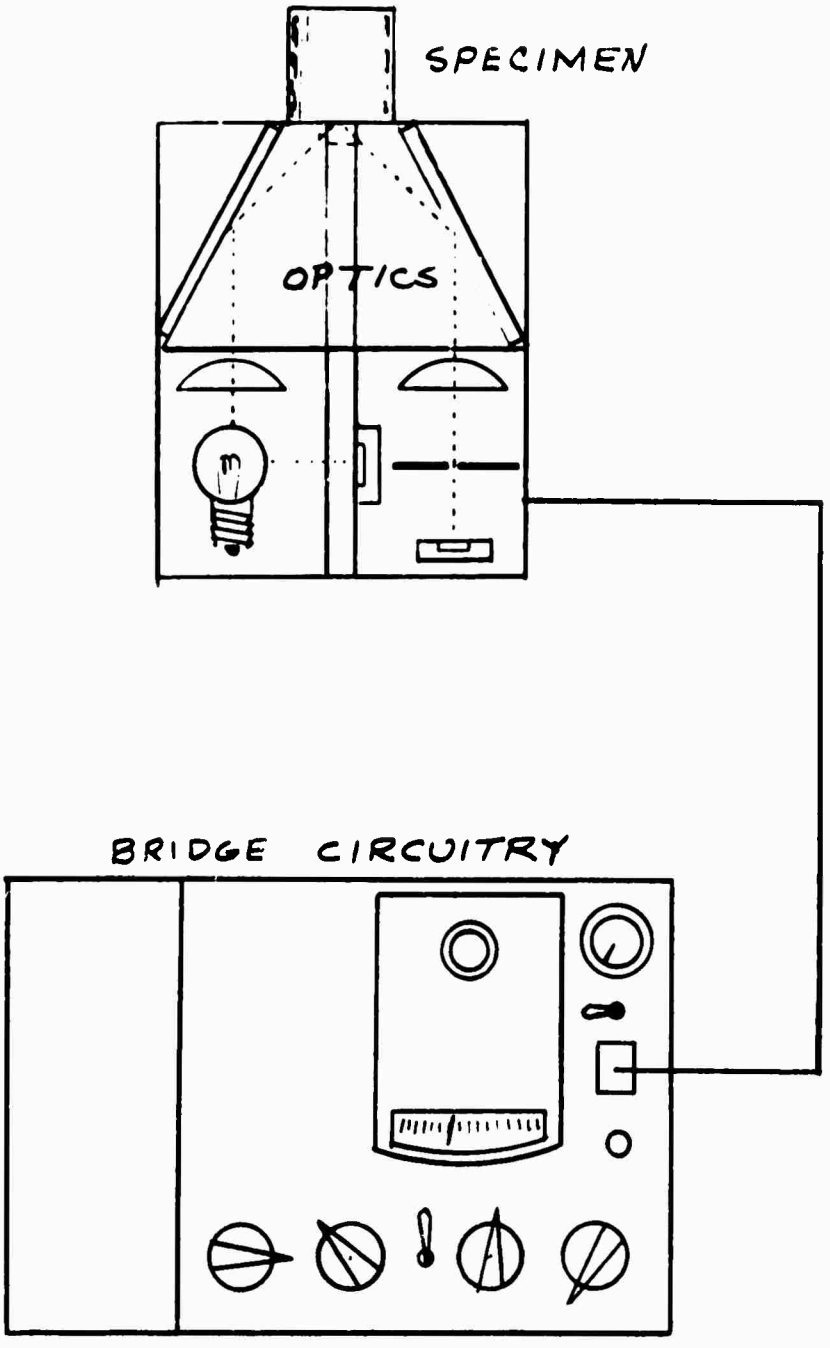

FIGURE 15. LIGHT REFLECTANCE TECHNIQUE USING A PHOTOVOLT GLOSSMETER

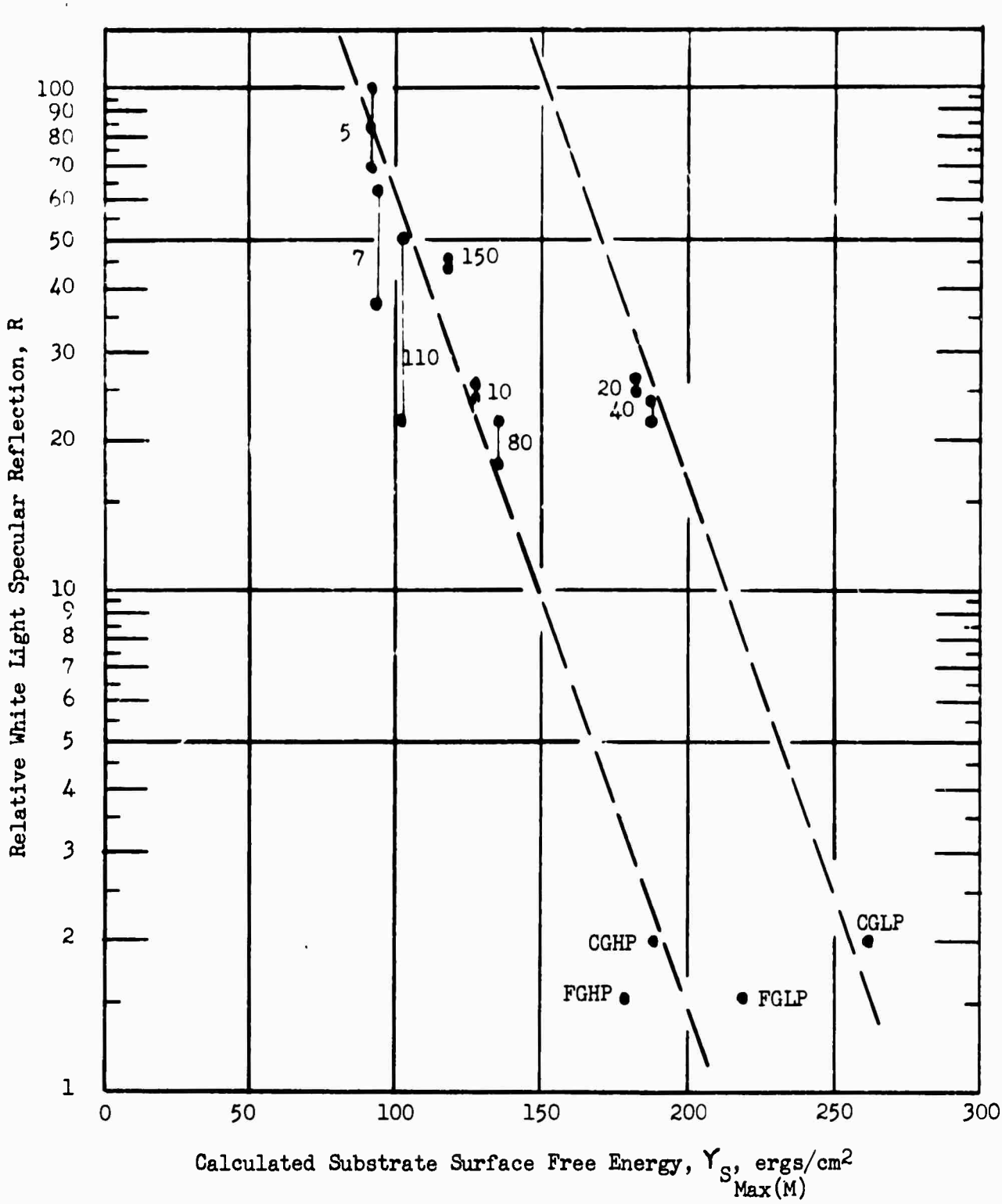

FIGURE 16. SURFACE FREE ENERGY VERSUS WHITE LIGHT REFLECTANCE CORRELATION

and methods of signal generation and processing.

These results, perhaps most importantly, support the validity of the Zurbrick equation for predicting bond adhesive strength.

REFERENCES

1. Lockyer, G. E. and E. A. Proudfoot, "Development of Nondestructive Tests for the Evaluation of Bonded Materials," Technical Report No. AVATD-0123-69-CR (Avco) for Naval Air Engineering Center, Warminster, Pa. (July 1969).

2. Marian, J. E., "Surface Texture in Relation to Adhesive Bonding," Symposium on Properties of Surfaces, ASTM Materials Science Series -4, ASTM STP-340, American Society for Testing and Materials (1963) pp 142-144.

3. Hughes, E. J., and Rutherford, J. L., "Study of Micromechanical Properties of Adhesive Bonded Joints," Technical Report No. 3744, General Precision Systems, Inc., Little Falls, N. J. (August 1968) (AD 673745).

4. "Sharp Receives Adhesive Age Award at Houston D-14 Meeting", Adhesives Age Vol 11, No 5, (May 1968), pp 42-44.

5. McClung, R. W., Oliver, R. B., and Rowand, R. R., "Section IV Technical Problem Areas" Nondestructive Testing, Publication NMAB-252, National Materials Advisory Board, NRC (June 1969)

6. Zisman, W. A., "Constitutional Effects on Adhesion and Abhesion," Adhesion and Cohesion, edited by P. Weiss, Elsevier Publishing Co., Amsterdam (1962), pp. 176-208.

7. Marian, I. E., "Surface Texture in Relation to Adhesive Bonding," Symposium on Properties of Surfaces, ASTM Materials Science Series -4, ASTM STP-340, American Society for Testing and Materials (1963).

8. Zurbrick, John R., "Development of Nondestructive Tests for Predicting Elastic Properties and Component Volume Fractions in Reinforced Plastic Composite Materials, Technical Report AFML-TR-68-233, Air Force Materials Laboratory, Wright-Patterson Air Force Base, Ohio (February 1969).

9. Pimentel, G. C., and R. D. Spratley, Chemical Bonding Clarified Through Quantum Mechanics, Holden-Day, Inc., San Francisco (1969).

10. Cagle, C. V., Adhesive Bonding, (McGraw-Hill Book Co., (1968).

11. Ramsey, J. A., "The Emission of Electrons from Aluminum, Abraded in Atmospheres of Air, Oxygen, Nitrogen, and Water Vapour," Surface Science, Vol. 8, (1967) pg 313.

12. Kortov, V. S., and Mints, R. I., "Exo-electronic Emission as a Method of Studying the Deformed Surface of Metals," Physics of Metals and Metallography, Vol. 19, (1965) pg 72.

13. Langenecker, J. A. M., and Ray, D. B., "Exo-Electron Emission Due to Ultrasonic Irradiation," Jour. of Applied Physics, Vol. 45 (1974) pps 2580-2588.

14. Uhlig, H. H., Ann. New York Academy of Science, Vol 58 (1954) p 843.

15. Langmuir, I., Jour. of American Chemical Society., Vol. 38 (1916) p 2221.

16. Zisman, W. A., "Constitutional Effects on Adhesion and Abhesion," Adhesion and Cohesion, edited by P. Weiss, Elsevier Publishing Co., Amsterdam (1962) pps 176-208.

17. Martin, G., The Early Detection of Fatigue Damage, First Semiannual Report, NA-69-173, 1968 July 1 - 1969 February 28, Advanced Research Project Agency (ARPA Order No. 1244).

18. Zashkvara, V. V., Korsunskii, M.I., and Dosmachev, O. S., "Focussing Properties of an Electrostatic Mirror with a Cylindrical Field," trans. from Zhurnal Tekhnicheskoi Fiziki, Vol 36, No. 1 (Jan. 1966) pp 132-138; in Soviet Physics - Technical Physics, Vol II, No. 1 (July 1966) pp 96-99.

19. Sar-el, H. Z., "Cylindrical Capacitor as an Analyzer I. Nonrelativistic Part, "The Review of Scientific Instruments, Vol 38, No. 9 (Sept. 1967) pp 1214 - 1216.

20. Hafner, H., Arol-Simpson, J., and Kuyatt, C. E., "Comparison of the Spherical Deflector and the Cylindrical Mirror Analyzers," The Review of Scientific Instruments, Vol 39, No. 1 (Jan. 1968) pp 33-35.

21. Hoenig, S. A., "Application of Exo-Electron Emission Techniques to the Measurement of Fatigue Damage and Cold Work," ARPA Program on Nondestructive Testing.

APPENDIX I

SPECIMEN DATA

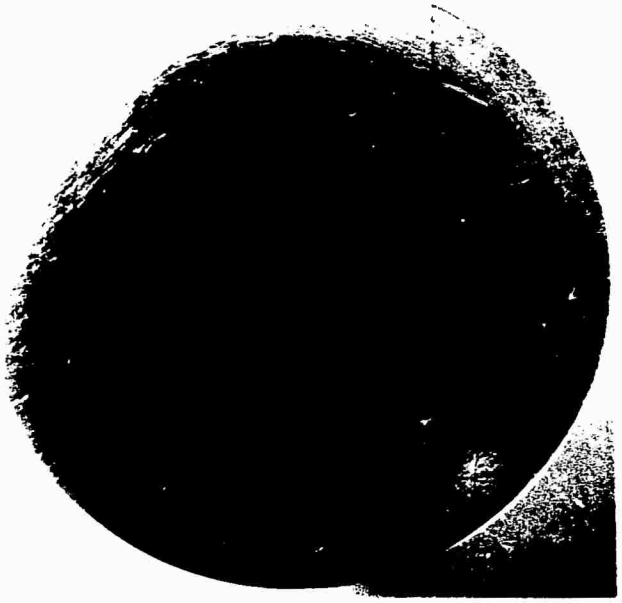

Photo Mag. = 4.4X

CLA = 1.2
RMS = 1.3

1 BT-3A (M) Before Etch

θ MAX	71.5
θ MIN	21.5
$\Delta\theta$	50.0

Photo Mag. = 4.5X

CLA = 10.0
RMS = 11.1

1 BT-3A (E) After Etch

θ MAX	45.5
θ MIN	9.0
$\Delta\theta$	36.5

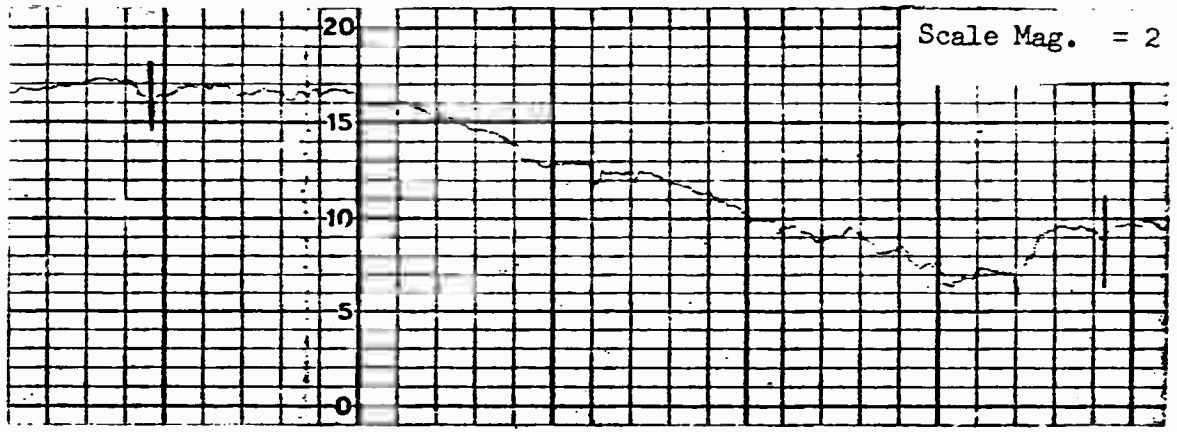

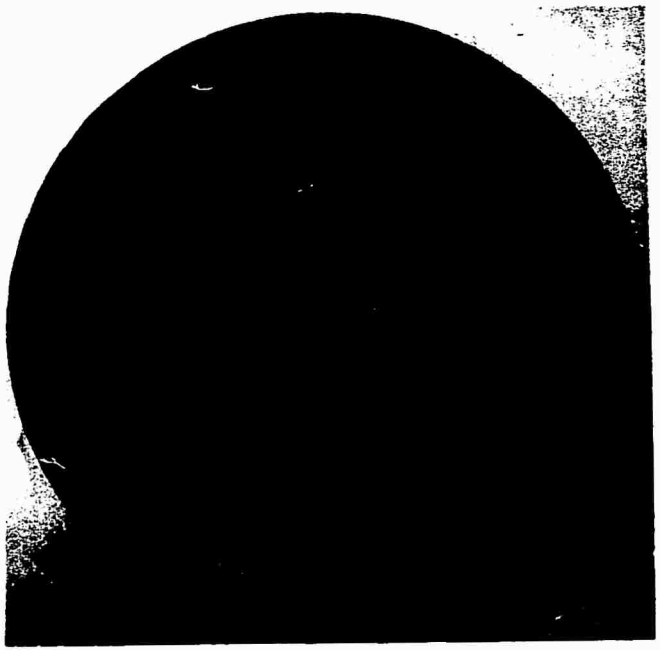

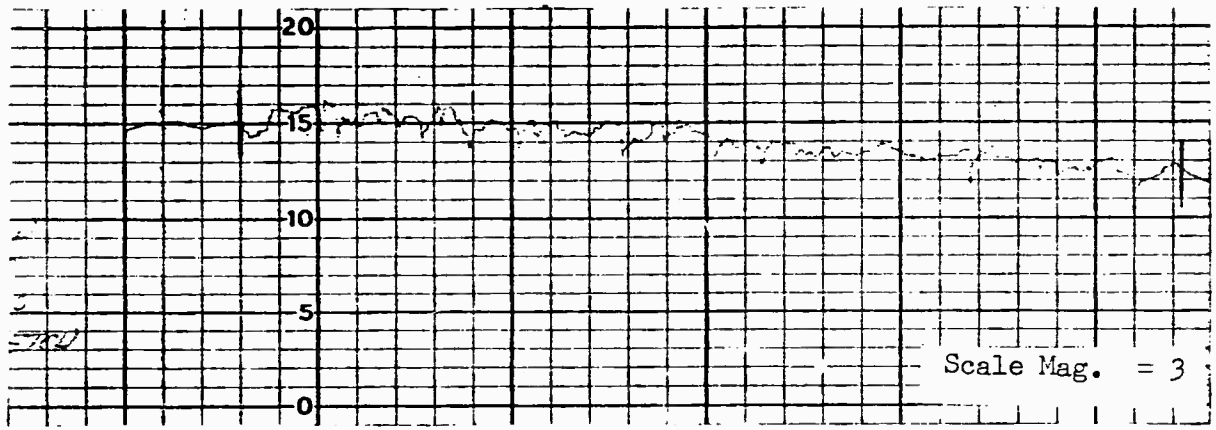

Photo Mag. = 4.4X

CLA = 6.0
RMS = 6.6

5BT-3A (M) Before Etch

θ MAX = 79.5
θ MIN = 25.0
Δθ 54.5

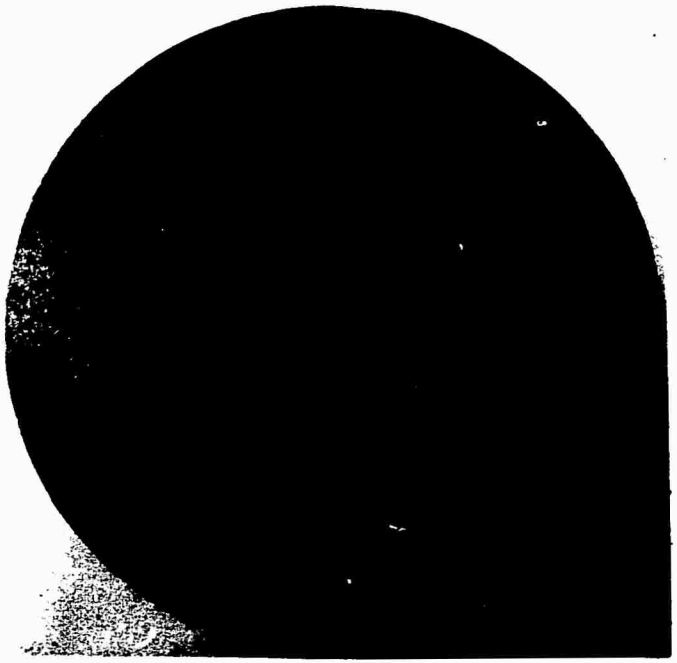

Photo Mag. = 4.5X

CLA = 14.0
RMS = 15.5

5BT-3A (E) After Etch

θ MAX = 35.5
θ MIN = 9.5
Δθ 26.0

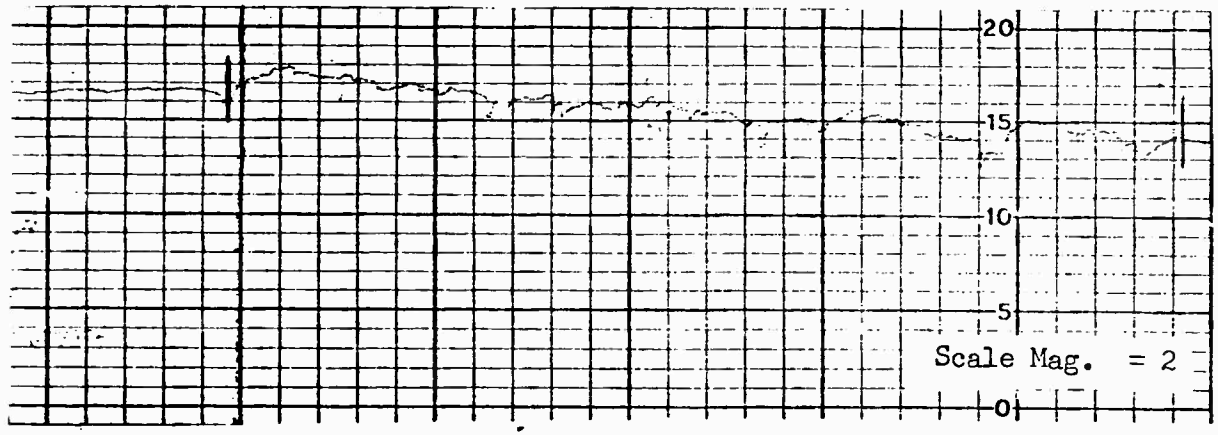

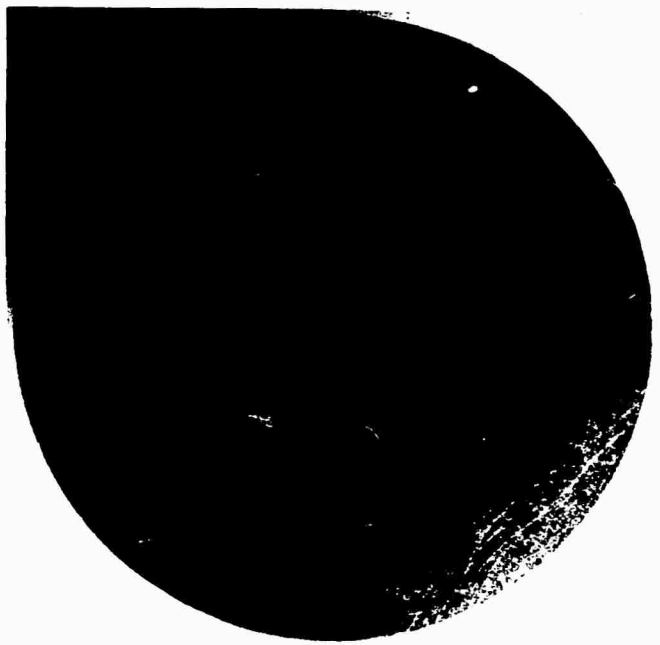

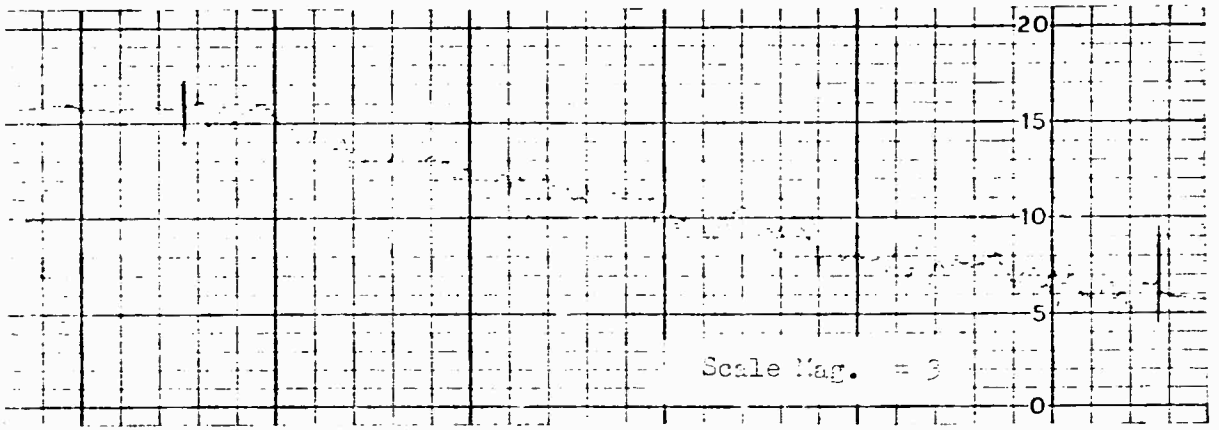

Photo Mag. = 4.4X

CLA = 9.2
RMS = 10.2

7 BT-3A (M) Before Etch

ϑ MAX	82.5
ϑ MIN	12.5
$\Delta\vartheta$	70.0

Photo Mag. = 4.5X

CLA = 15.0
RMS = 16.7

7 BT-3A (E) After Etch

ϑ MAX	52.5
ϑ MIN	15.5
$\Delta\vartheta$	37.0

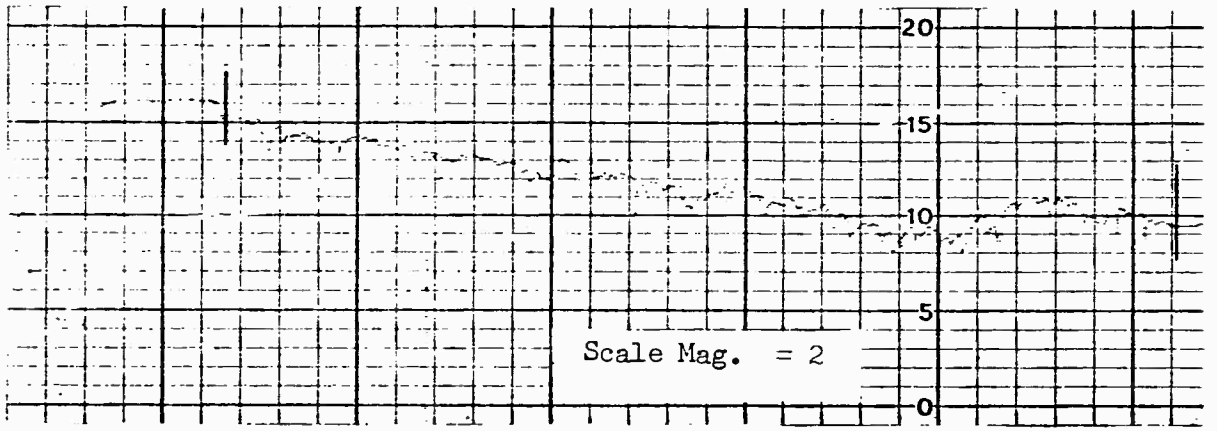

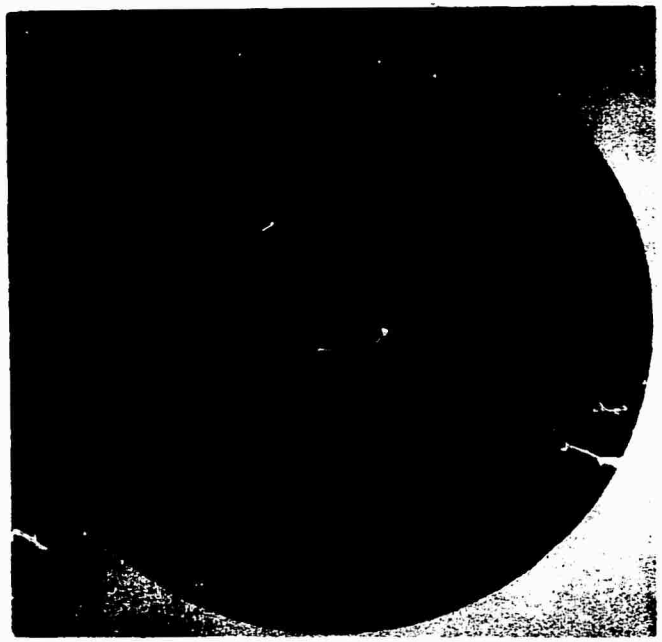

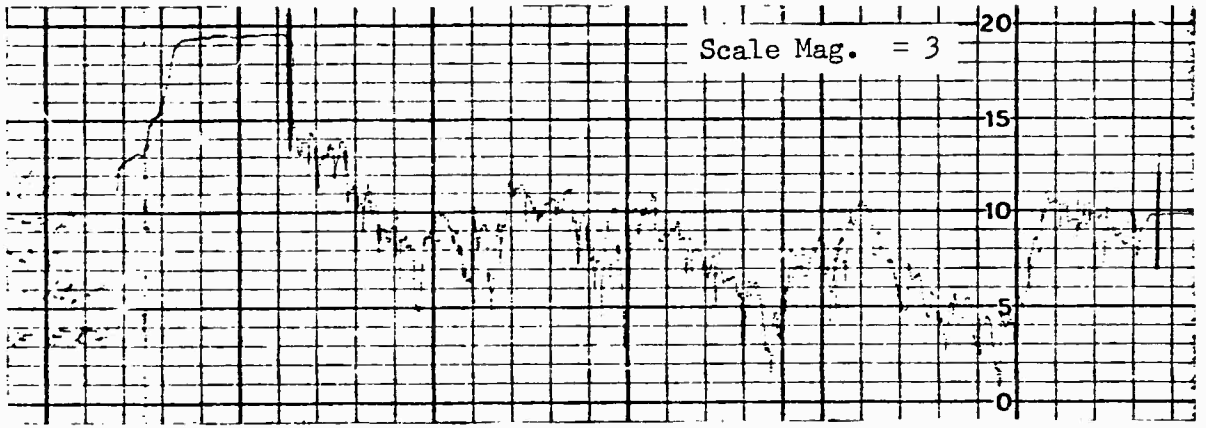

Photo Mag. = 4.4X

CLA = 14.4
RMS = 16.0

10 BT-3A (M) Before Etch

θ MAX	83.5
θ MIN	(9.0)
$\Delta\theta$	74.5

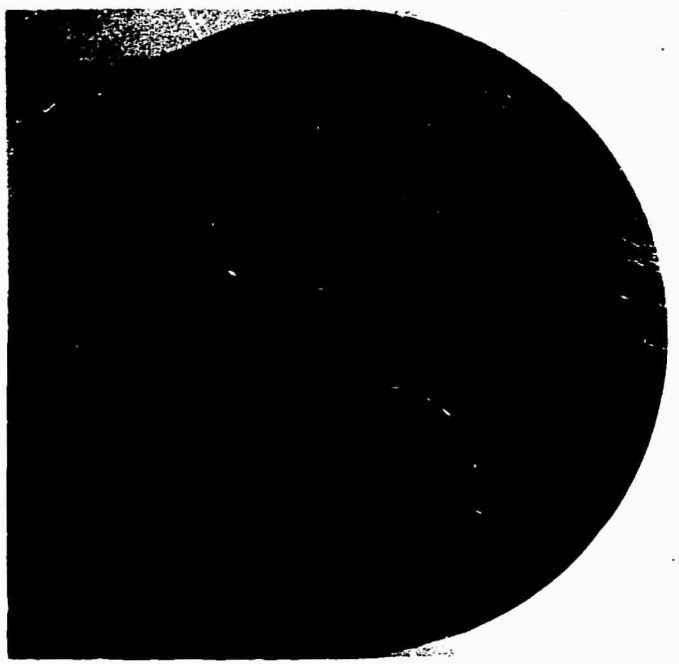

10 BT-3A (E) After Etch

Photo Mag. = 4.5X

CLA = 24.0
RMS = 26.6

θ MAX	54.0
θ MIN	8.5
$\Delta\theta$	45.5

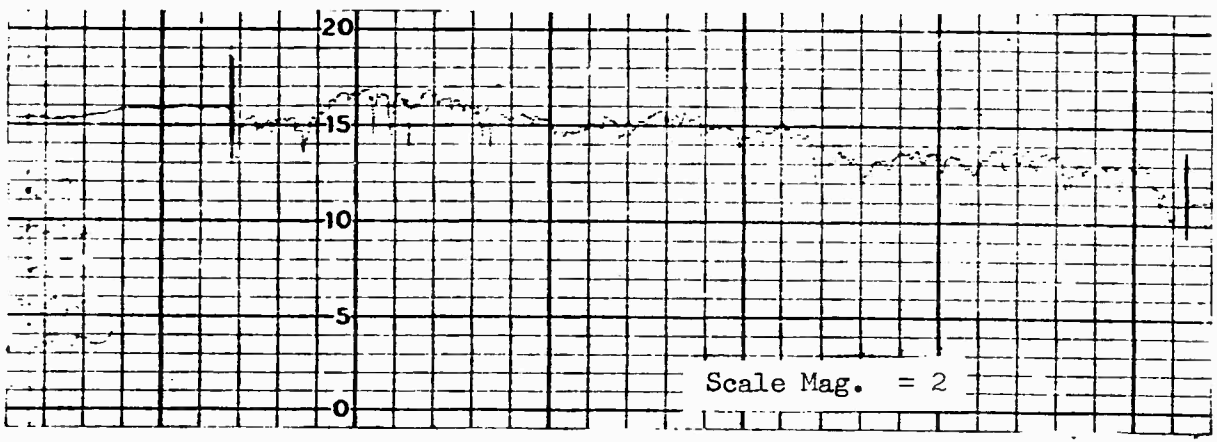

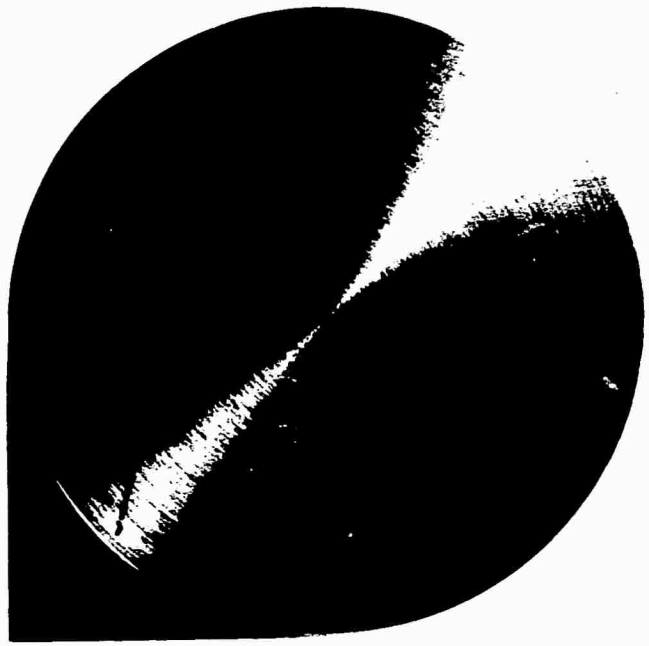

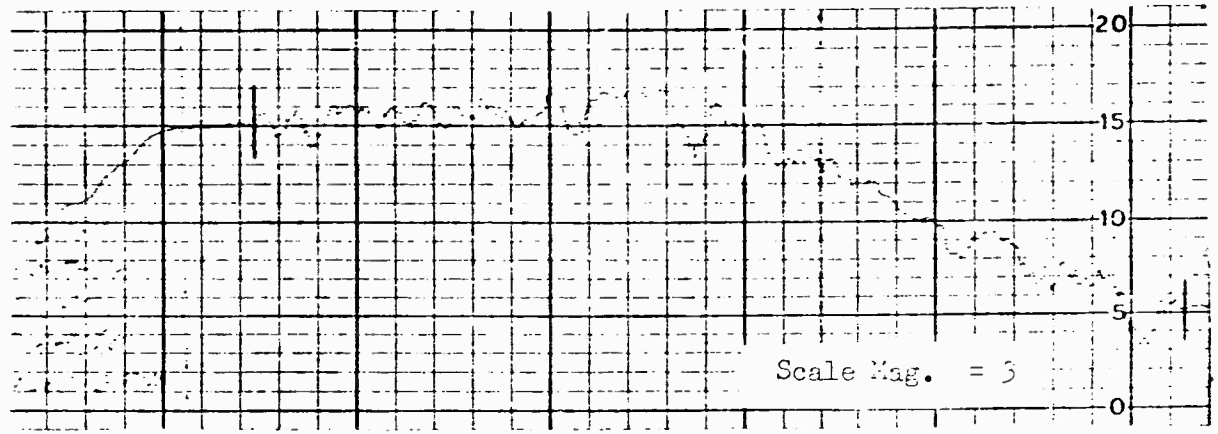

Photo Mag. = 4.4X

CLA = 7.0
RMS = 7.8

20 BT-3A (M) Before Etch

ϑ MAX	70.0
ϑ MIN	12.5
$\Delta\theta$	57.5

Photo Mag. = 4.5X

CLA = 14.0
RMS = 15.5

20 BT-3A (E) After Etch

θ MAX	36.0
ϑ MIN	13.5
$\Delta\theta$	22.5

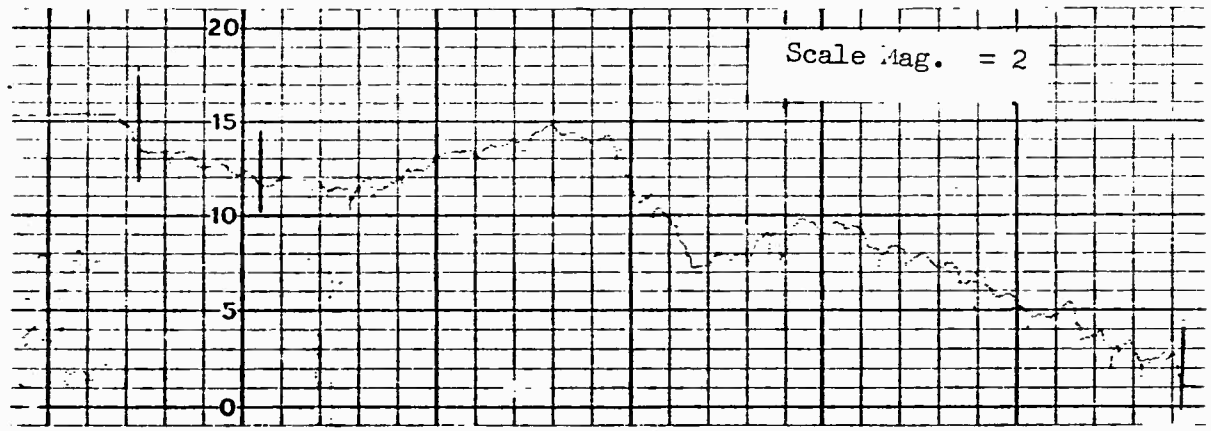

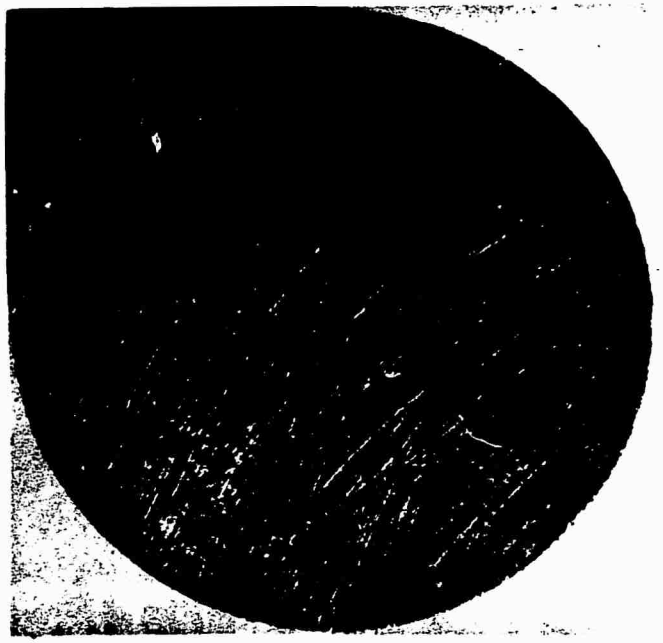

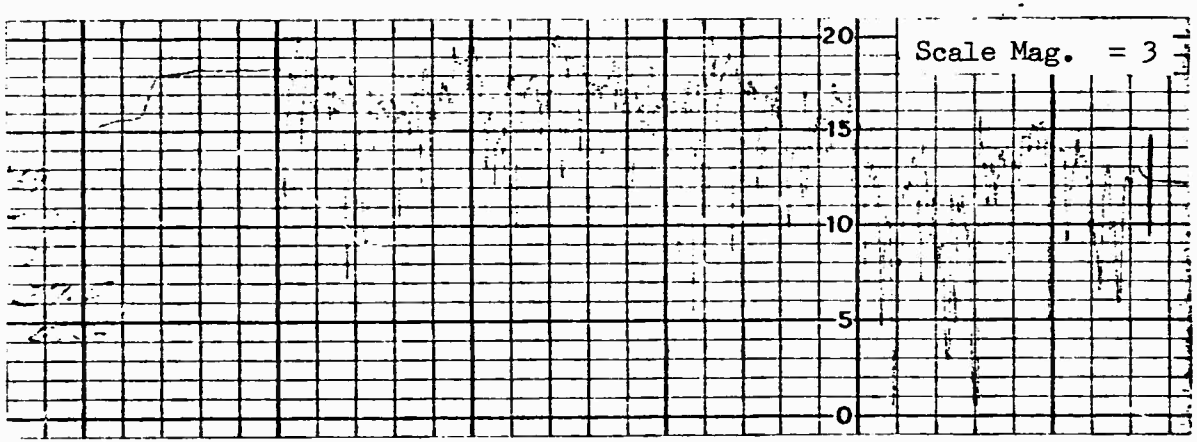

Photo Mag. = 4.4X

CLA = 37.5
RMS = 41.6

40 BT-3A (M) Before Etch

θ MAX	63.5
θ MIN	4.0
$\Delta\theta$	59.5

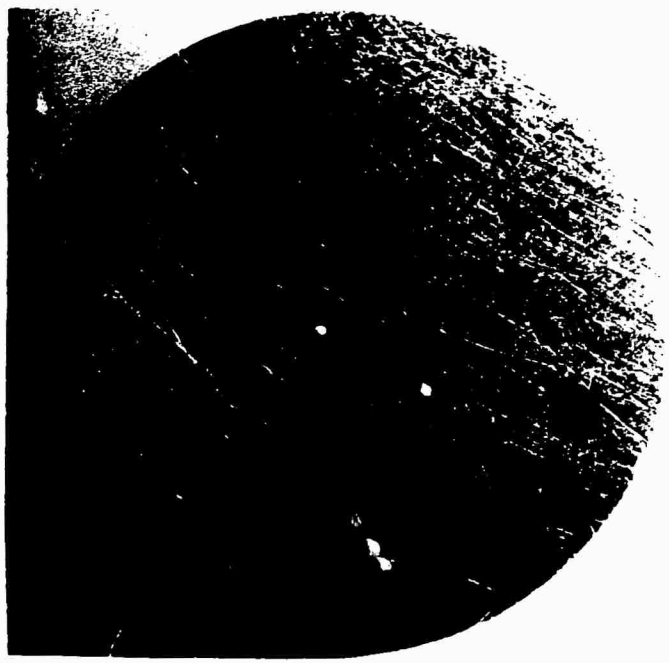

Photo Mag. = 4.5X

CLA = 35.0
RMS = 38.8

40 BT-3A (E) After Etch

θ MAX	19.0
θ MIN	5.0
$\Delta\theta$	14.0

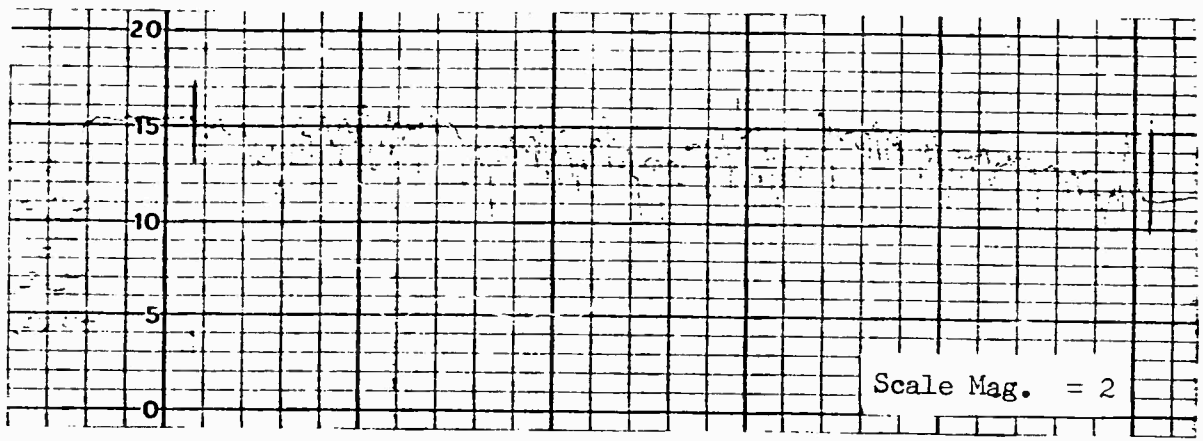

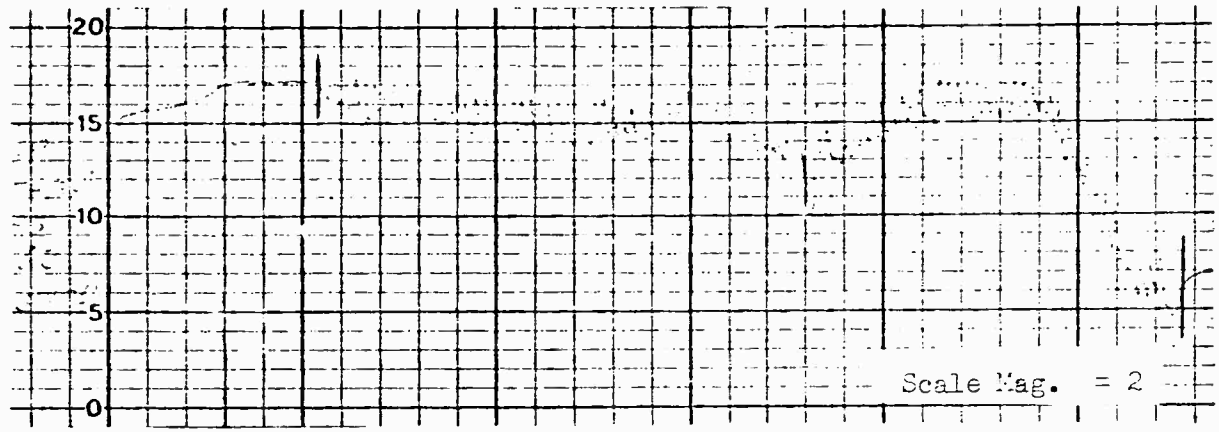

Photo Mag. = 4.4X

CLA = 63
RMS = 69.9

80 BT-3A (E) Before Etch

θ MAX	78.5
θ MIN	12.5
$\Delta\theta$	66.0

Photo Mag. = 4.5X

CLA = 45.0
RMS = 49.9

80 BT-3A (E) After Etch

θ MAX	43.0
θ MIN	5.5
$\Delta\theta$	37.5

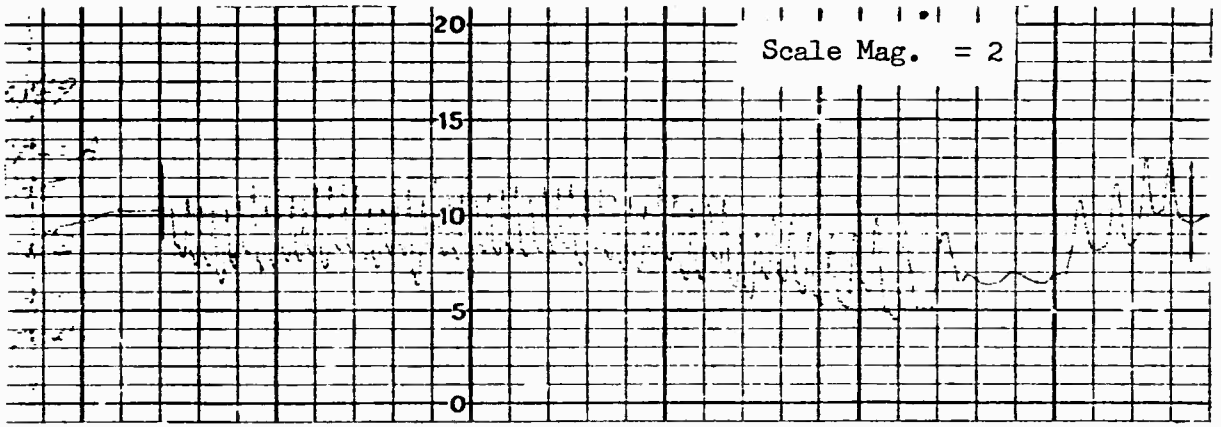

Photo Mag. = 4.4X

CLA = 62
RMS = 68.9

110 BT-3A (M) Before Etch

θ MAX	80.5
θ MIN	17.5
$\Delta\theta$	63.0

Photo Mag. = 4.5X

CLA = 60.0
RMS = 66.6

110 BT-3A (E) After Etch

θ MAX	32.5
θ MIN	8.0
$\Delta\theta$	24.5

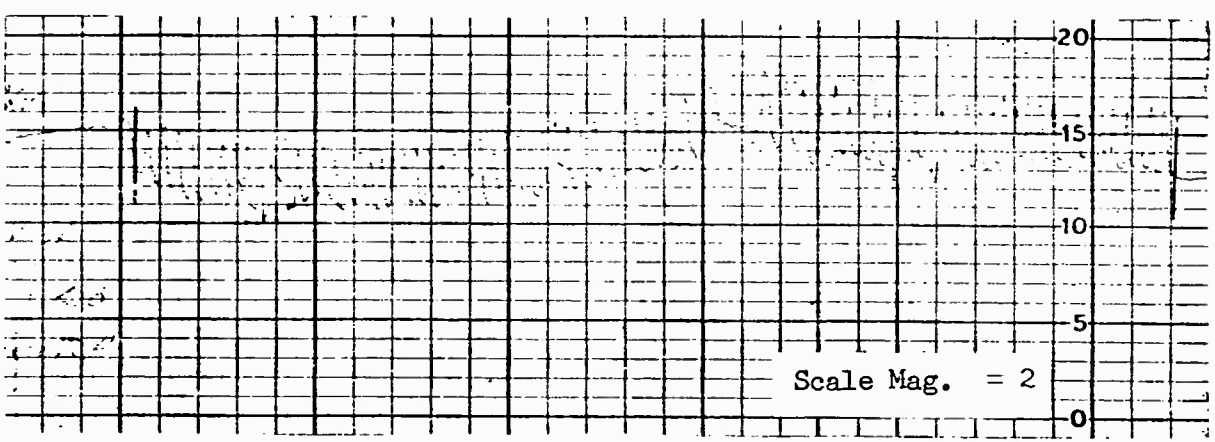

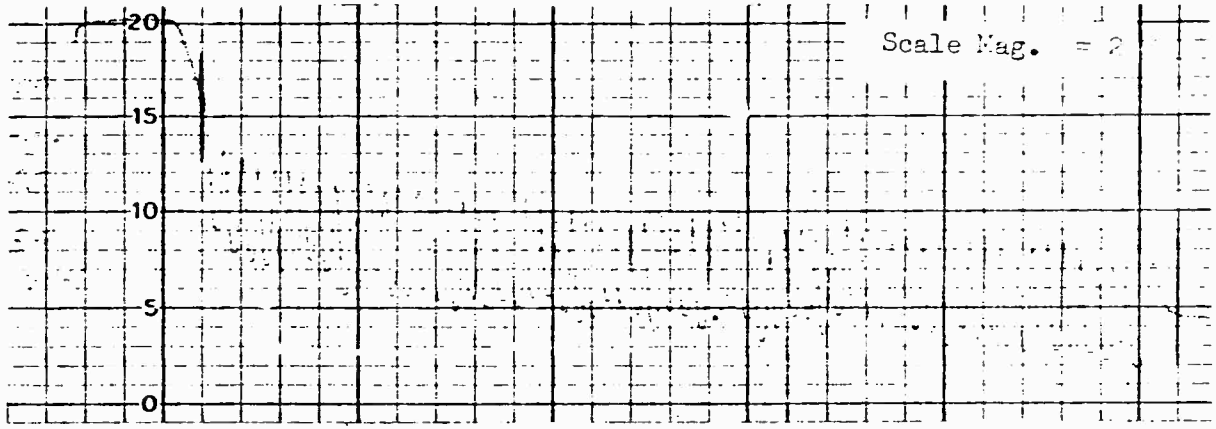

Photo Mag. = 4.4X

CLA = 84
RMS = 93.2

150 BT-3A (E) Before Etch

θ MAX	83.5
θ MIN	27.0
$\Delta\theta$	56.5

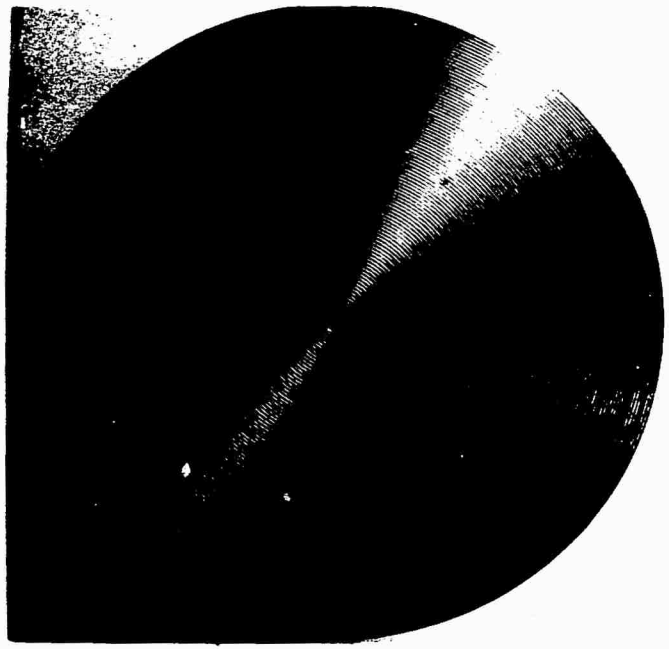

Photo Mag. = 4.5X

CLA = 77.0
RMS = 85.5

150 BT-3A (E) After Etch

θ MAX	46.5
θ MIN	12.0
$\Delta\theta$	34.5

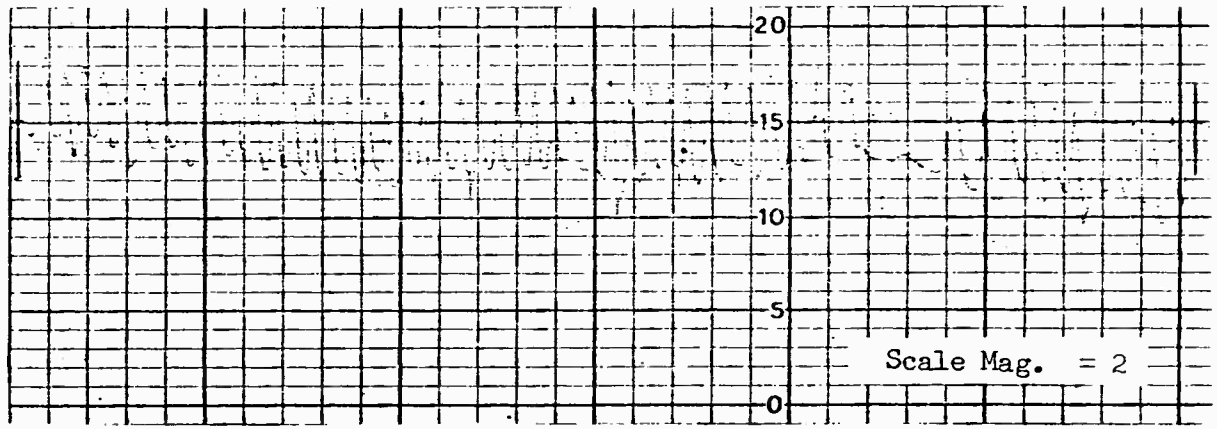

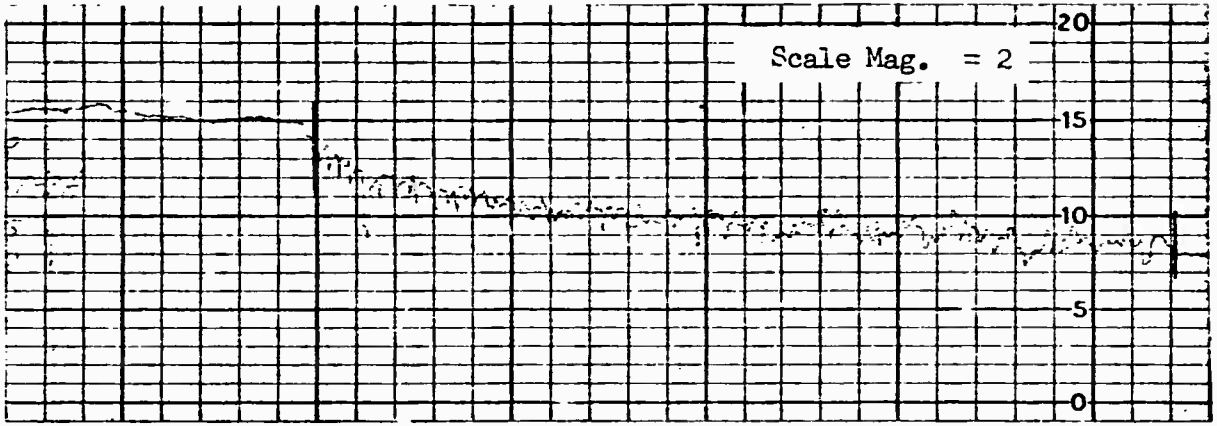

Photo Mag. = 4.4X

CLA = 22
RMS = 24.4

FGLP-BT-3A (M) Before Etch

θ MAX	56.0
θ MIN	20.0
$\Delta\theta$	36.0

Photo Mag. = 4.5X

CLA = 25.0
RMS = 27.7

FGLP-BT-3A (E) After Etch

θ MAX	44.5
θ MIN	9.5
$\Delta\theta$	35.0

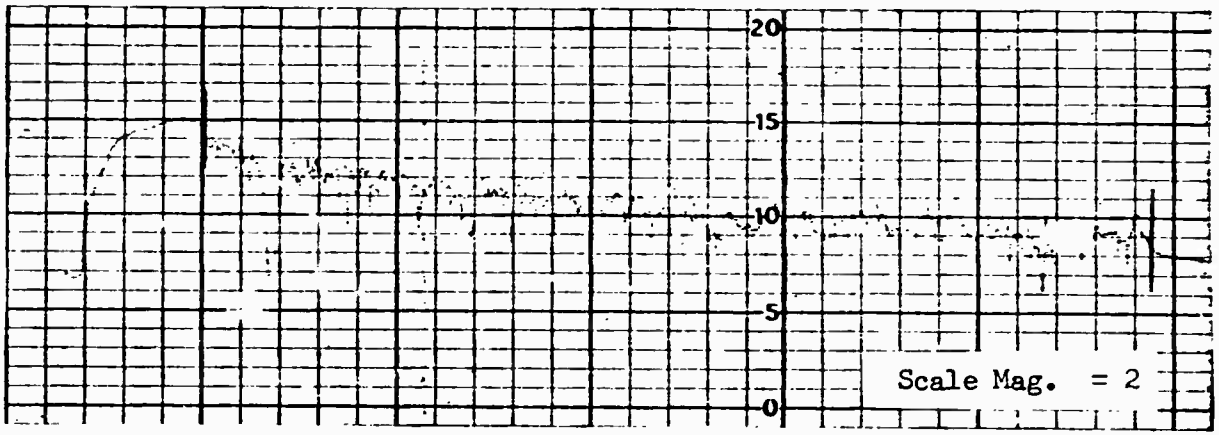

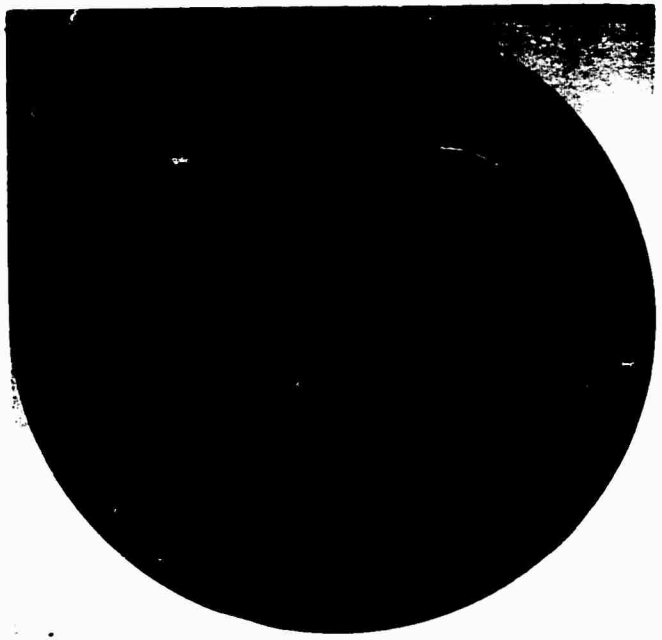

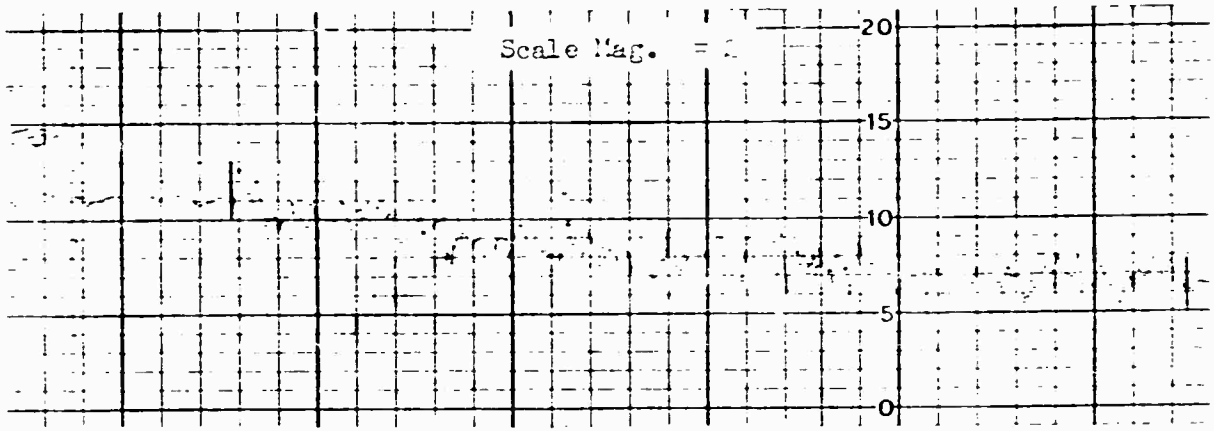

Photo Mag. = 4.4X

CLA = 29
RMS = 32.2

FGHP-BT-3A (M) before Etch

θ MAX	56.0
θ MIN	20.0
$\Delta\theta$	36.0

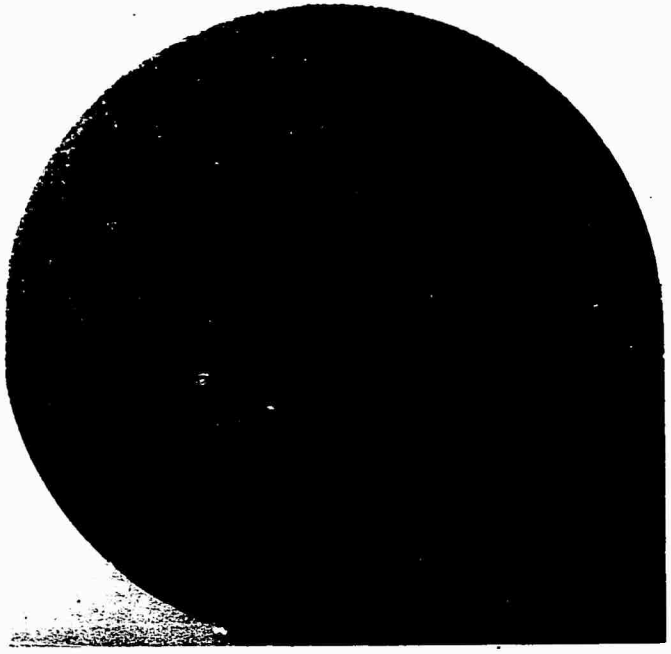

Photo Mag. = 4.5X

CLA = 50.0
RMS = 55.5

FGHP-BT-3A (E) After Etch

θ MAX	59.0
θ MIN	($\ll$ 31.0)
$\Delta\theta$	--(>28)

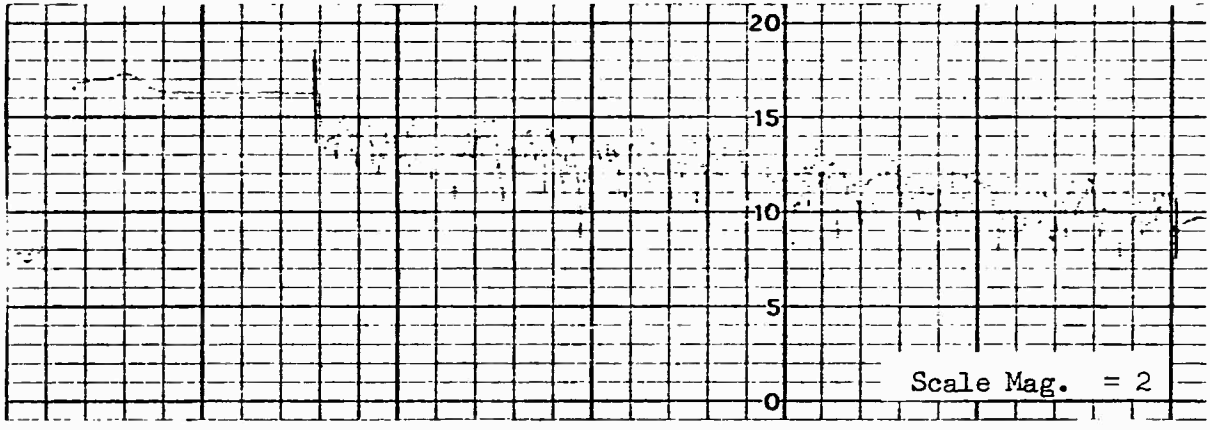

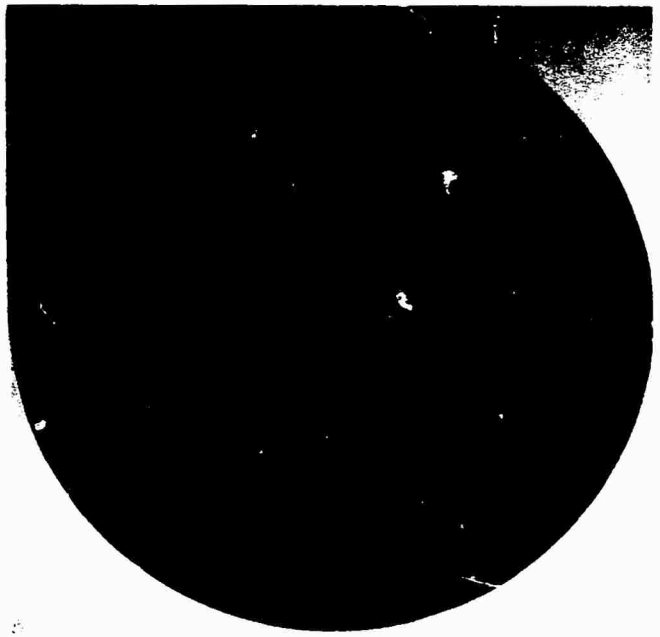

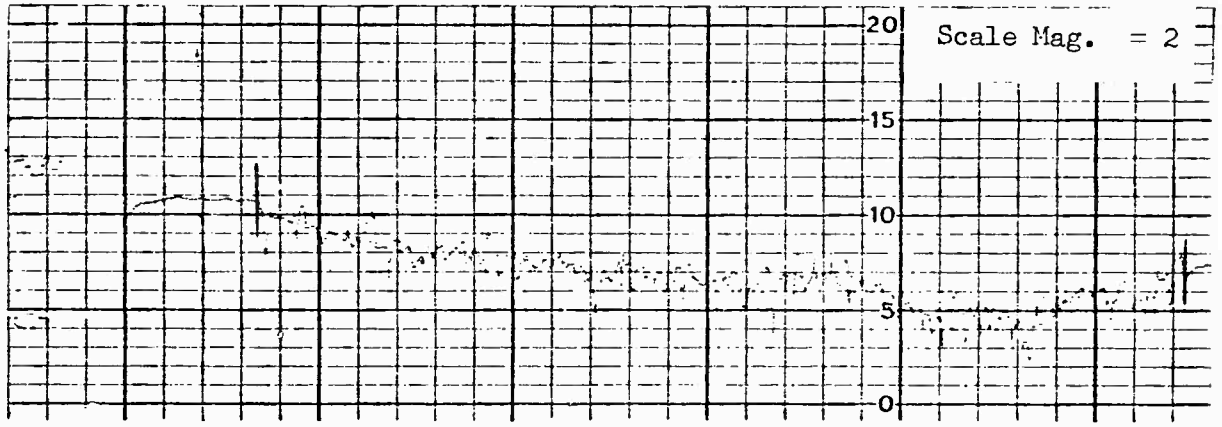

Photo Mag. = 4.4X

CLA = 31.0
RMS = 34.4

CGLP-BT-3A (M) Before Etch

θ MAX	76.0
θ MIN	15.5
$\Delta\theta$	60.5

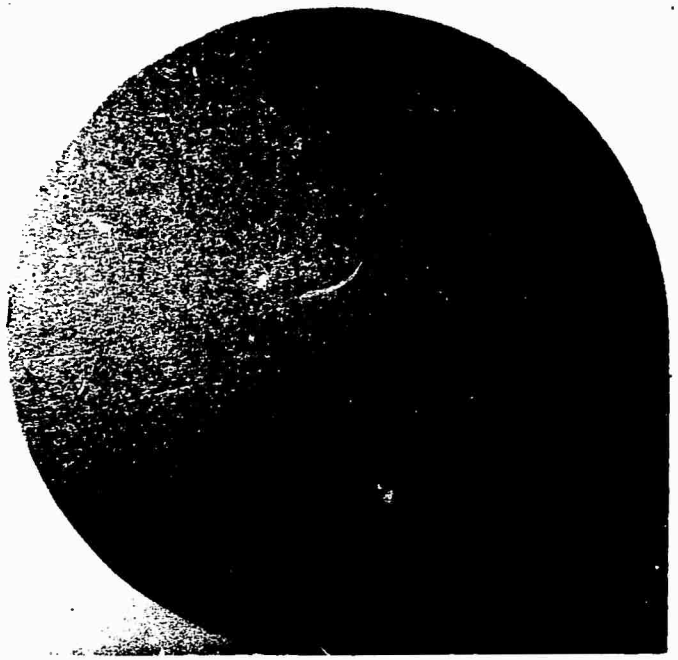

CGLP-BT-3A (E) After Etch

Photo Mag. = 4.5X

CLA = 30.0
RMS = 33.3

θ MAX	54.5
θ MIN	10.5
$\Delta\theta$	44.0

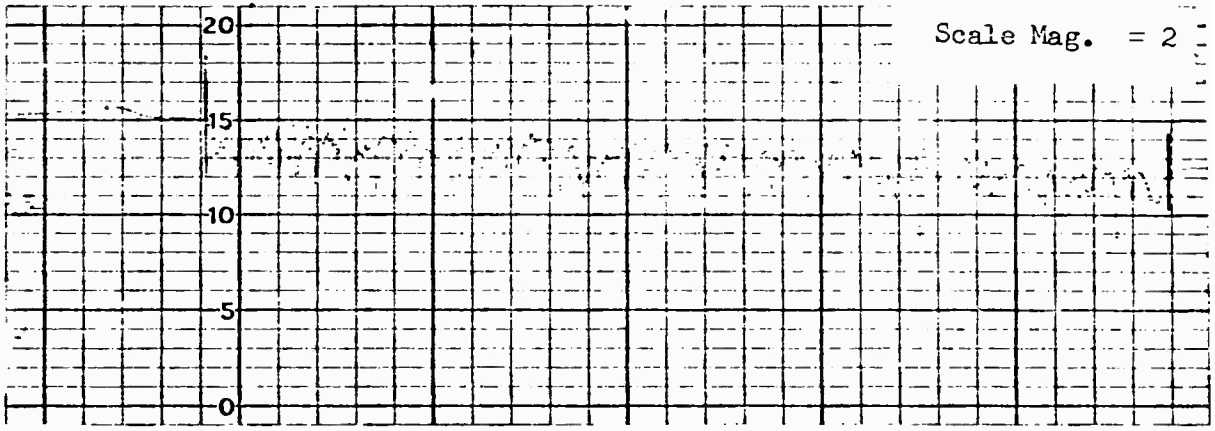

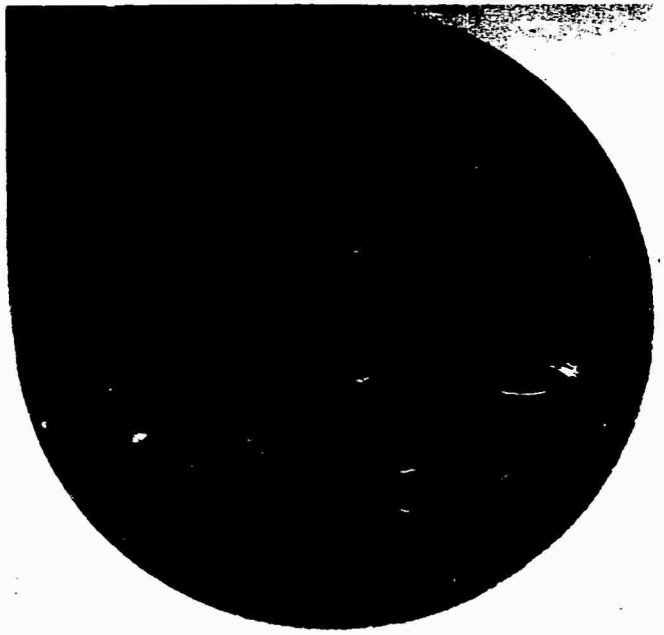

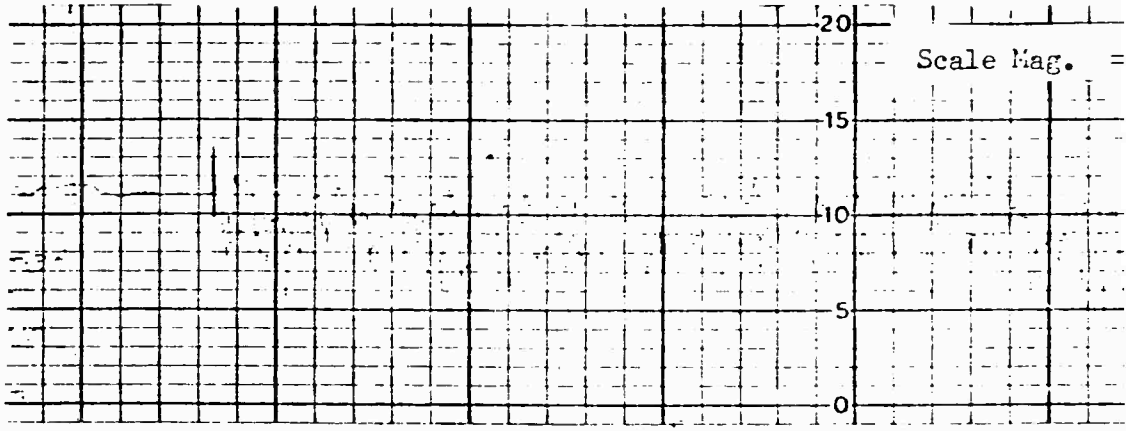

Photo Mag. = 4.4X

CLA = 55.0
RMS = 61.0

CGHP-BT-3A (M) Before

θ MAX	78.0
θ MIN	13.0
$\Delta\theta$	65.0

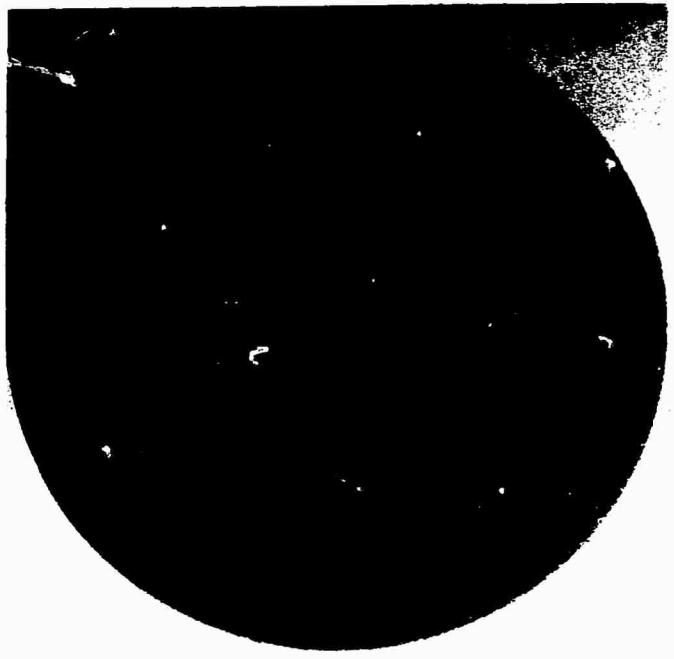

Photo Mag. = 4.5X

CLA = 70.0
RMS = 77.7

CGHP-BT-3A (E) After

θ MAX	40.5
θ MIN	9.0
$\Delta\theta$	31.5

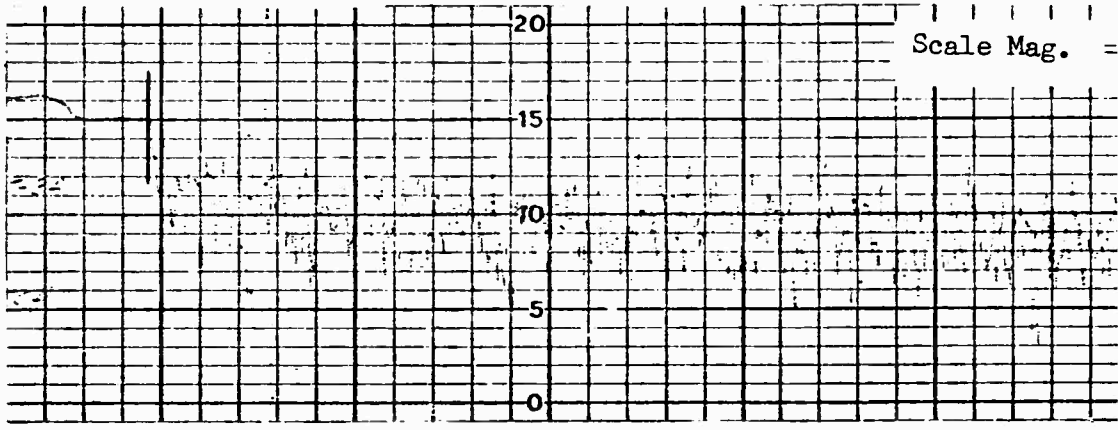

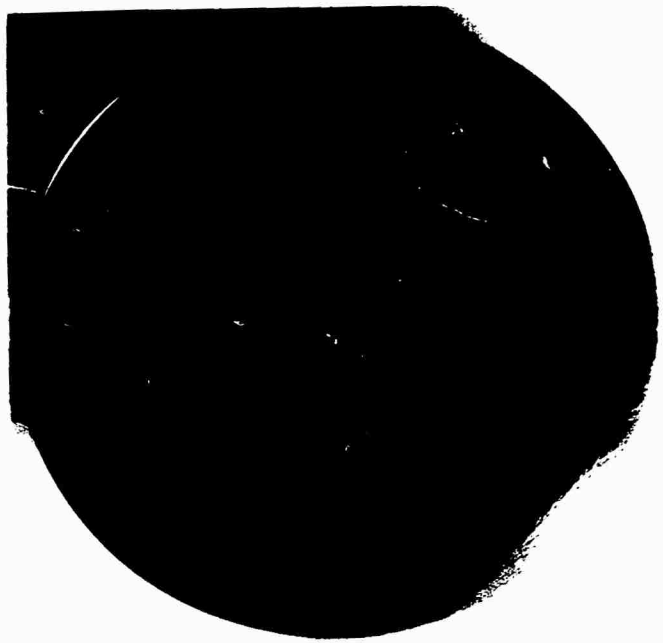

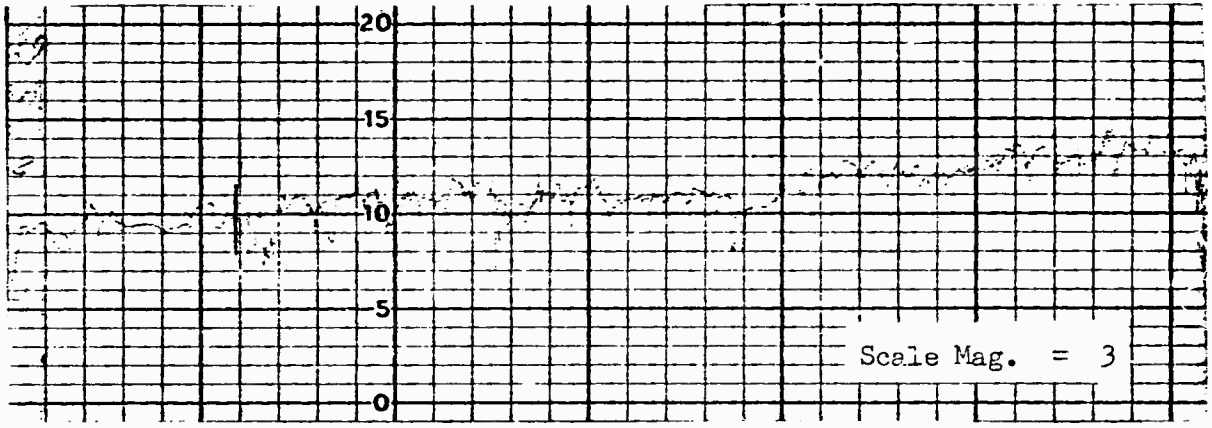

Photo Mag. = 4.4X

CLA = 2.2
RMS = 2.4

1 CS-3A (M) Before Etch

θ MAX	88.0
θ MIN	44.5
$\Delta\theta$	43.5

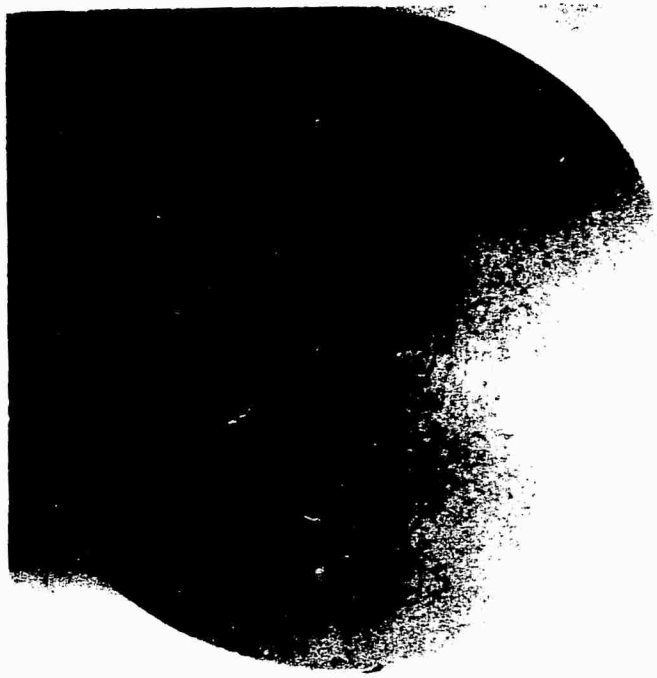

Photo Mag. = 4.7X

CLA = 2.5
RMS = 2.8

1 CS-3A (E) After Etch

θ MAX	24.5
θ MIN	4.5
$\Delta\theta$	20.0

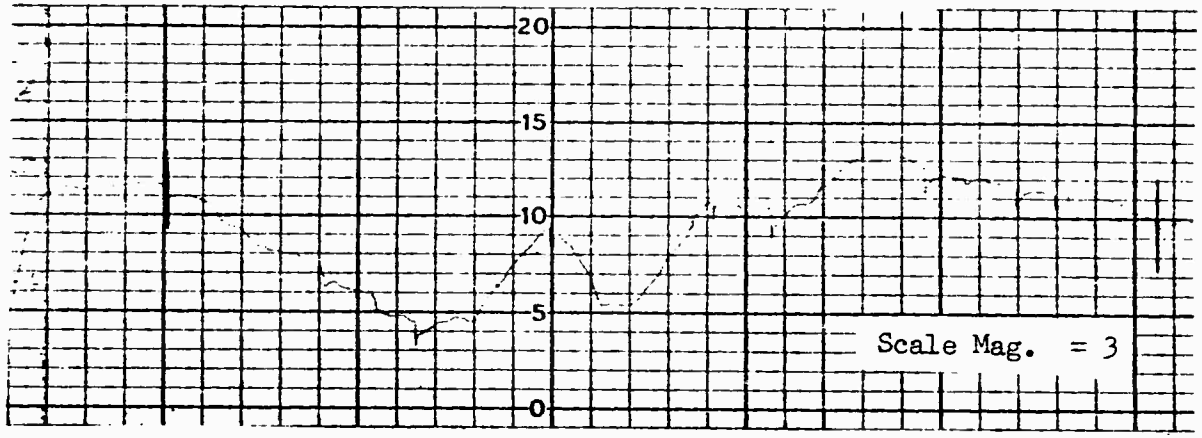

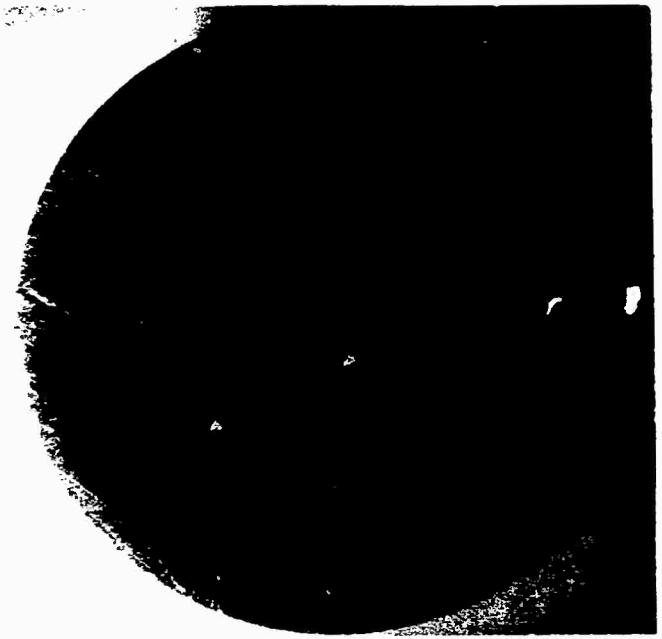

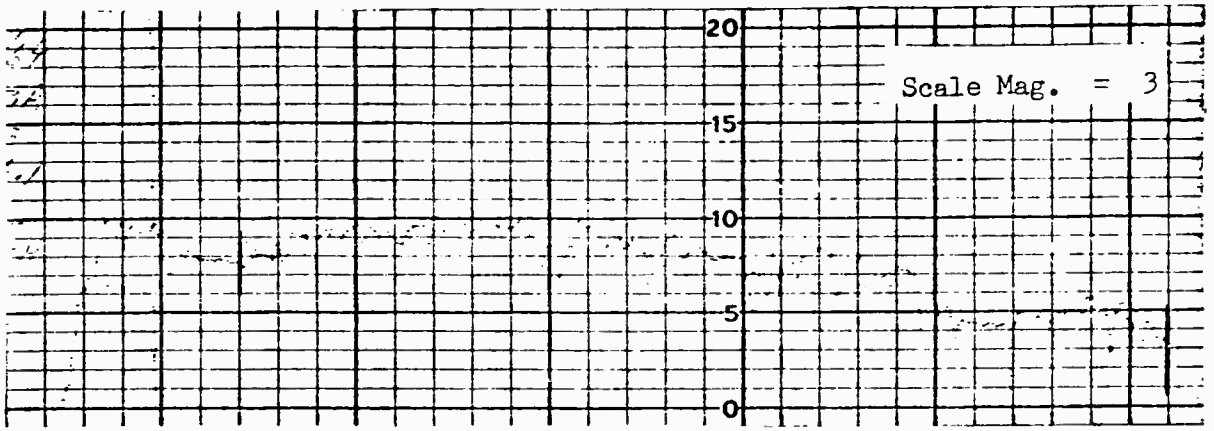

Photo mag. = 4.4X

CLA = 4.1
RMS = 4.5

5 CS-3A (M) Before Etch

θ MAX	74.0
θ MIN	15.0
$\Delta\theta$	59.0

Photo Mag. = 4.5X

CLA = 6.5
RMS = 7.2

5 CS-3A (E) After Etch

θ MAX	15.0
θ MIN	4.5
$\Delta\theta$	10.5

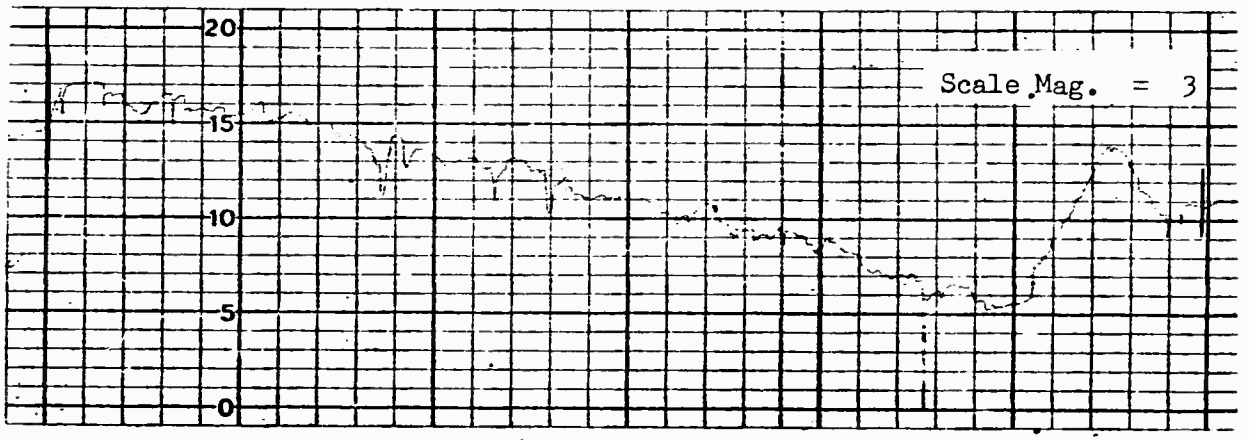

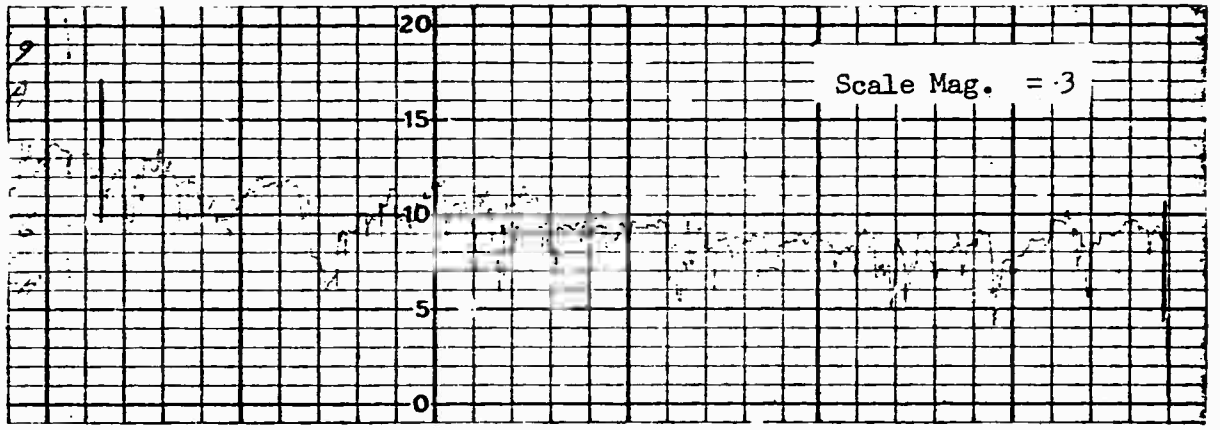

Photo mag. = 3.7X

CLA = 9.6
RMS = 10.6

7CS-3A (M) Before Etch

θ MAX	81.0
θ MIN	15.5
$\Delta\theta$	65.5

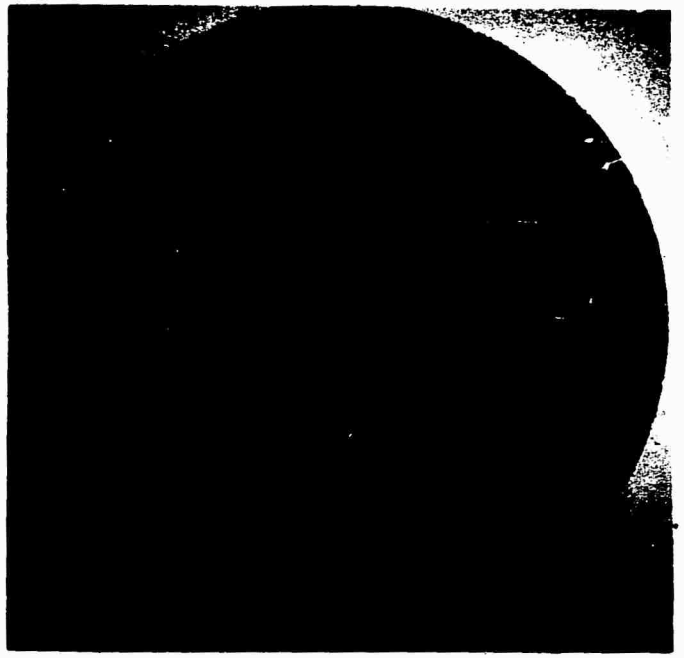

Photo Mag. = 4.5X

CLA = 18.0
RMS = 20.0

7 CS-3A (E) After Etch

θ MAX	18.0
θ MIN	5.0
$\Delta\theta$	13.0

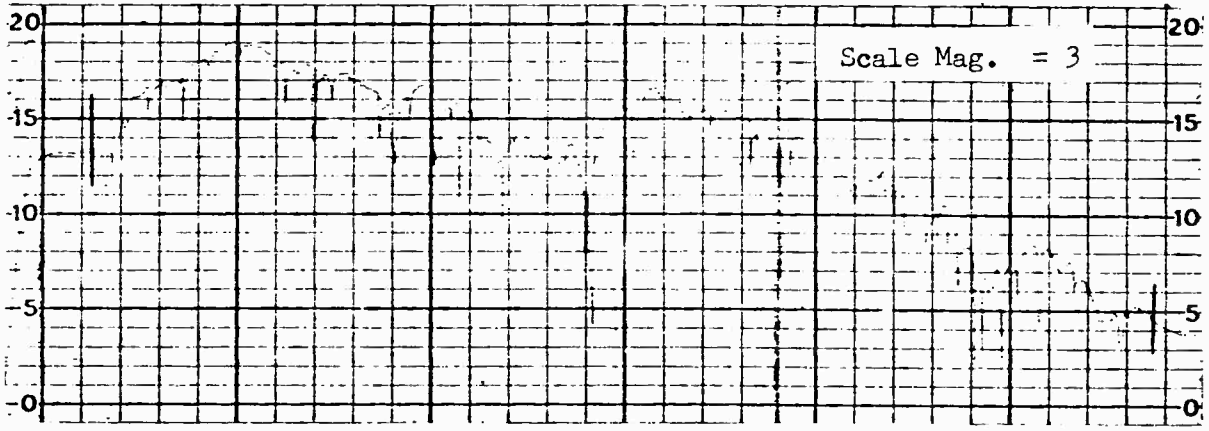

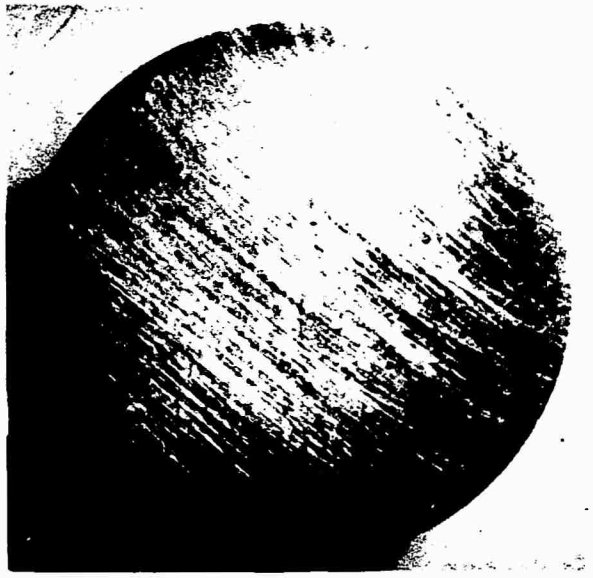

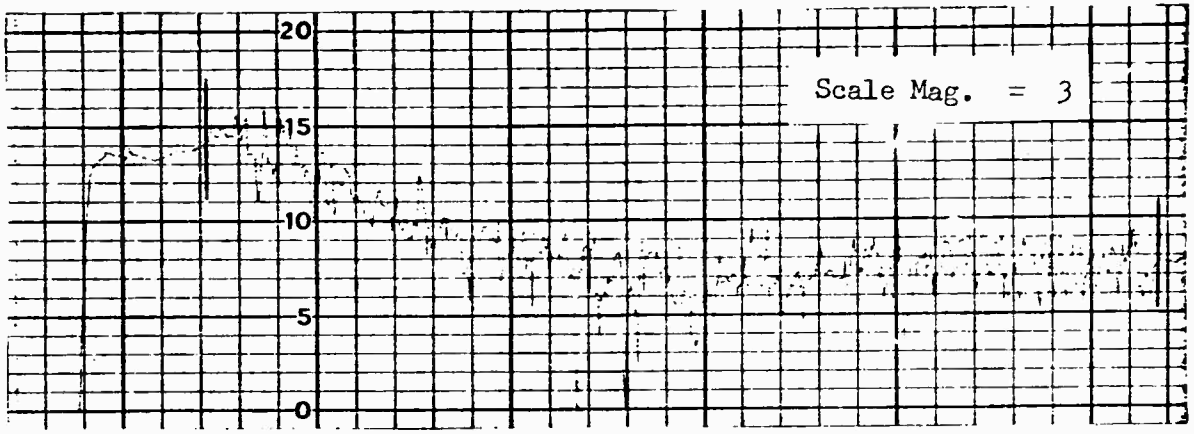

Photo Mag. = 3.7X

CLA = 8.6
RMS = 9.5

10 CS-3A (M) Before Etch

θ MAX 72.0
θ MIN 16.0
$\Delta\theta$ 56.0

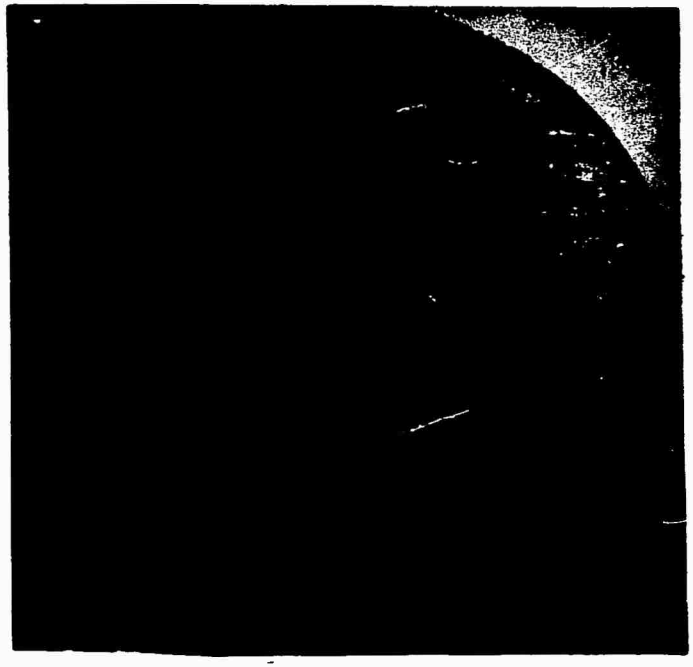

Photo Mag. = 4.5X

CLA = 12.5
RMS = 13.9

10 CS-3A (E) After Etch

θ MAX 28.0
θ MIN 6.0
$\Delta\theta$ 22.0

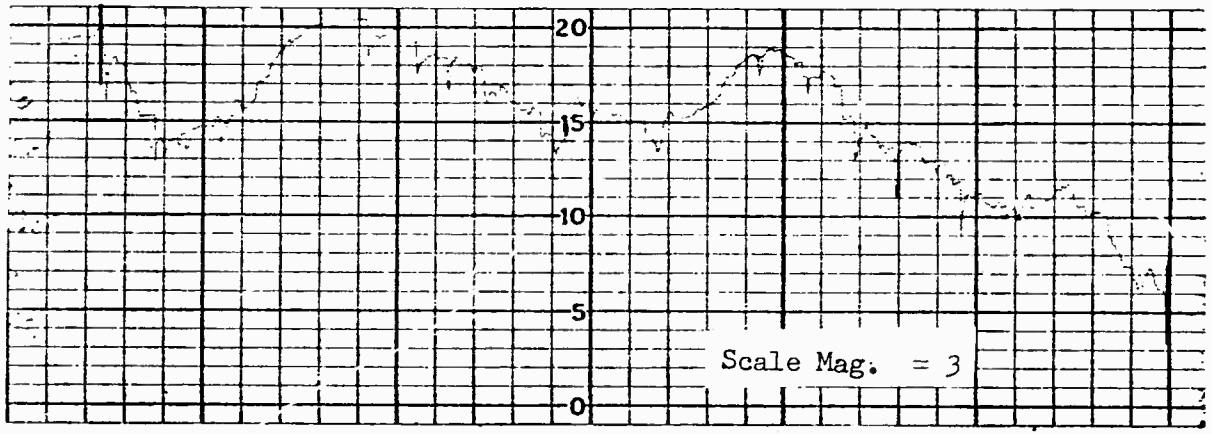

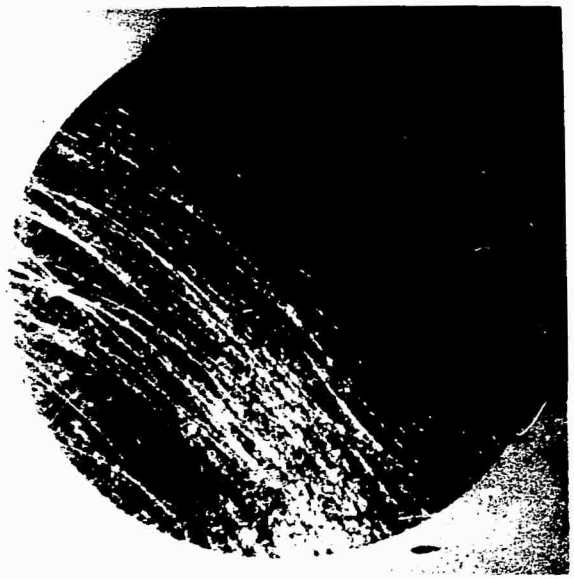

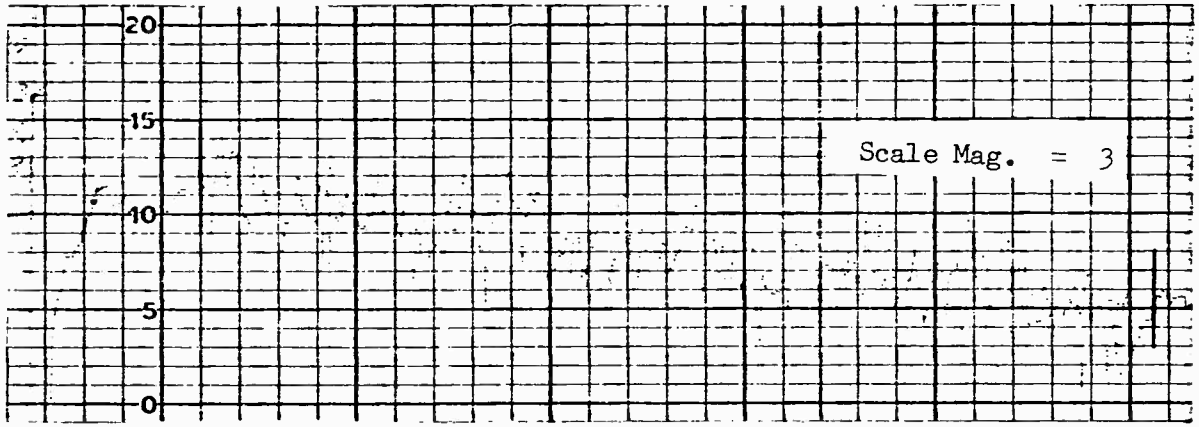

Photo Mag. = 3.7X

CLA = 23.0
RMS = 25.5

20 CS 3A (M) Before Etch

θ MAX	73.5
θ MIN	14.0
$\Delta\theta$	59.5

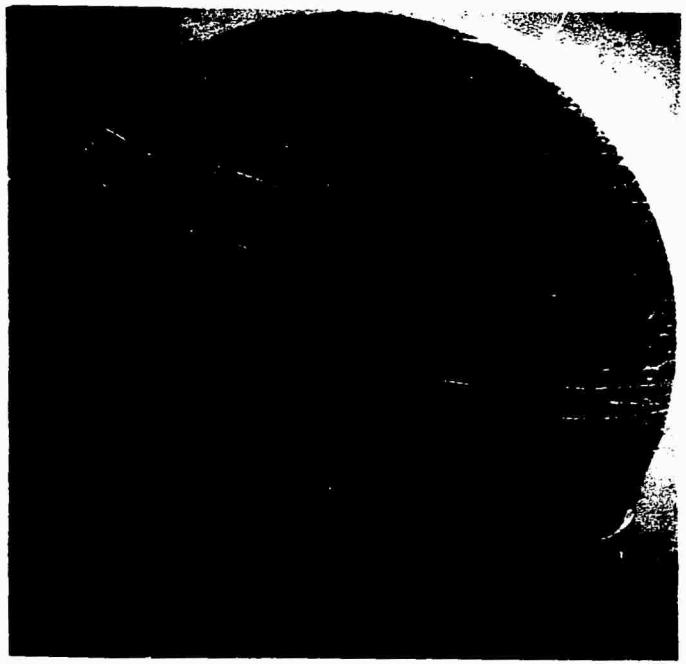

Photo Mag. = 4.5X

CLA = 17.0
RMS = 18.9

20 CS-3A (E) After Etch

θ MAX	28.5
θ MIN	6.0
$\Delta\theta$	22.5

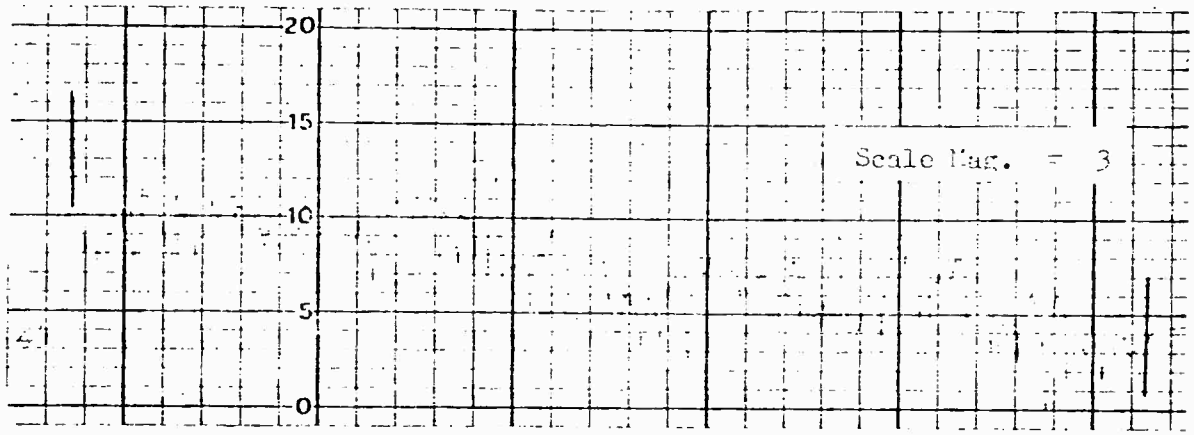

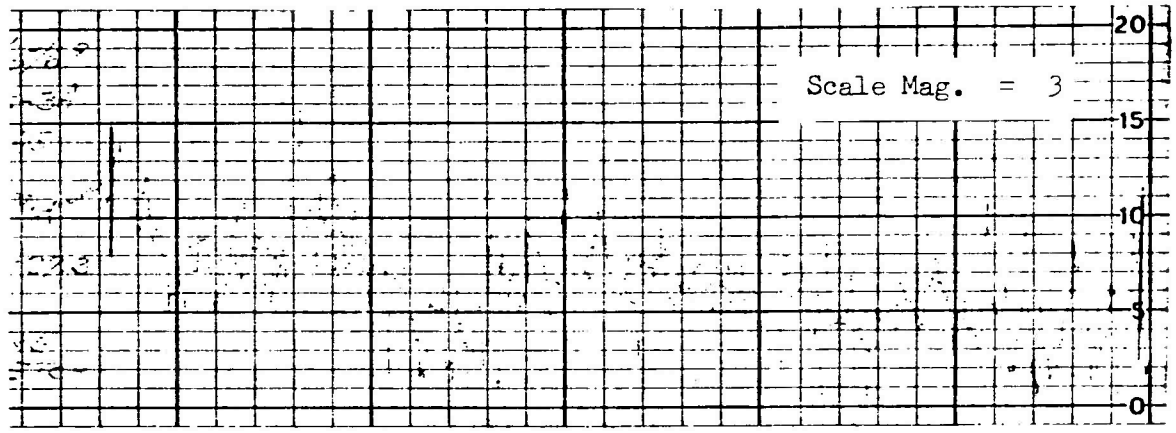

Photo Mag. = 3.7X

CLA = 27.3
RMS = 30.3

40 CS-3A (M) Before Etch

θ MAX	76.0
θ MIN	12.5
$\Delta\theta$	63.5

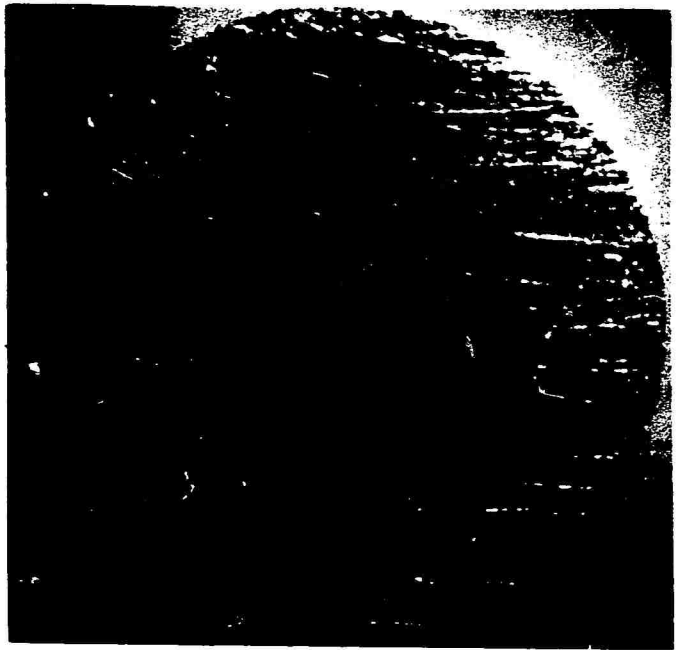

Photo Mag. = 4.5X

CLA = 26.0
RMS = 28.8

40 CS-3A (E) After Etch

θ MAX	25.0
θ MIN	(6.5)
$\Delta\theta$	(18.5)

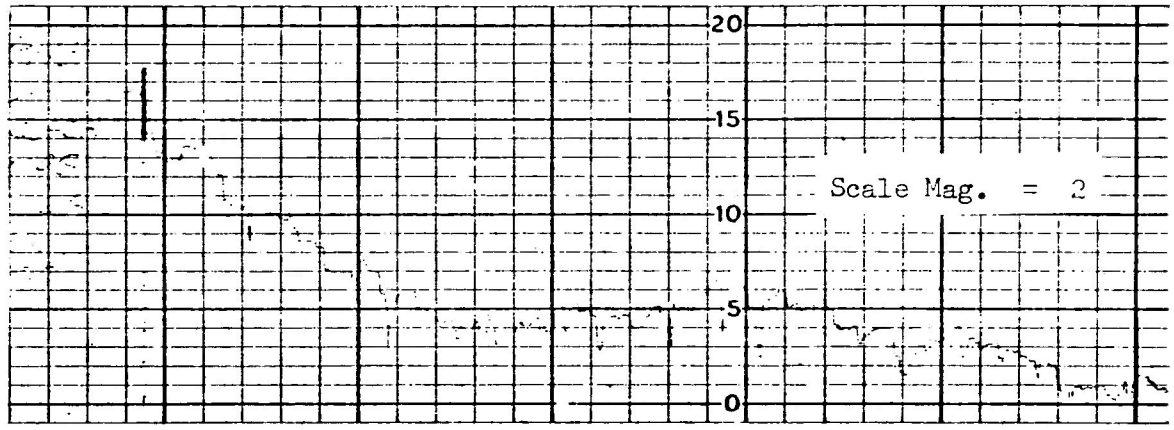

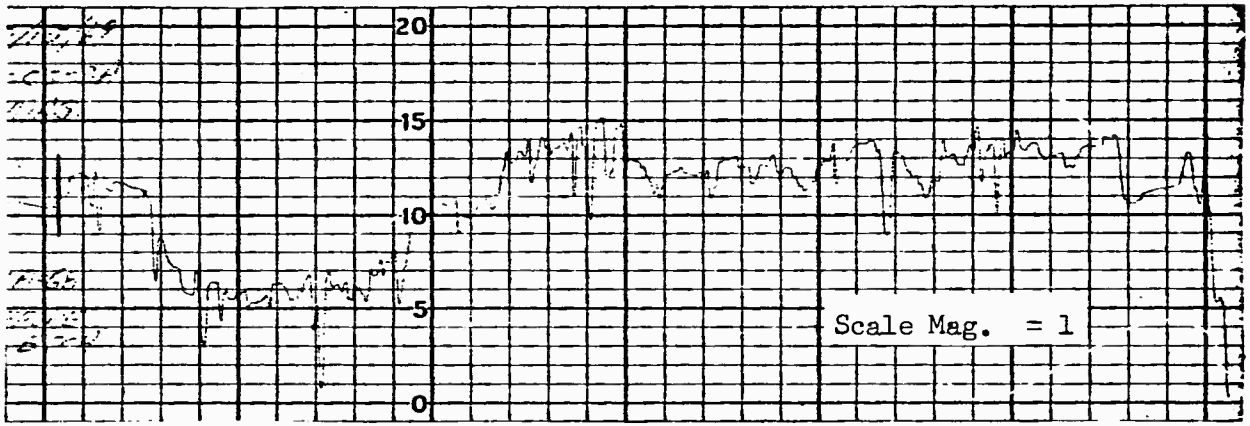

Photo Mag. = 3.7X

CLA = 68.0
RMS = 75.5

80 CS-3A (M) Before Etch

θ MAX	77.5
θ MIN	11.5
$\Delta\theta$	66.0

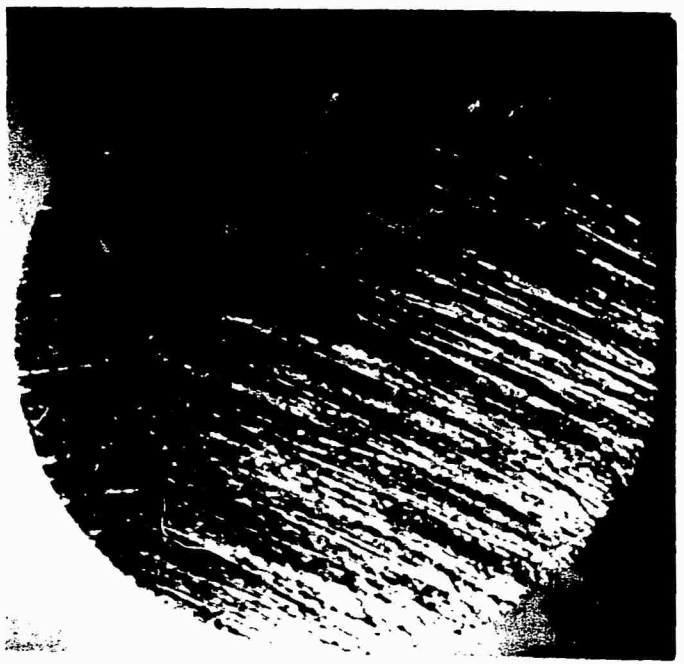

Photo Mag. = 4.5X

CLA = 70.0
RMS = 77.7

80 CS-3A (E) After Etch

θ MAX	31.0
θ MIN	(5.0)
$\Delta\theta$	(26.0)

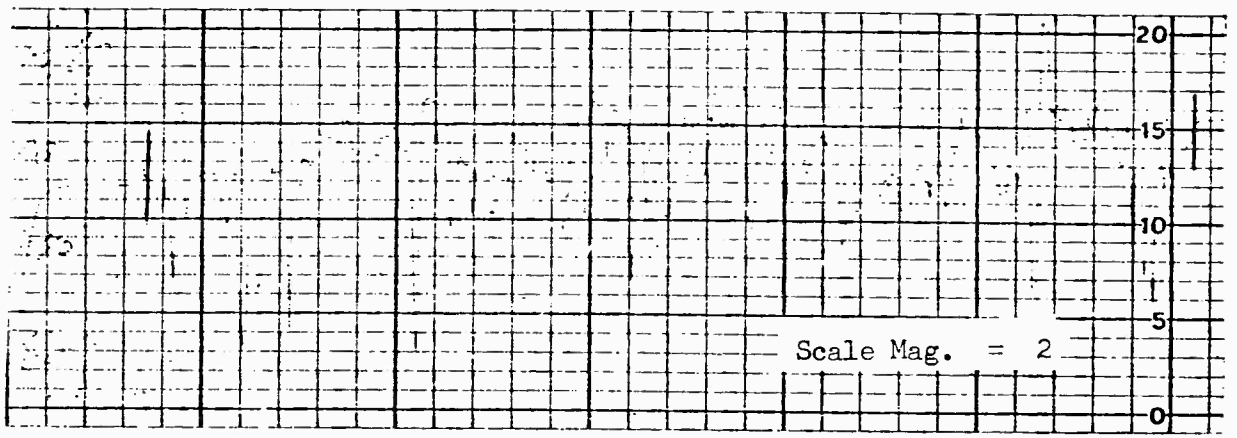

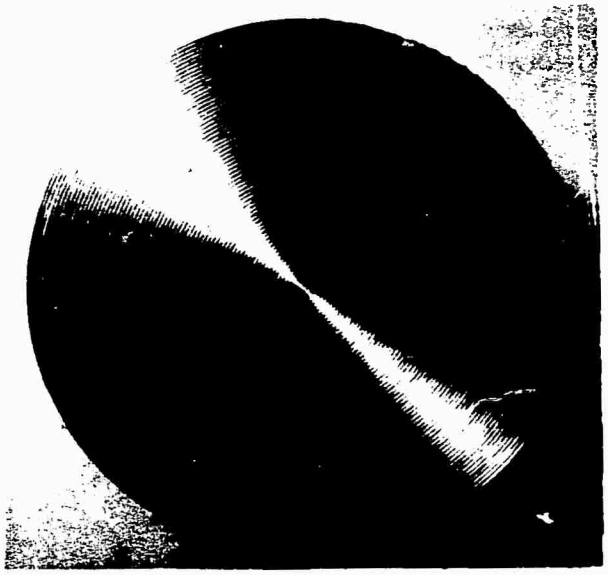

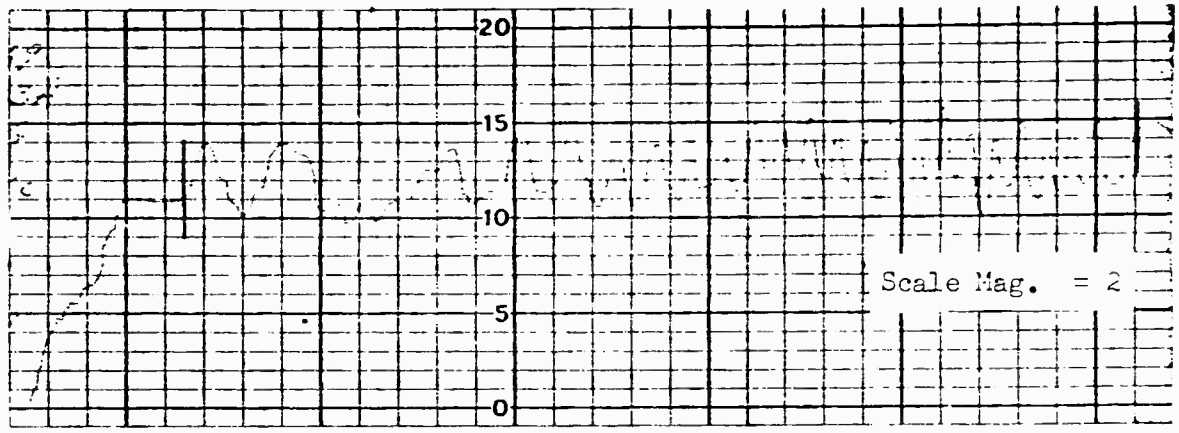

Photo Mag. = 3.7X

CLA = 60.0
RMS = 66.6

110 CS-3A (M) Before Etch

θ MAX	73.0
θ MIN	21.0
$\Delta\theta$	52.0

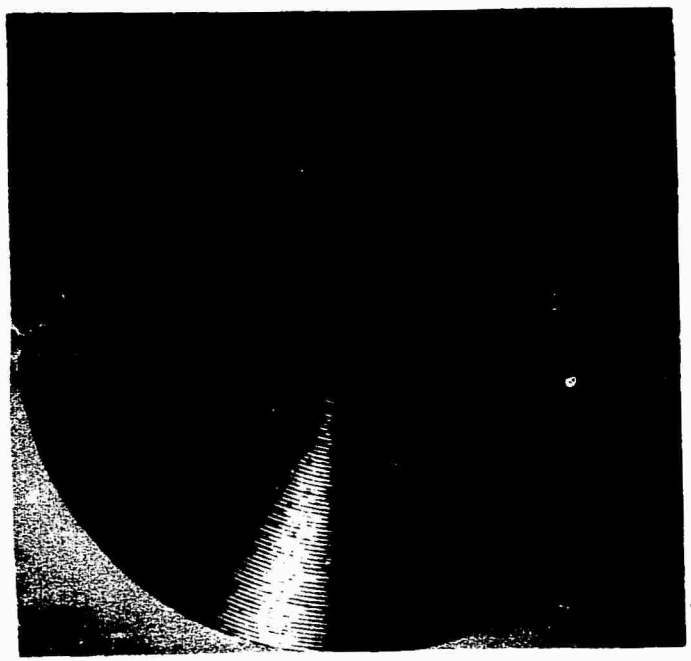

Photo Mag. = 4.5X

CLA = 70.0
RMS = 77.7

110 CS-3A (E) After Etch

θ MAX	32.0
θ MIN	(3.0)
$\Delta\theta$	(29.0

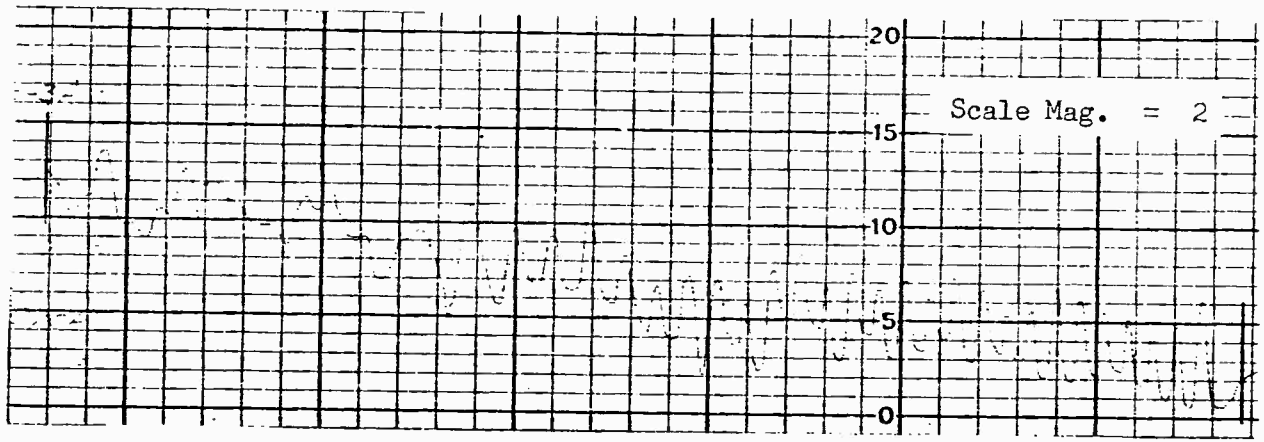

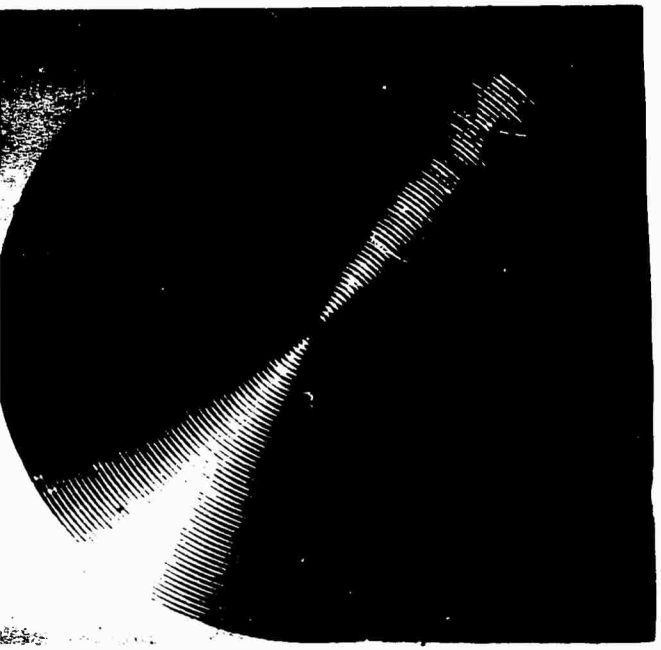

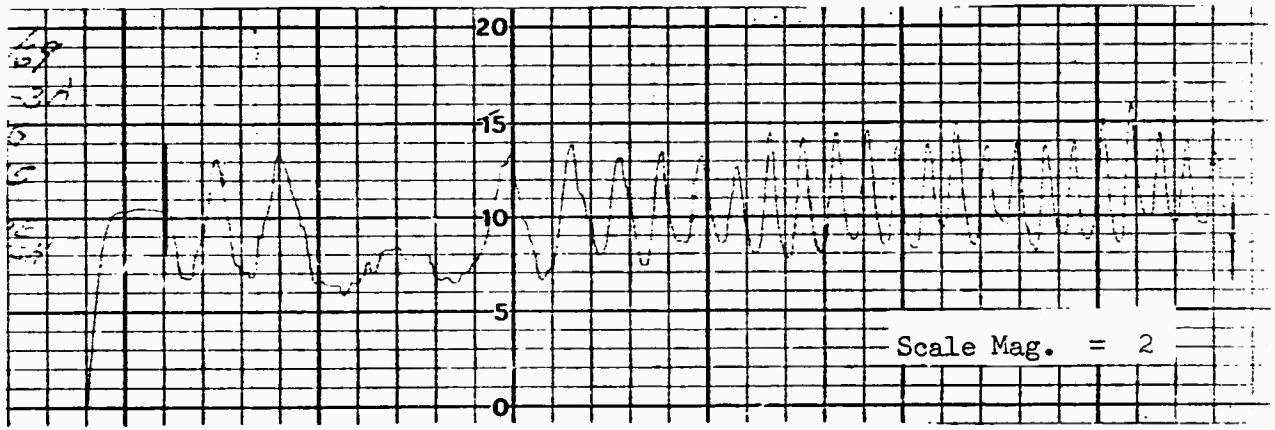

Photo Mag. = 4.4X

CLA = 95.0
RMS = 105.4

150 CS=3A (M) Before Etch

θ MAX	72.5
θ MIN	15.0
$\Delta\theta$	57.5

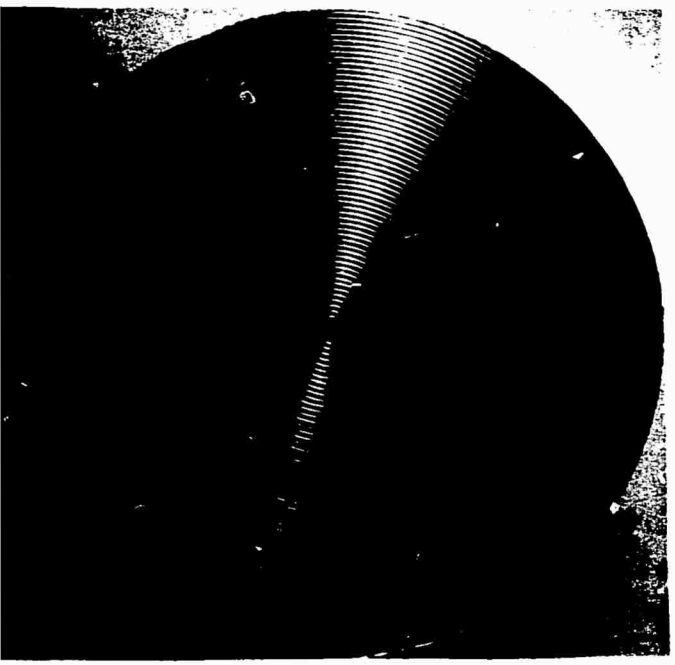

Photo Mag. = 4.5X

CLA = 70.0
RMS = 77.7

150 CS-3A (E) After Etch

θ MAX	37.5
θ MIN	(7.5)
$\Delta\theta$	(30.0)

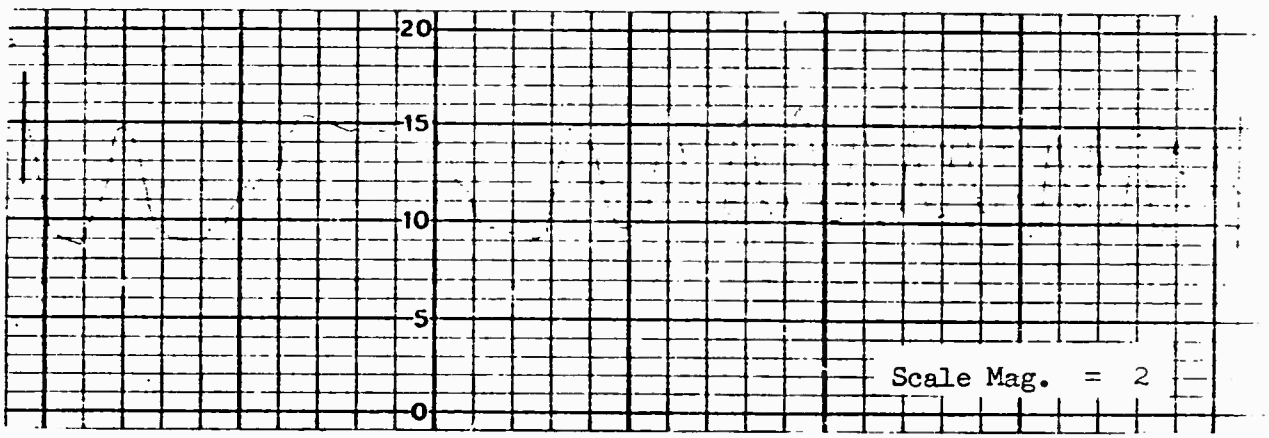

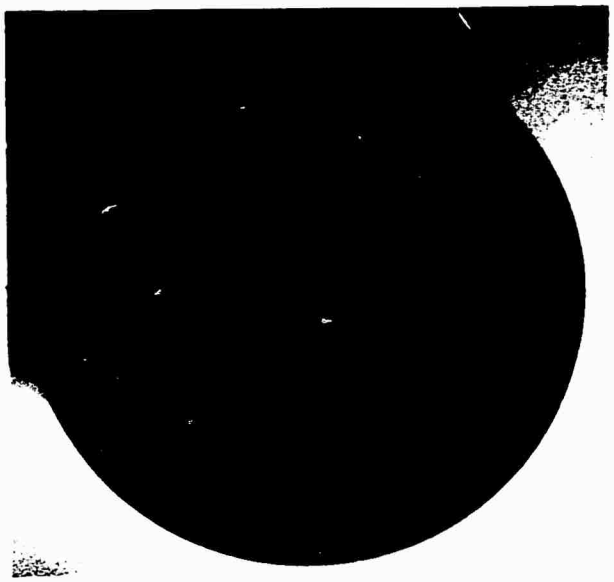

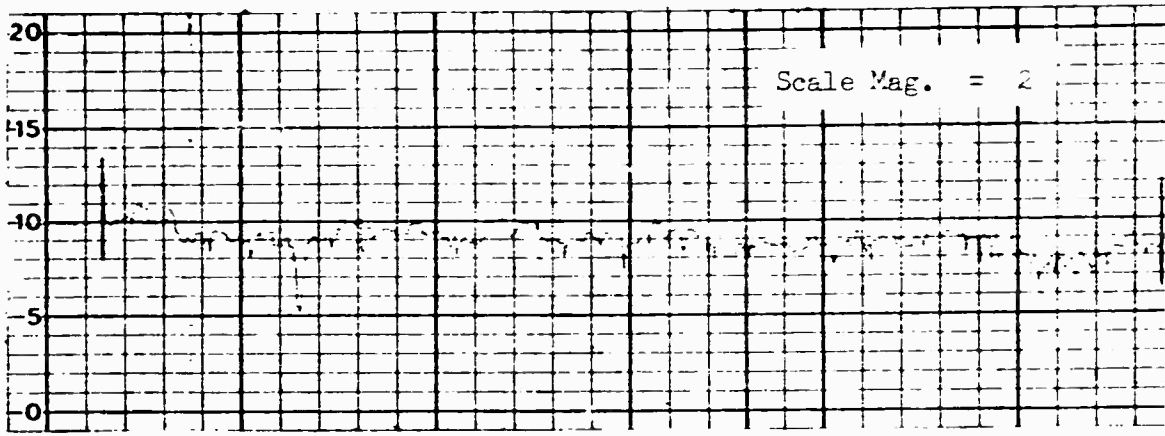

Photo Mag. = 3.7X

CLA = 22.0
RMS = 24.4

FGLP-CS-3A (M) Before E

θ MAX	52.0
θ MIN	11.0
$\Delta\theta$	41.0

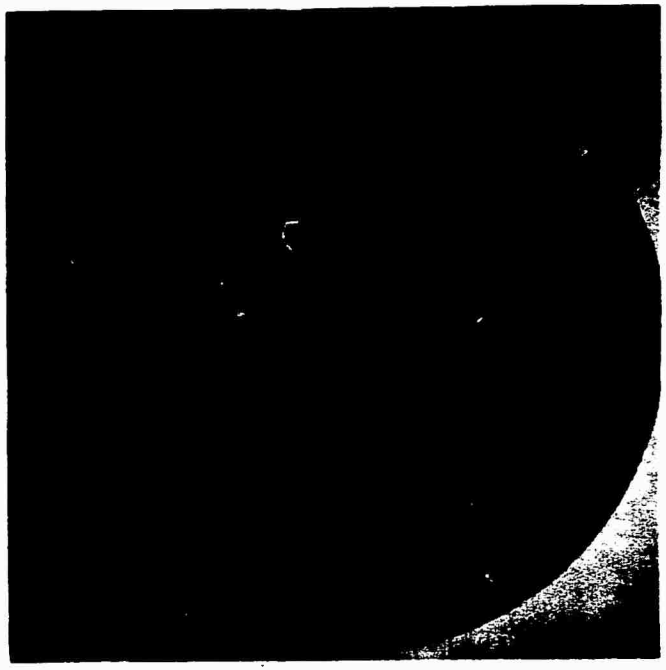

Photo Mag. = 4.5X

CLA = 41.0
RMS = 45.5

FGLP-CS-3A (E) After Et

θ MAX	8.0
θ MIN	2.0
$\Delta\theta$	6.0

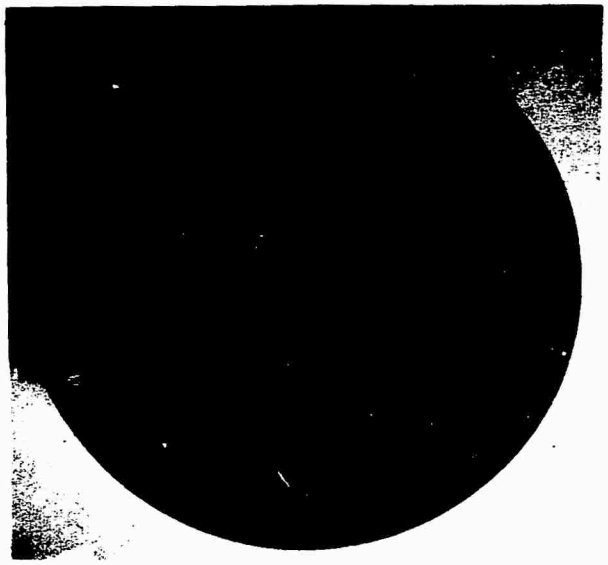

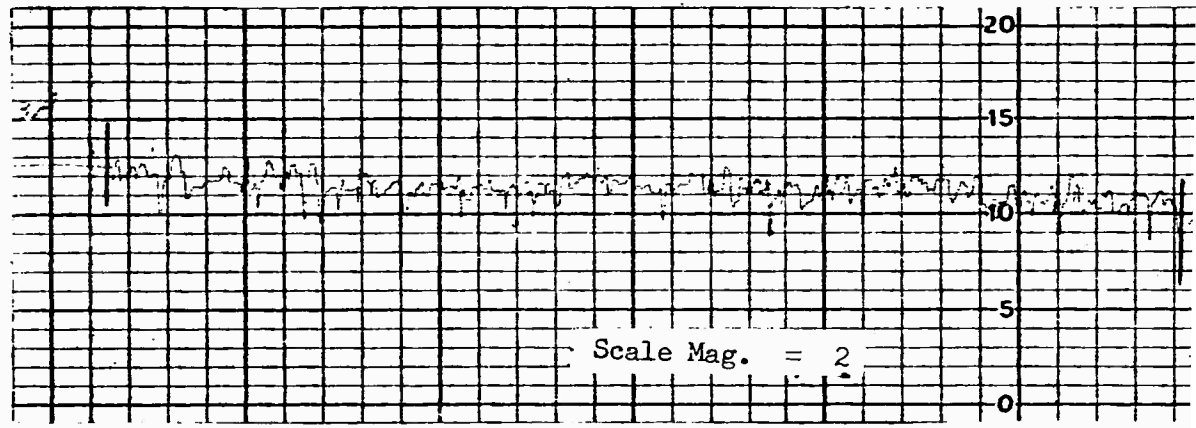

Photo Mag. = 37.X

FGHP-CS-3A (M) Before Etch

CLA	= 45.0	θ MAX	47.5
RMS	= 50.0	θ MIN	14.5
		$\Delta\theta$	33.0

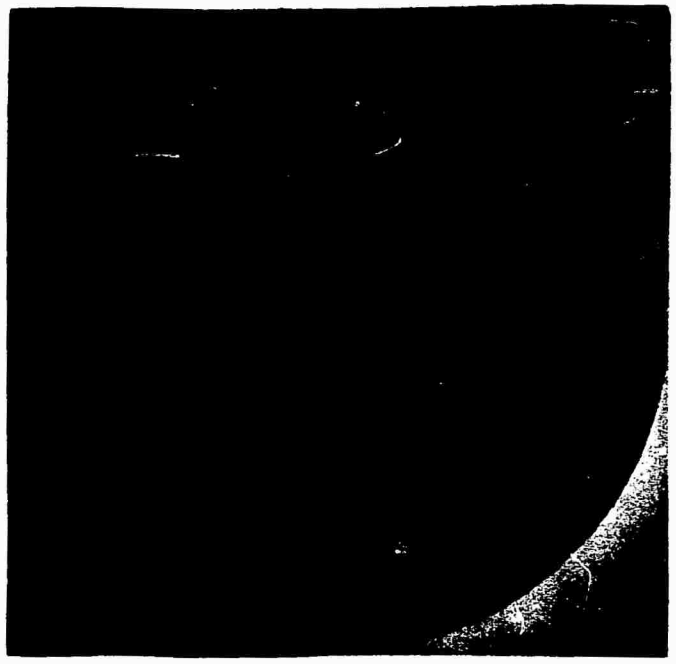

Photo Mag. = 4.5X

FGHP-CS-3A (E) After Etch

CLA	= 48.0	θ MAX	0.5
RMS	= 53.3	θ MIN	<0.5
		$\Delta\theta$	--

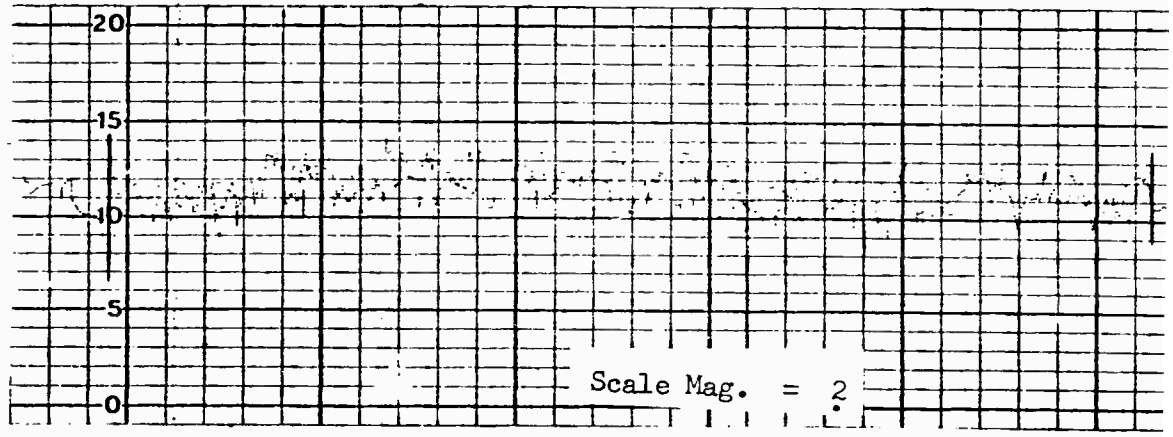

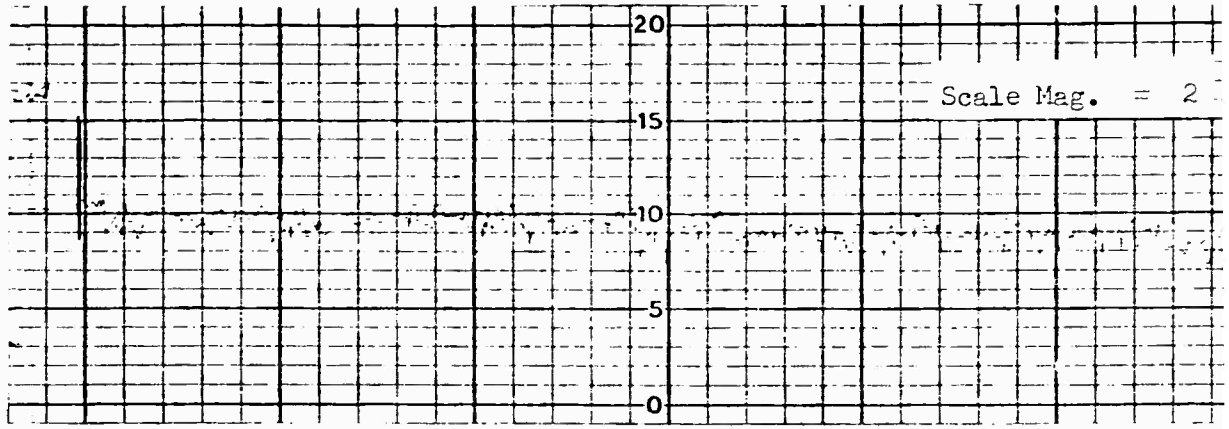

Photo Mag. = 3.7X

CLA = 25.0
RMS = 27.7

CGLP-CS-3A (M) Before Etch

θ MAX	61.0
θ MIN	17.0
$\Delta\theta$	44.0

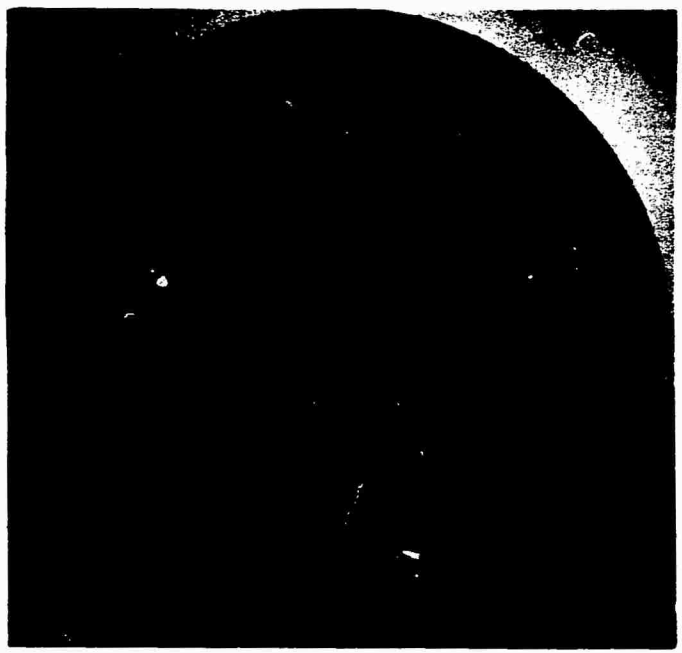

Photo Mag. = 4.5X

CLA = 35.0
RMS = 38.8

CGLP-CS-3A (E) After Etch

θ MAX	7.0
θ MIN	2.0
$\Delta\theta$	5.0

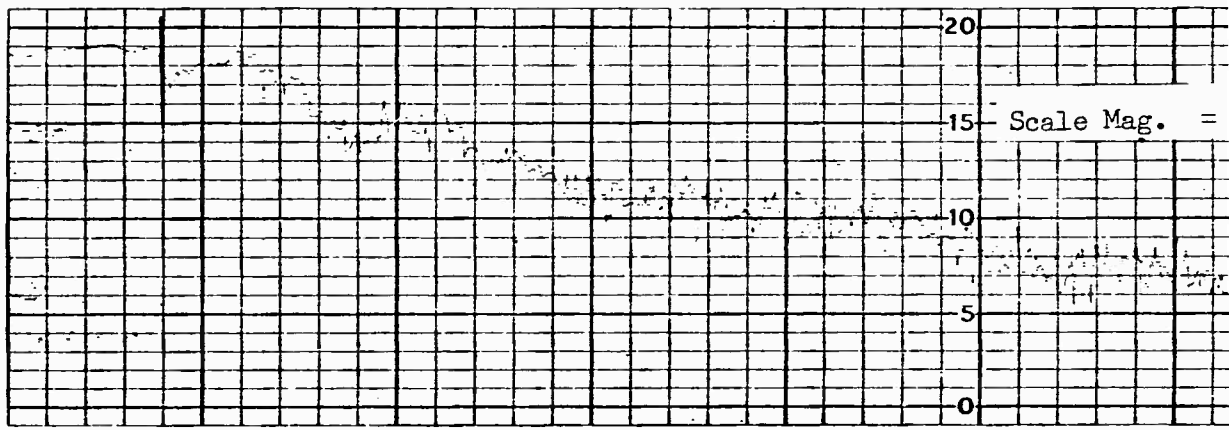

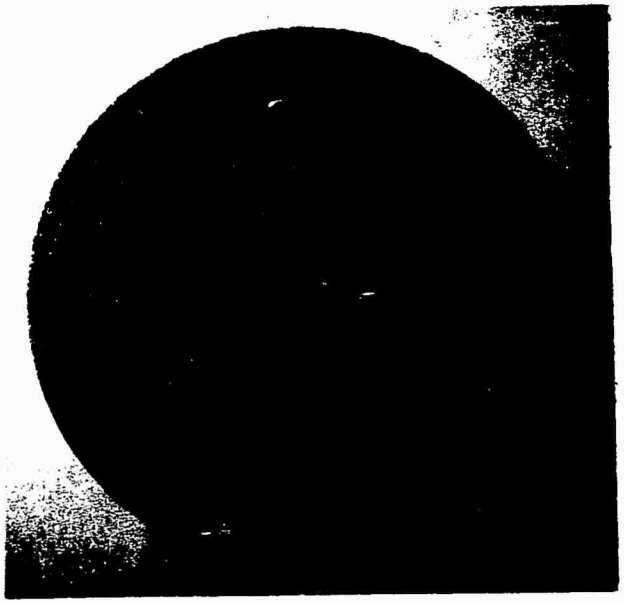

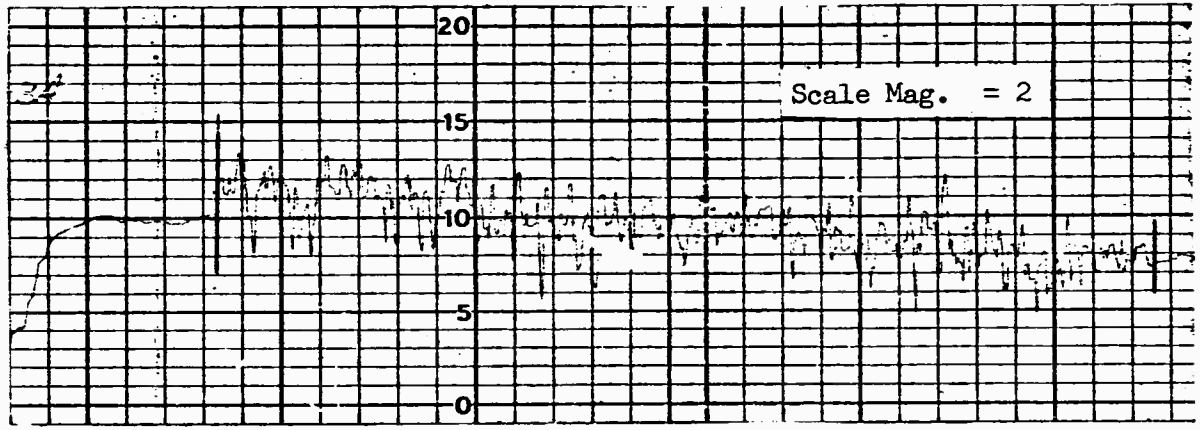

Photo Mag. = 3.7X

CLA = 48.0
RMS = 53.3

CGHP-CS-3A (M) Before Etch

θ MAX	76.0
θ MIN	4.0
$\Delta\theta$	72.0

Photo Mag. = 4.5X

CLA = 80.0
RMS = 88.8

CGHP-CS-3A (E) After Etch

θ MAX	7.0
θ MIN	1.0
$\Delta\theta$	6.0

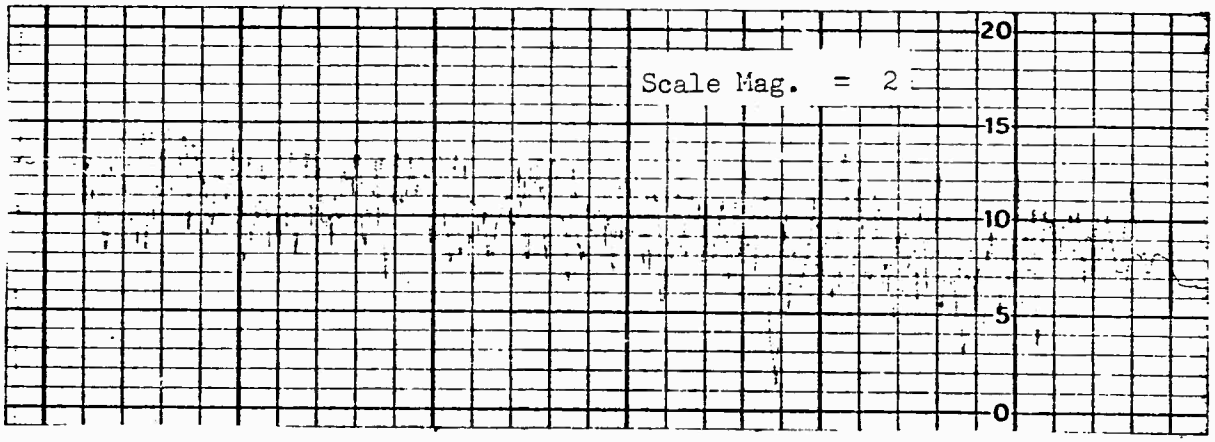

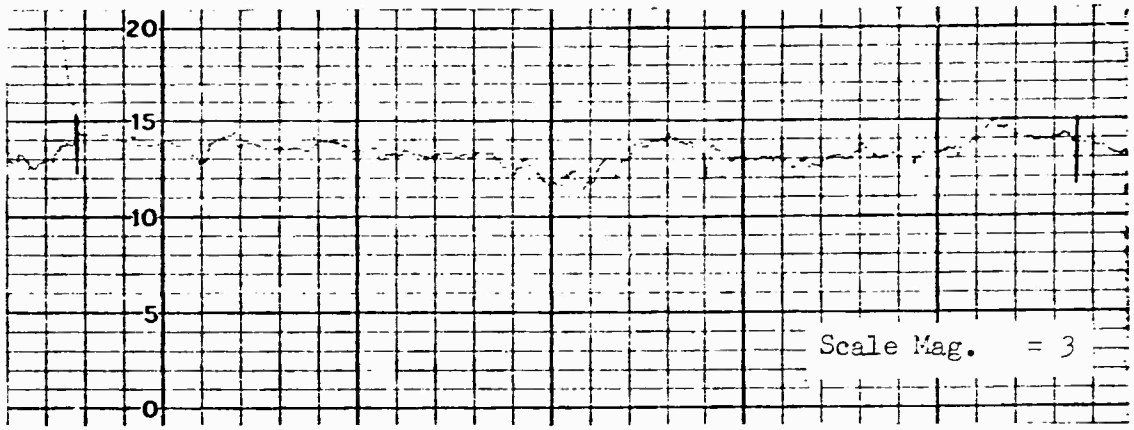

Photo Mag. = 2.7X

CLA = 1.2
RMS = 1.3

1 LS-3A (M) Before Etch

θ MAX	66.0
θ MIN	21.5
$\Delta\theta$	44.5

Photo Mag. = 2.7X

CLA = 7.0
RMS = 7.8

1 LS-3A (E) After Etch

θ MAX	70.0
θ MIN	(12.5)
$\Delta\theta$	(57.5)

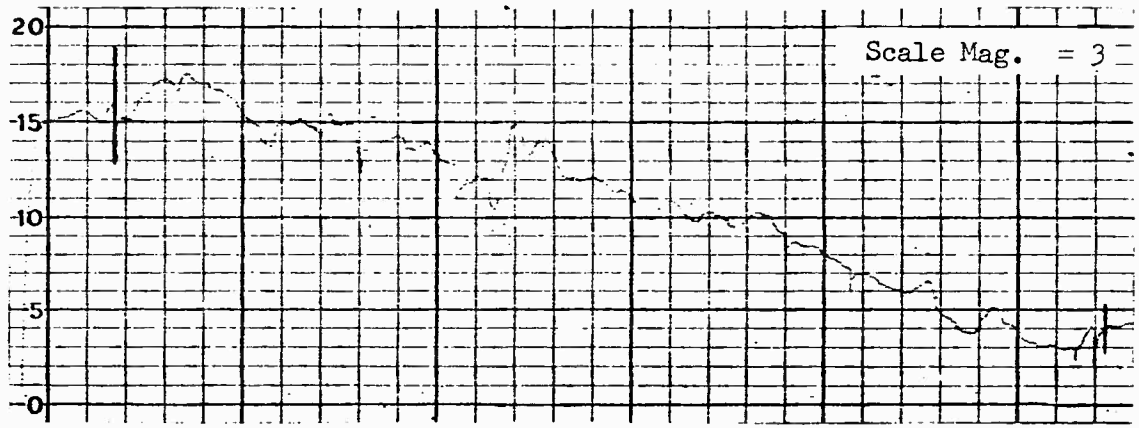

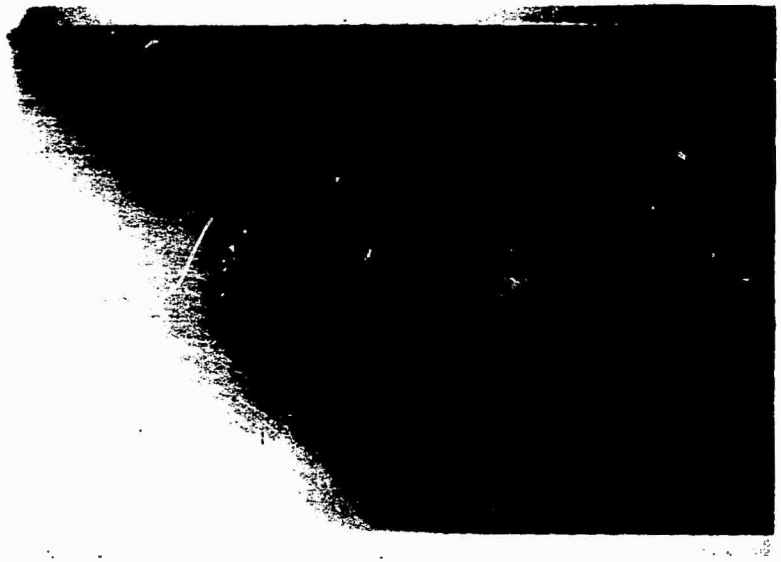

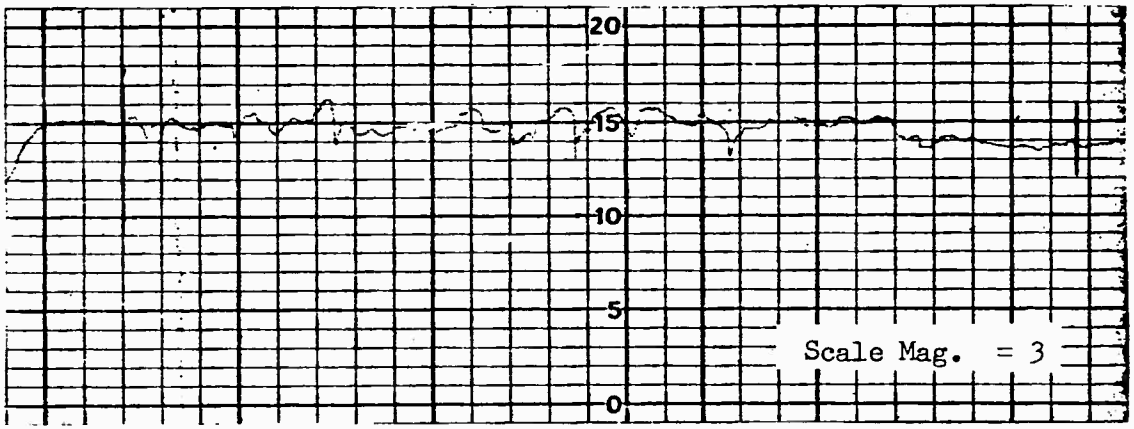

Photo Mag. = 2.7X

CLA = 4.5
RMS = 5.0

5 LS-3A (M) Before Etch

θ MAX	87.0
θ MIN	36.0
$\Delta\theta$	51.0

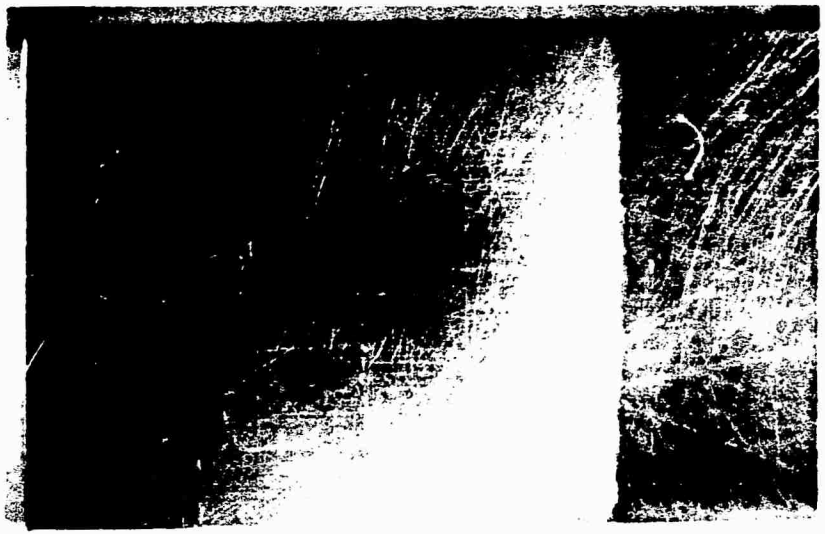

Photo Mag. = 2.7X

CLA = 7.0
RMS = 7.8

5LS-3A (E) After Etch

θ MAX	74.0
θ MIN	19.0
$\Delta\theta$	55.0

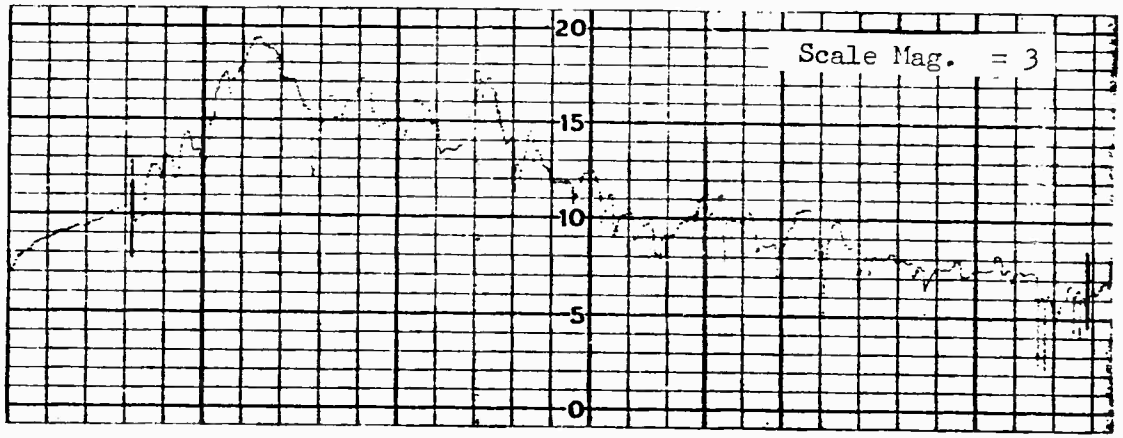

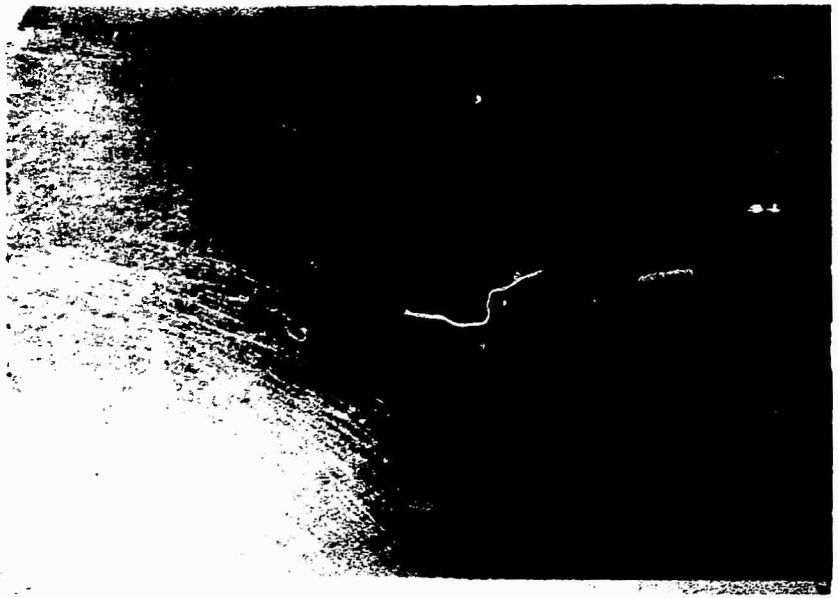

Photo Mag. = 2.9X

7 LS-3A (M) Before Etch

CLA	= 7.2
RMS	= 8.0

θ MAX	70.0
θ MIN	15.5
$\Delta\theta$	54.5

Photo Mag. = 2.7X

7 LS-3A (E) After Etch

CLA	= 9.0 - 9.5
RMS	= 10.0 - 10.6

θ MAX	64.0
θ MIN	(7.0)
$\Delta\theta$	(57.0)

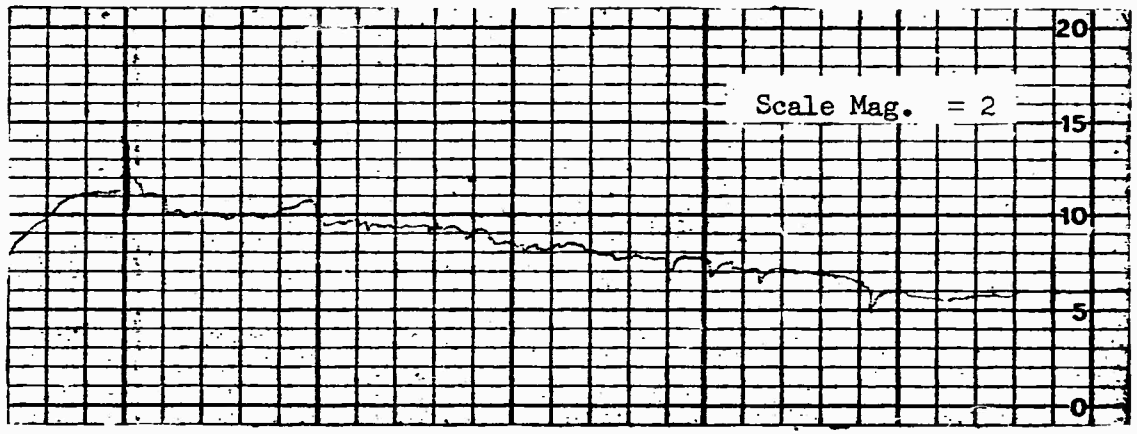

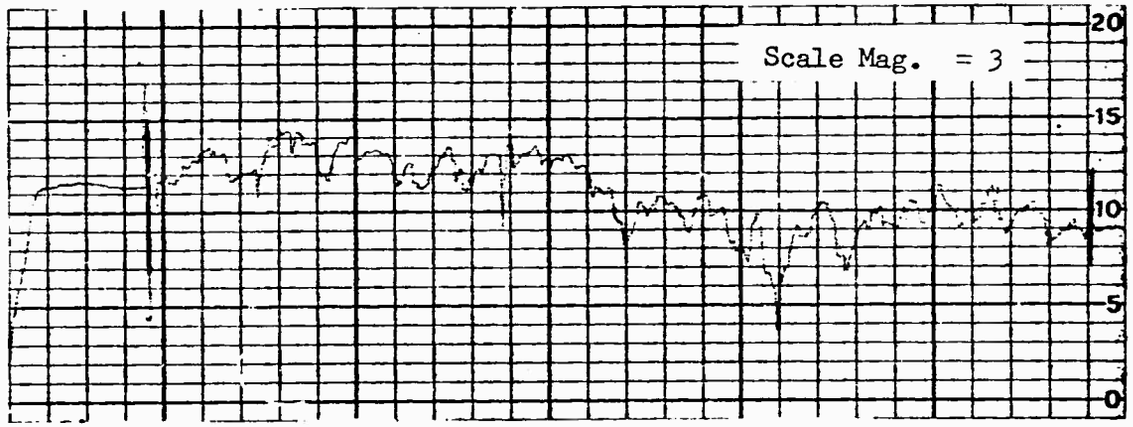

Photo Mag. = 2.7X

CLA = 8.5
RMS = 9.4

10 LS-3A (M) Before Etch

θ MAX	62.0
θ MIN	19.0
$\Delta\theta$	43.0

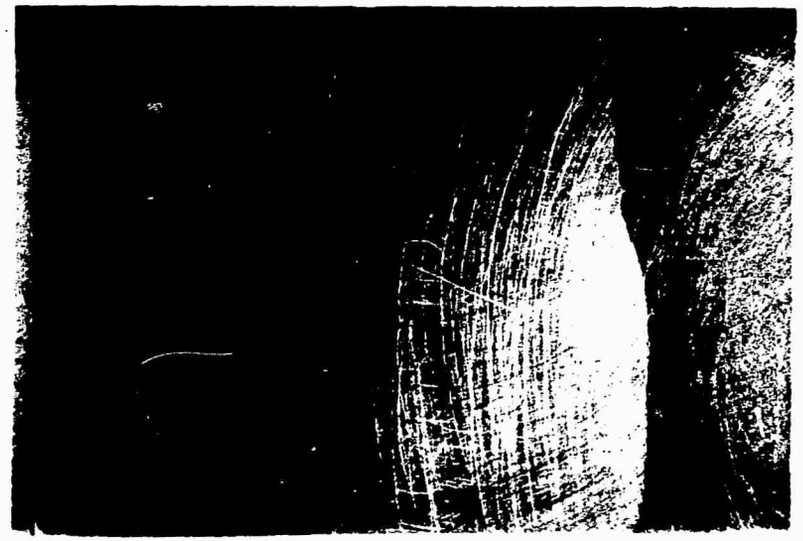

Photo Mag. = 2.7X

CLA = 10.8 - 11.0
RMS = 12.0 - 12.2

10 LS-3A (E) After Etch

θ MAX	79.0
θ MIN	10.5
$\Delta\theta$	68.5

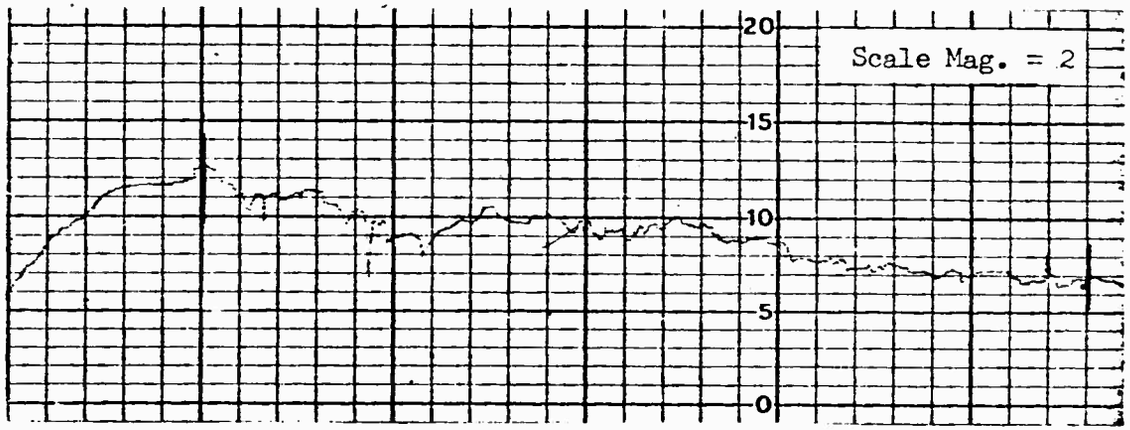

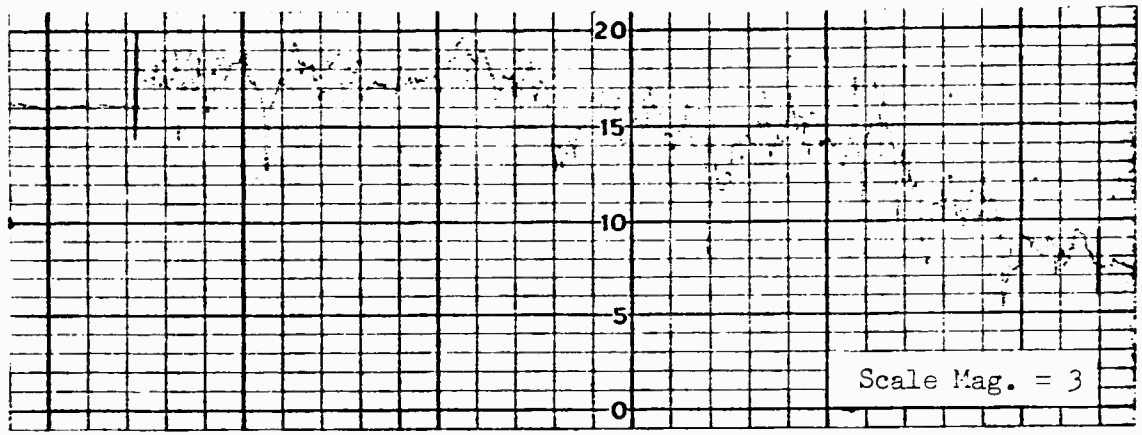

Photo Mag. = 2.7X

CLA = 17.0
RMS = 18.9

20 LS-3A (M) Before Etch

θ MAX 69.0
θ MIN 19.5
$\Delta\theta$ 49.5

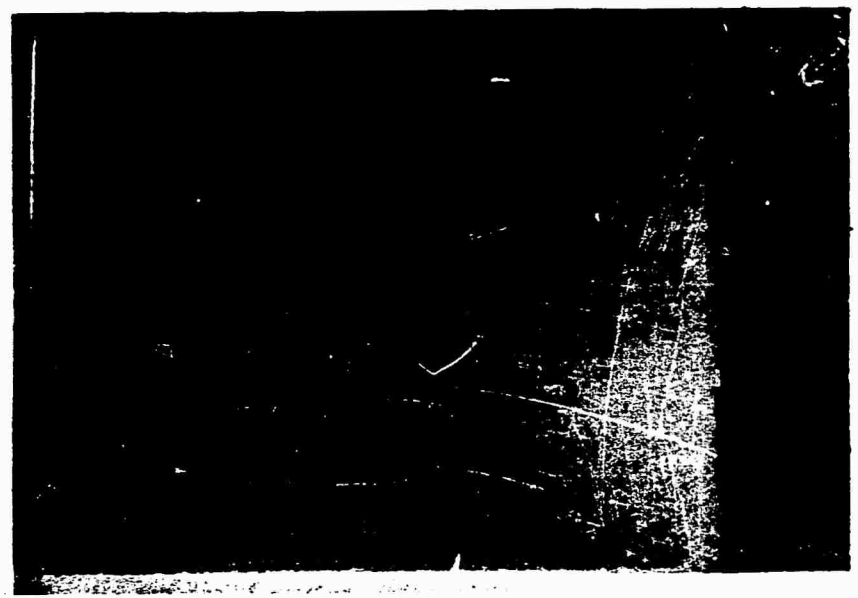

Photo Mag. = 2.7X

CLA = 32.0
RMS = 35.5

20 LS-3A (E) After Etch

θ MAX 62.0
θ MIN 16.0
$\Delta\theta$ 46.0

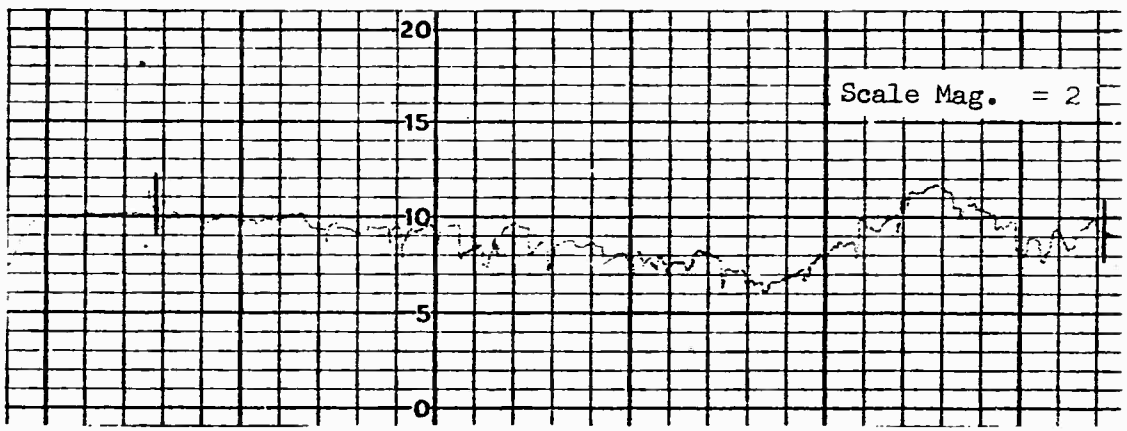

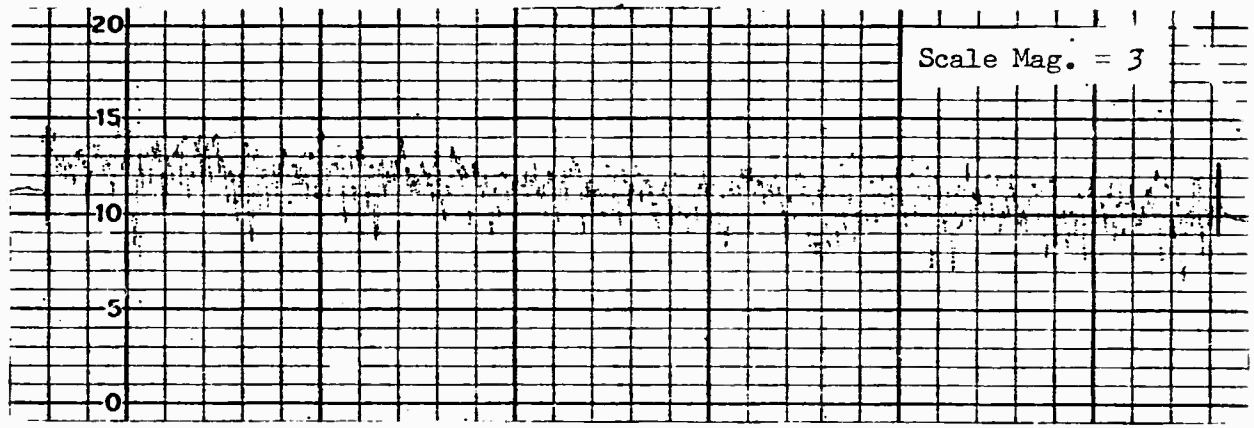

Photo Mag. = 2.9X

CLA = 21.0
RMS = 23.3

40 LS-3A (M) Before Etch

θ MAX 75.0
θ MIN 14.0
$\Delta\theta$ 61.0

Photo Mag. = 2.9X

CLA = 22.0
RMS = 24.4

40 LS-3A (E) After Etch

θ MAX 23.5
θ MIN 7.5 (irregular droplet)
$\Delta\theta$ 16.0

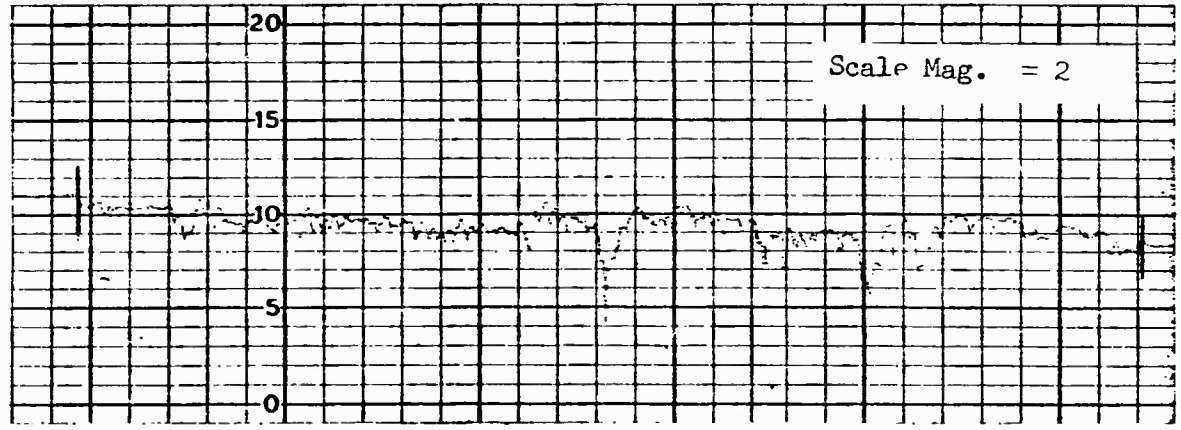

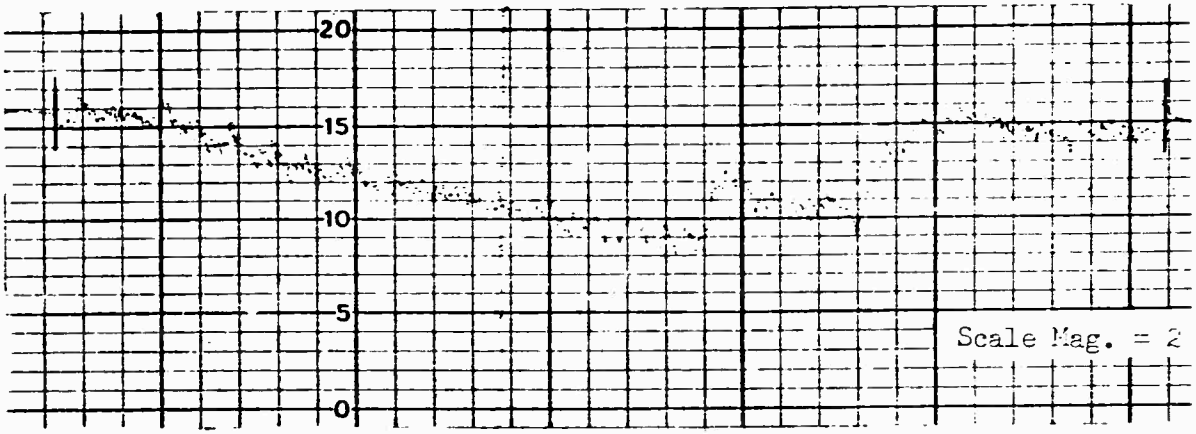

Photo Mag. = 2.9X

CLA = 36.0 - 38.0
RMS = 40.0 - 42.0

80 LS-3A (M) Before Etch

θ MAX	63.0
θ MIN	25.0
$\Delta\theta$	38.0

Photo Mag. = 2.8X

CLA = 32.0
RMS = 35.5

80 LS-3A (E) After Etch

θ MAX	56.0
θ MIN	13.5
$\Delta\theta$	42.5

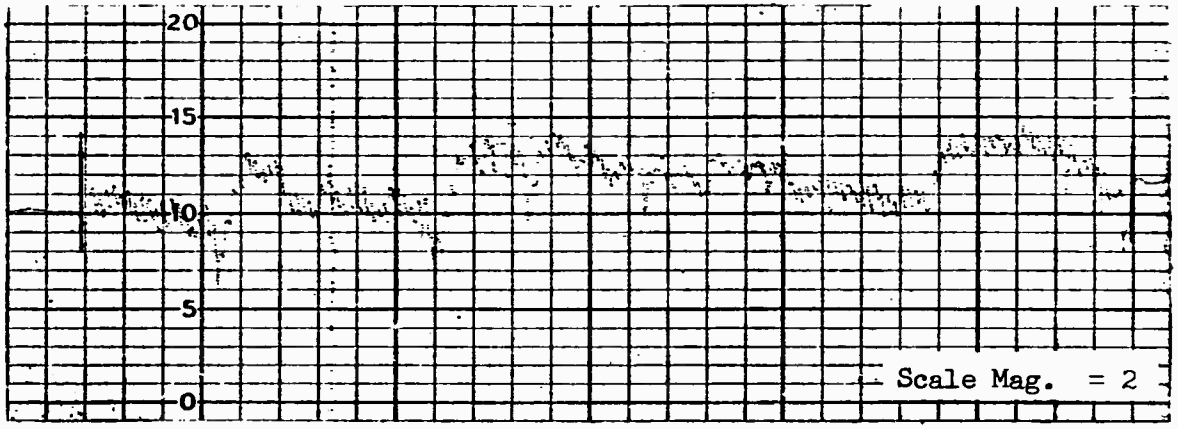

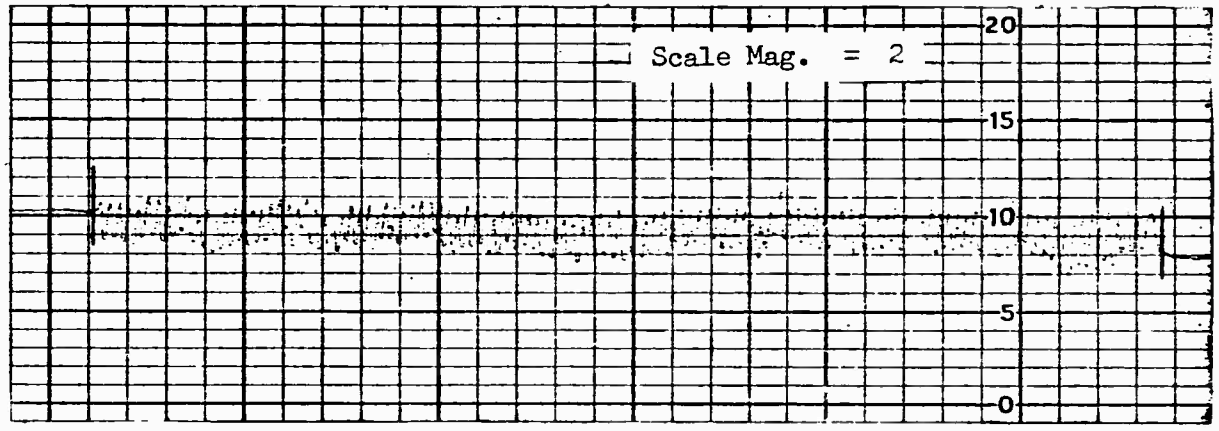

Photo Mag. = 2.9X

110 LS-3A (M) Before Etch

CLA	= 47.0	θ MAX	66.5
RMS	= 52.2	θ MIN	26.5
		$\Delta\theta$	40.0

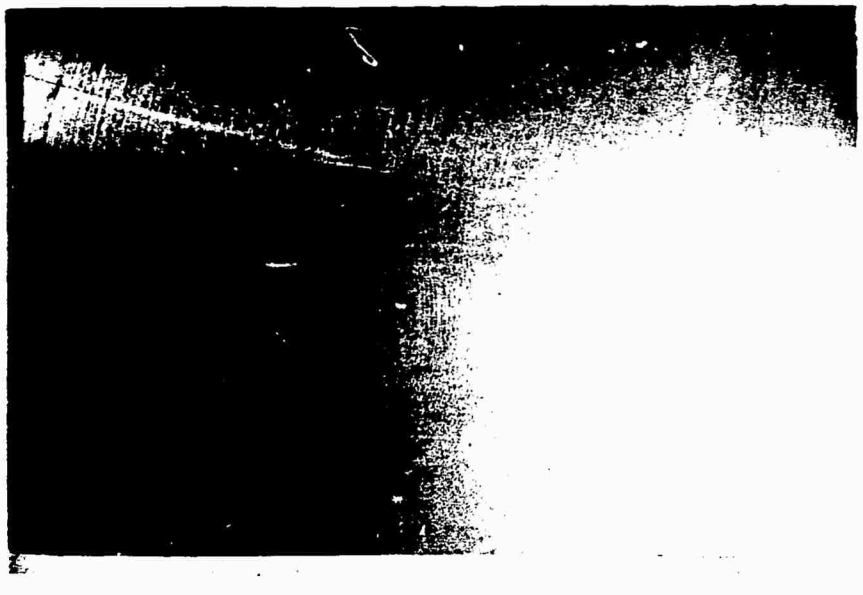

Photo Mag. = 2.8X

110 LS-3A (E) After Etch

CLA	= 58.0	θ MAX	17.0
RMS	= 64.4	θ MIN	2.5 (Irregular droplet)
		$\Delta\theta$	14.5

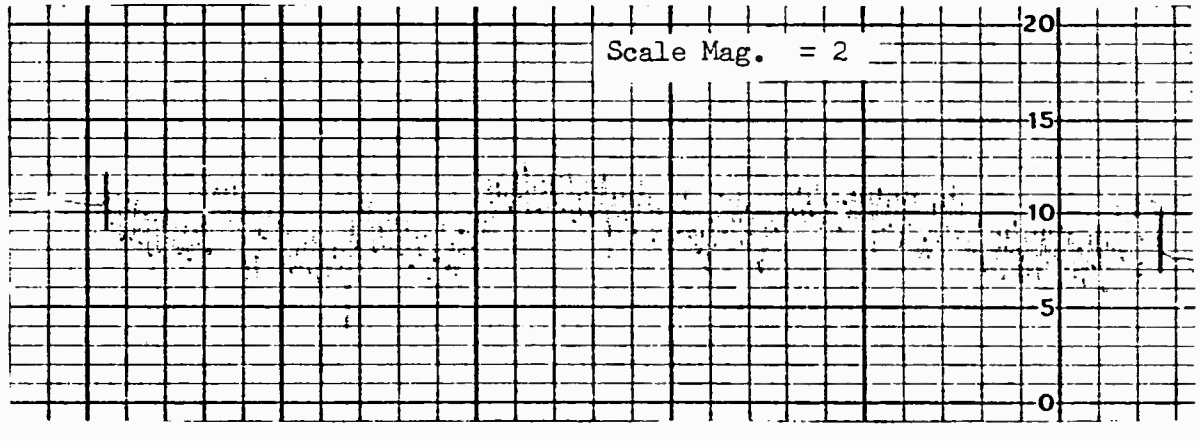

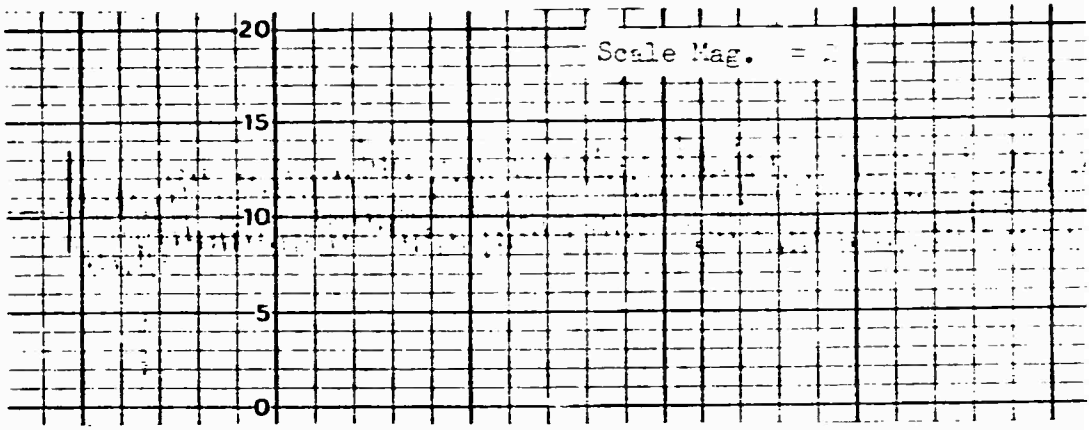

Photo Mag. = 2.9X

CLA = 72.0
RMS = 80.0

150 LS-3A (M) Before E

θ MAX 79.0
θ MIN 22.0
$\Delta\theta$ 57.0

Photo Mag. = 2.8X

CLA = 72.0
RMS = 80.0

150 LS-3A (E) After Et

θ MAX 86.0
θ MIN 19.0
$\Delta\theta$ 67.0

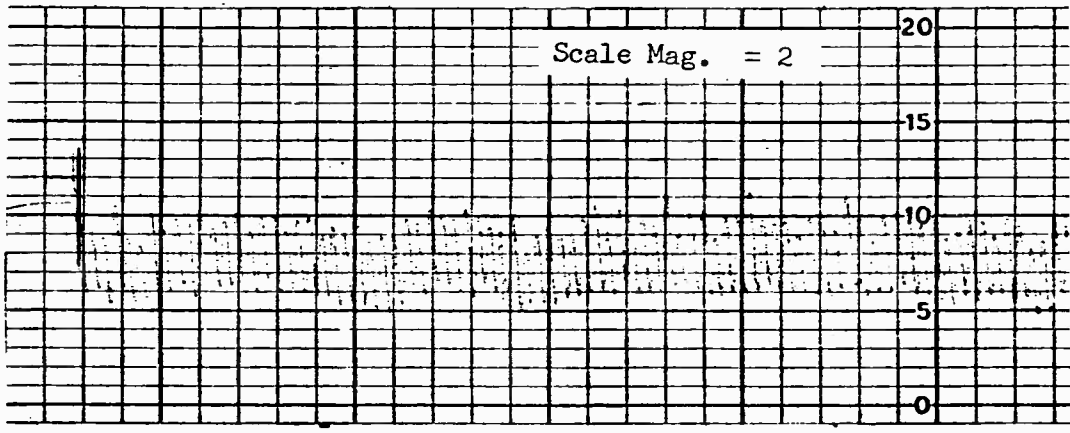

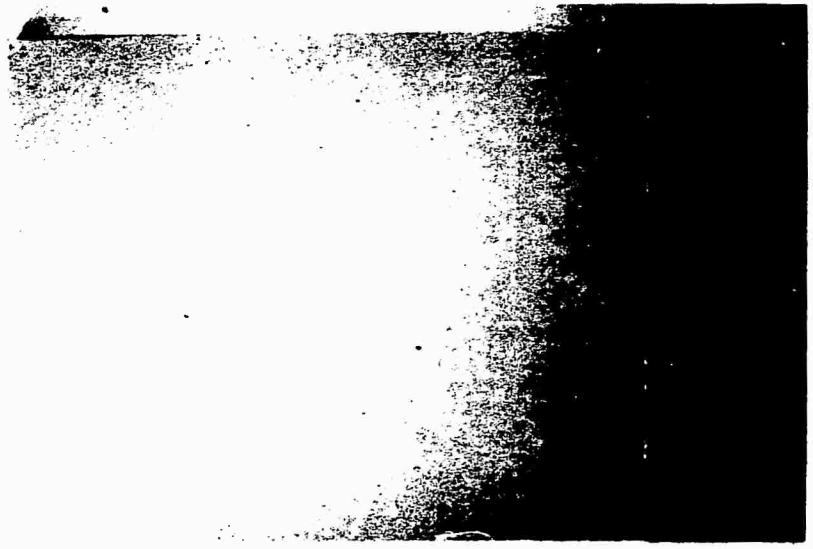

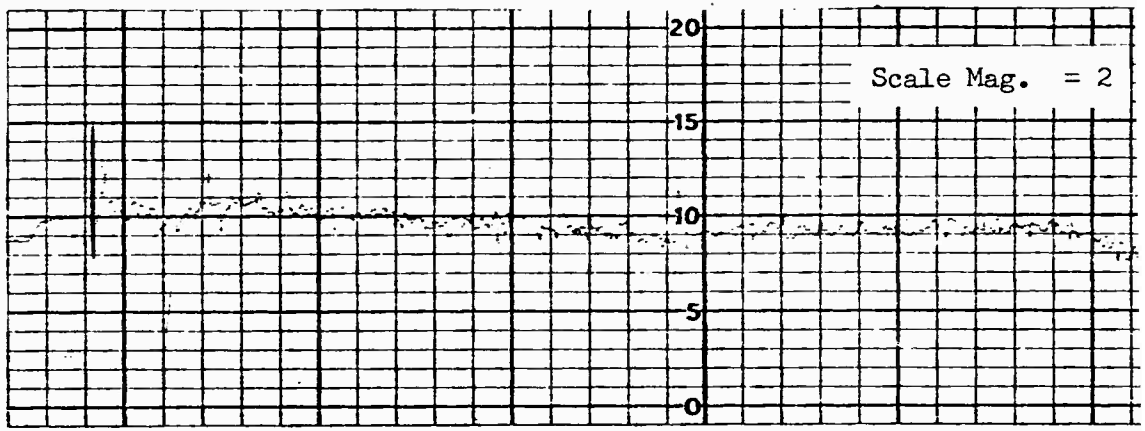

Photo Mag. = 2.7X

CLA = 20.0
RMS = 22.2

FGLP-LS-3A (M) Before Et

θ MAX	58.5
θ MIN	10.5
$\Delta\theta$	48.0

Photo Mag. = 2.8X

CLA = 20.0
RMS = 22.2

FGLP-LS-3A (E) After Etcl

θ MAX	74.0
θ MIN	18.5
$\Delta\theta$	55.5

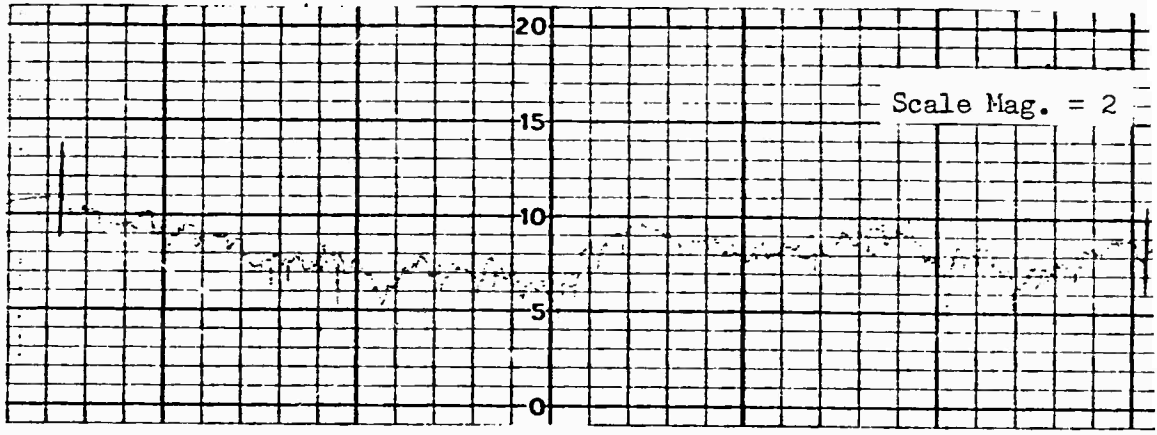

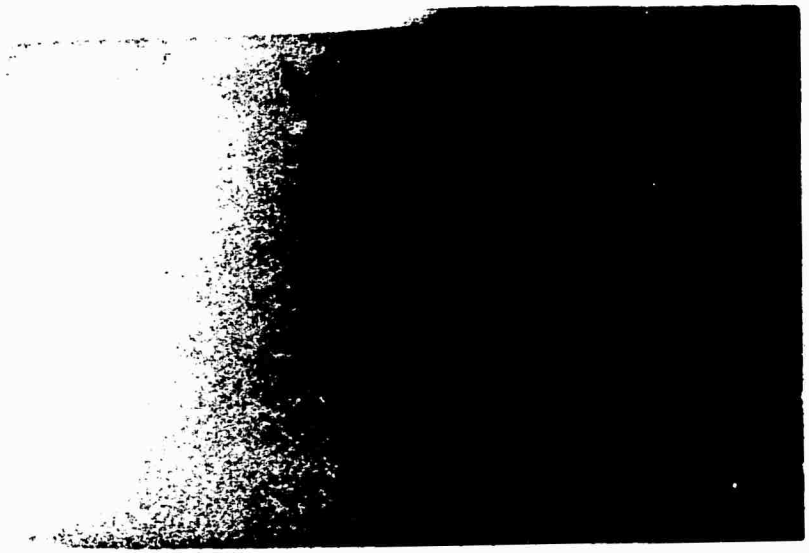

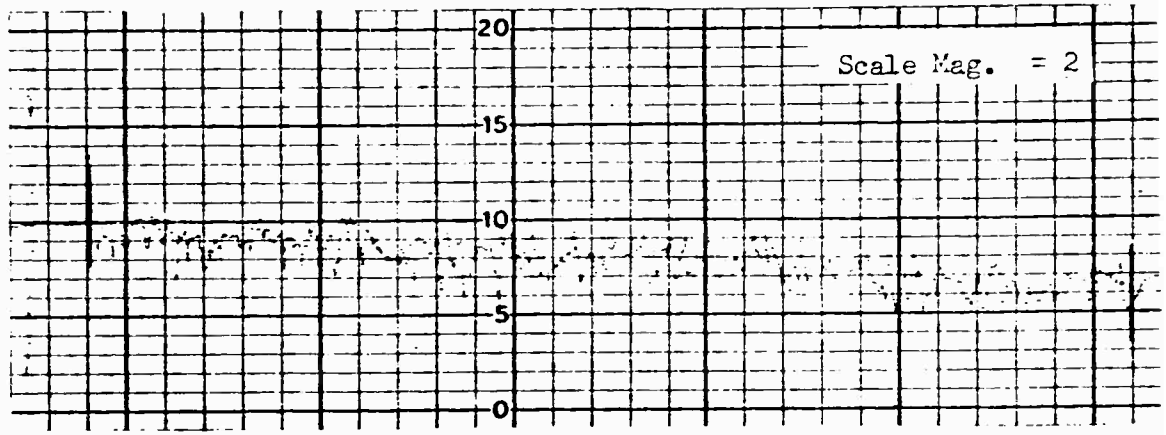

Photo Mag. = 2.7X

CLA = 32.5
RMS = 35.6

FGHP-LS-3A (M) Before Etch

θ MAX 39.0
θ MIN 14.0
$\Delta\theta$ 25.0

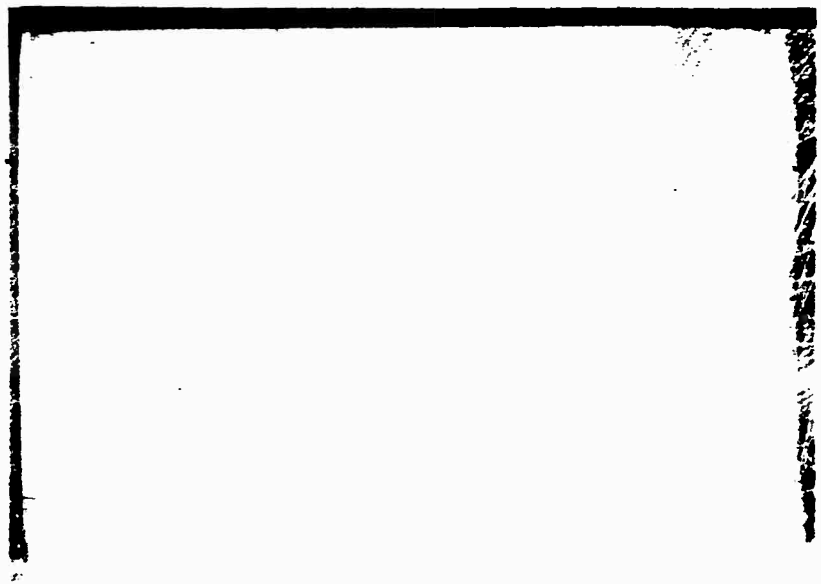

Photo Mag. = 2.8X

CLA = 45.0
RMS = 50.0

FGHP-LS-3A (E) After Etch

θ MAX = 63.5
θ MIN = 15.0
$\Delta\theta$ 48.5

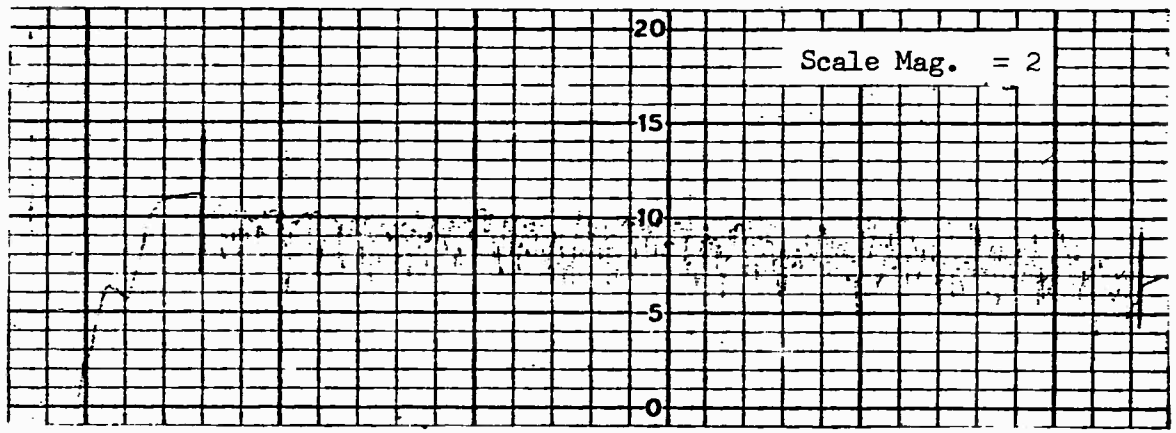

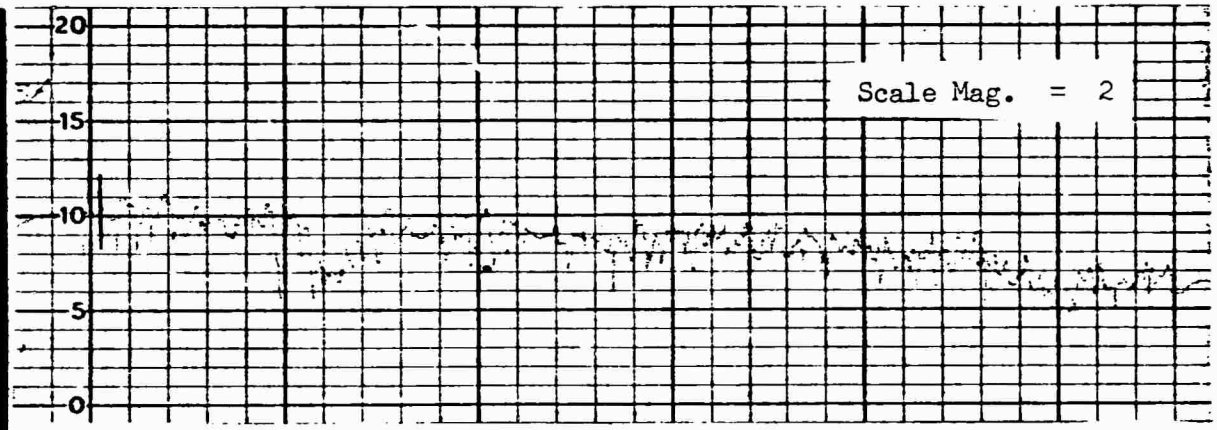

Photo Mag. = 2.7X

CLA = 34.0
RMS = 38.8

CGLP-LS-3A (M) Before Etch

θ MAX 81.5
θ MIN 18.0
$\Delta\theta$ 63.5

Photo Mag. = 2.8X

CLA = 36.0
RMS = 39.9

CGLP-LS-3A (E) After Etch

θ MAX 13.0
θ MIN 3.0
$\Delta\theta$ 10.0

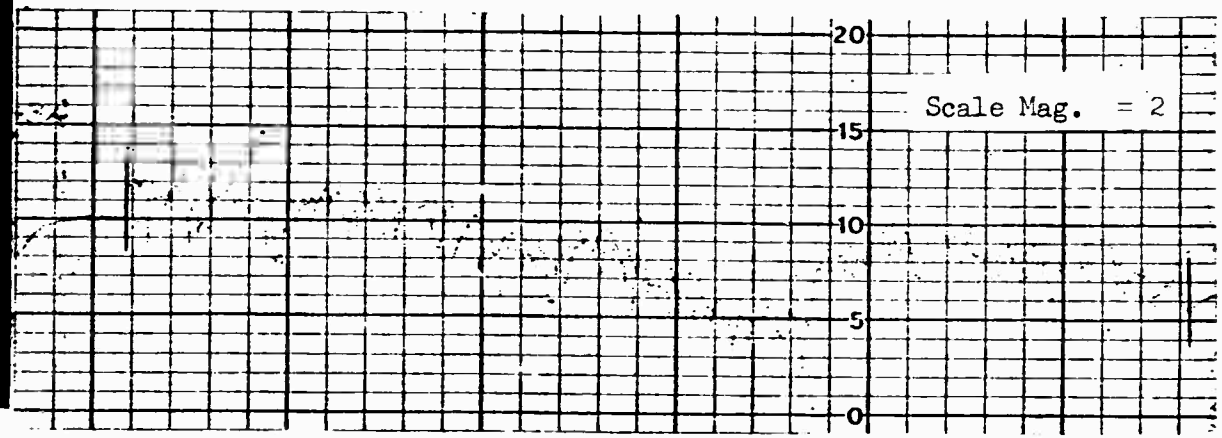

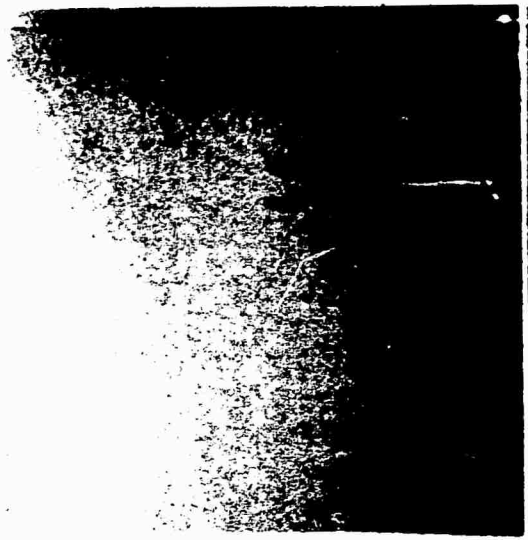

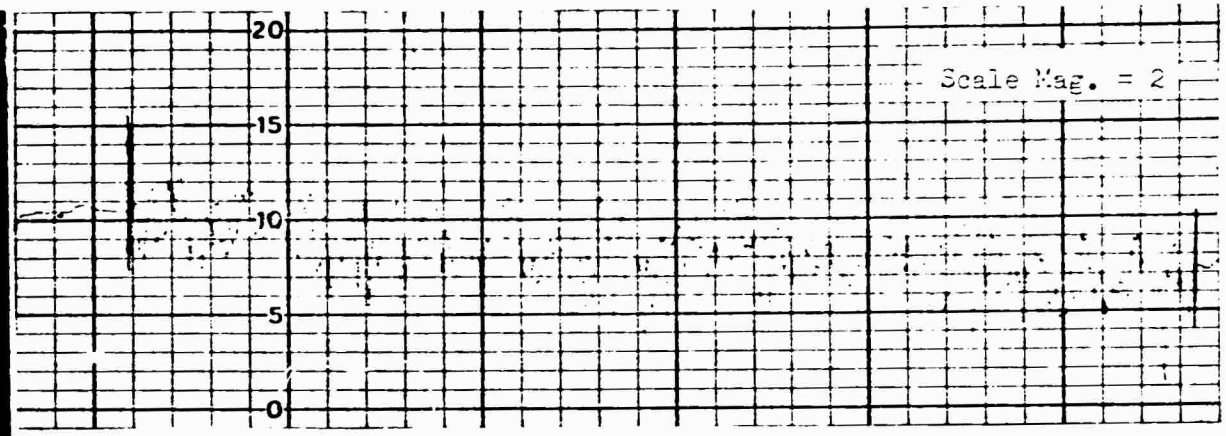

Photo Mag. = 2.7X

CLA = 55.0
RMS = 61.0

CGHP-LS-3A (M) Before Etch

θ MAX	83.5
θ MIN	25.0
$\Delta\theta$	58.5

Photo Mag. = 2.8X

CLA = 60.0
RMS = 66.6

CGHP-LS-3A (E) After Etch

θ MAX	88.0+
θ MIN	31.0
$\Delta\theta$	57.0

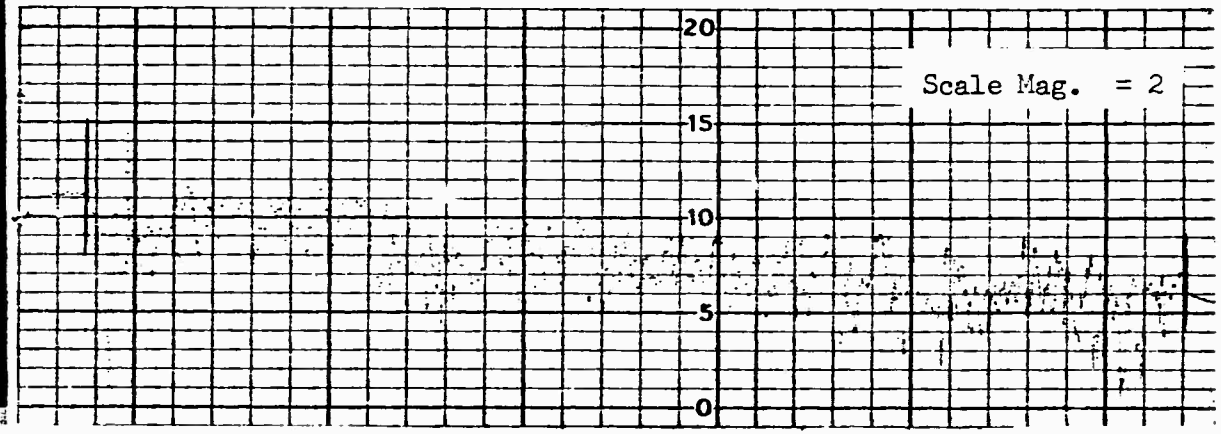

APPENDIX II

CALCULATION OF SUBSTRATE SURFACE FREE ENERGY

TABLE I

Calculation of Surface Free Energies

Specimen Type: BUTT TENSILE k_o = 0.500 γ_L = 72.8 ergs/ cm^2

Code	Specimen 1A			Specimen 2A			Specimen 3A			Average
	Bond Strength psi	Bondline Thickness inch	γ_{L_S} ergs/cm^2	Bond Strength psi	Bondline Thickness inch	γ_{L_S} ergs/cm^2	Bond Strength psi	Bondline Thickness inch	γ_{L_S} ergs/cm^2	γ_L ergs/cm^2
1	3900	.0055	93.91	3750	.003[illegible]	[illegible].39	3[illegible]00	.00[illegible]	[illegible]	[illegible]
5	5770	.0044	111.15	4780	.00[illegible]	[illegible]7.90	55[illegible]0	.00[illegible]	10[illegible]	131.[illegible]
7	3600	.0100	157.61	3920	.004[illegible]	[illegible]0.[illegible]	5190	.00[illegible]	15[illegible]	1[illegible]0.1[illegible]
10	4100	.0071	127.45	5040	.0066	145.64	2660	.004[illegible]	[illegible]8.91	107.33
20	5580	.0076	185.67	6930	.0069	197.21	4750	.0059	114.3	165.75
40	4070	.0061	108.70	3920	.0069	111.56	4240	.0052	96.53	105.60
80	5300	.0047	109.06	4210	.0064	117.97	5100	.00[illegible]7	149.[illegible]	125.[illegible]
110	4450	.0083	161.71	4080	.0075	133.97	3630	.00[illegible]1	12[illegible].73	141.47
150	5750	.0077	193.84	5510	.00[illegible]9	11[illegible].21	5320	.0060	139.[illegible]	1[illegible].[illegible]
FGLP	7590	.0061	202.71	5210	.005[illegible]	1[illegible]7.[illegible]	7300	.00[illegible]5	145.[illegible]	1[illegible].09
FGHP	6930	.0066	200.25	7160	.005[illegible]	1[illegible].[illegible]	5560	.0055	133.[illegible]	171.9[illegible]
CGLP	5110	.0073	163.32	6720	.0060	176.[illegible]3	4710	.00[illegible]6	94.[illegible]	144.90
CGHP	6110	.0044	117.70	5760	.0027	68.09	6770	.0053	157.09	114.29

TABLE I (Continued)

Code	Cos θ Max (M)	Cos θ Max (E)	Max (M) γ_S ergs/cm^2	Max (E) γ_S ergs/cm^2	Cos θ Min (M)	Cos θ Min (E)	Min (M) γ_S ergs/cm^2	Min (E) γ_S ergs/cm^2	CLA (M) μin	CLA (E) μin
1	.31730	.70091	98.08	126.01	.93042	.98769	142.71	146.88	1.2	10.0
5	.18224	.81412	115.19	161.19	.90631	.98629	167.90	173.72	6.0	14.0
7	.23053	.60876	139.67	174.49	.97630	.96363	201.24	200.32	9.2	15.0
10	.11320	.58779	115.57	150.12	.98769	.98902	179.23	179.33	14.4	24.0
20	.34202	.80902	190.65	224.65	.97630	.97237	236.82	236.54	7.0	14.0
40	.44620	.94552	138.08	174.43	.99756	.99619	178.22	178.12	37.5	35.0
80	.19937	.73135	140.05	178.78	.97630	.99540	196.61	198.01	63.0	45.0
110	.16505	.84339	153.49	202.87	.95372	.99027	210.90	213.56	62.0	60.0
150	.11320	.68835	158.84	200.71	.89101	.97815	215.47	221.31	54.0	77.0
FGLP	.55919	.71325	198.80	210.01	.93969	.98629	226.50	229.79	22.0	25.0
FGHP	.55919	.51540	212.69	209.50	.93969	.985 est.	240.39	243.69	29.0	50.0
CGLP	.24192	.56070	162.51	187.17	.96303	.98325	215.05	216.46	31.0	30.0
CGHP	.20791	.76041	129.43	169.65	.97437	.98769	165.22	166.19	55.0	70.0

TABLE II

Calculation of Surface Free Energies

Specimen Type: CORE SHEAR $\qquad k_o = 0.833 \qquad \gamma_L = 72.8$ [illegible] cm^2

Code	Specimen 1A Bond Strength psi	Specimen 1A Bondline Thickness inch	Specimen 1A γ_L erg/cm	Specimen [illegible] Bond Strength psi	Specimen [illegible] Bondline Thickness inch	Specimen [illegible] γ_L erg/cm	Specimen [illegible] Bond Strength psi	Specimen [illegible] Bondline Thickness inch	γ	γ
1	[illegible]	.00?7	13?.??	[illegible]	[illegible]	[illegible]	[illegible]	[illegible]	[illegible]	[illegible]
[illegible]	[illegible]	.005?	51.??	1?7?	[illegible]	[illegible]		[illegible]		[illegible]
[illegible]	1?10	.005?	61.07	1?90	[illegible]	[illegible]	[illegible]	[illegible]		[illegible]
10	?310	.0051	85.93	3000	[illegible]	9?.?3	[illegible]	[illegible]	[illegible]	[illegible]
[illegible]	[illegible]	.0063	1??.??	?370	.009?	[illegible]	20??	[illegible]	[illegible]	[illegible]
40	2?40	.008?	156.??	29?0	[illegible]	17?.??	30??	.?7?	[illegible]	[illegible]
60	2320	.0074	1?5.22	4710	[illegible]	[illegible]	[illegible]	[illegible]	[illegible]	[illegible]
110	3280	.0056	133.9?	2000	.005?	[illegible]	?90	[illegible]	[illegible]	[illegible]
150	1610	.0060	70.4?	2470	.007?	135.1?	[illegible]	[illegible]	[illegible]	[illegible]
FGLP	4440	.0081	262.33	4160	.0066	2?0.?7	1400	[illegible]	[illegible]	[illegible]
FGHP	1540	.0055	61.78	51?0	.0046	17?.?0	4260	.0049	[illegible]	[illegible]
CGLP	5250	.0060	229.76	4770	.0073	253.99	?730	.0057	19? ??	[illegible]
CGHP	5480	.0039	155.89	5270	.0054	207.57	5070	.0040	147 ??	17?.?6

* [illegible] range

TABLE II (Continued)

Code	Cos θ Max (M)	Cos θ Max (E)	Max (M) γ_S ergs/cm²	Max (E) γ_S ergs/cm²	Cos θ Min (M)	Cos θ Min (E)	Min (M) γ_S ergs/cm²	Min (E) γ_S ergs/cm²	CLA (M) μin	CLA (E) μin
1	.03490	.90996	103.27	166.96	.71325	.99692	152.65	173.31	[illegible]	[illegible]
5	.27564	.96593	91.80	142.05	.96593	.99692	142.05	144.31	[illegible]	[illegible]
7	.15643	.95106	93.64	151.49	.96363	.99619	152.40	154.77	9.0	[illegible]
10	.30902	.88295	126.54	168.32	.96126	.99452	174.02	176.44	8.6	[illegible]
20	.28402	.87882	184.63	227.93	.97030	.99452	234.59	236.35	23.0	17.0
40	.24192	.90631	186.82	235.19	.97630	.99257	240.28	241.54	27.3	26.0
80	.21644	.85717	136.29	182.93	.97992	.99619	191.87	193.05	55.0	[illegible]
110	[illegible]	[illegible]	[illegible]	143.45	[illegible]	[illegible]	[illegible]	[illegible]	[illegible]	[illegible]
150	.30071	.79335	[illegible]	154.30	.96593	.99144	[illegible]	[illegible]	[illegible]	[illegible]
FGLP	.61566	.99027	218.76	246.03	.96163	.99939	245.40	[illegible]	[illegible]	[illegible]
FGHP	.67559	.99996	178.13	201.75	.96815	.99996	199.43	201.75	[illegible]	[illegible]
CGLP	.46481	.99255	262.09	299.06	.95630	.99939	296.42	299.56	25.0	35.0
CGHP	.24192	.99255	188.07	242.72	.99756	.99955	243.08	243.25	[illegible]	30.0

TABLE III

Calculation of Surface Free Energies

Specimen Type: LAP SHEAR $k_o = 4.000$ $\gamma_L = 72.8$ ergs/cm^2

Code	Specimen 1A			Specimen 2A			Specimen 3A			
	Bond Strength psi	Bondline Thickness inch	γ_{L_g} ergs/cm^2	Bond Strength psi	Bondline Thickness inch	γ_{L_g} ergs/cm^2	Bond Strength psi	Bondline Thickness inch	γ_{L_g} ergs/cm^2	γ_L ergs/cm^2
1	1360	.0021	100.03	1320	.0039	180.31	910	.0017	[illegible]	[illegible]
5	1260	.0026	114.74	1390	.0010	46.59	910	.003	101.99	[illegible]
7	1240	.0050	217.16	1320	.0020	92.47	1100	.00131	[illegible]	[illegible]
10	1100	.0012	48.76	1280	.0023	103.11	1000	.0032	139.10	[illegible]
20	.990	.0039	135.23	1200	.0031	130.29	1120	.0019	74.53	113.35
40	1000	.0045	157.61	1000	.0046	161.12	822	.0036	103.65	140.79
80	1130	.0072	284.97	1060	.0061	226.47	830	.0044	127.91	213.12
110	940	.0036	118.53	970	.0059	200.45	760	.0064	170.36	163.11
150	860	.0050	150.61	1120	.0027	105.92	770	.0028	75.51	110.61
FGLP	975	.0037	126.35	940	.0044	144.87	975	.0039	133.18	134.50
FGHP	1050	.0037	136.07	1040	.0030	109.28	1060	.0048	178.21	141.19
CGLP	925	.0022	71.28	1230	.0013	56.01	1180	.0027	111.59	79.63
CGHP	1230	.0030	129.24	965	.0052	175.76	1130	.0053	209.47	171.59

TABLE III (Continued)

Code	Cos θ Max (M)	Cos θ Max (E)	Max (M) γ_S ergs/cm^2	Max (E) γ_S ergs/cm^2	Cos θ Min (M)	Cos θ Min (E)	Min (M) γ_S ergs/cm^2	Min (E) γ_S ergs/cm^2	CLA (M) μin	CLA (E) μin
1	.40674	.34202	151.74	147.03	[illegible]	[illegible]	[illegible]	[illegible]	[illegible]	[illegible]
5	.05234	[illegible]	92.2[illegible]	[illegible]	[illegible]	[illegible]	147.37	[illegible]	[illegible]	[illegible]
7	.34202	[illegible]	[illegible]	[illegible]	.96363	[illegible]	[illegible]	[illegible]	[illegible]	[illegible]
10	[illegible]	[illegible]	[illegible]	[illegible]	[illegible]	[illegible]	[illegible]	[illegible]	[illegible]	[illegible]
[illegible]	[illegible]	[illegible]	[illegible]	[illegible]	[illegible]	[illegible]	[illegible]	[illegible]	[illegible]	[illegible]
[illegible]	[illegible]	[illegible]	[illegible]	[illegible]	[illegible]	[illegible]	[illegible]	[illegible]	[illegible]	[illegible]
[illegible]	[illegible]	[illegible]	[illegible]	[illegible]	[illegible]	[illegible]	[illegible]	[illegible]	[illegible]	[illegible]
[illegible]	[illegible]	[illegible]	[illegible]	[illegible]	[illegible]	[illegible]	[illegible]	[illegible]	[illegible]	[illegible]
[illegible]	[illegible]	[illegible]	[illegible]	[illegible]	[illegible]	[illegible]	[illegible]	[illegible]	[illegible]	[illegible]
FGLP	[illegible]	[illegible]	[illegible]	[illegible]	[illegible]	[illegible]	[illegible]	[illegible]	[illegible]	[illegible]
FGHP	.77715	[illegible]	197.77	173.57	.97030	[illegible]	211.63	[illegible]	[illegible]	[illegible]
CGLP	.14781	[illegible]	90.39	[illegible]	[illegible]	[illegible]	[illegible]	[illegible]	[illegible]	[illegible]
CGHP	.11320	.03490	179.83	174.13	.90631	[illegible]	[illegible]	[illegible]	[illegible]	[illegible]

BLANK PAGE

UNCLASSIFIED

Security Classification

DOCUMENT CONTROL DATA - R & D

(Security classification of title, body of abstract and indexing annotation must be entered when the overall report is classified)

1. ORIGINATING ACTIVITY (Corporate author)	2a. REPORT SECURITY CLASSIFICATION
Avco Government Products Group Systems Division 201 Lowell Street Wilmington, Massachusetts 01887	2b. GROUP

3. REPORT TITLE

Nondestructive Test Technique Development Based on the Quantitative Prediction of Bond Adhesive Strength

4. DESCRIPTIVE NOTES (Type of report and inclusive dates)

Contract Annual Report (1969 July 21 - 1970 July 20)

5. AUTHOR(S) (First name, middle initial, last name)

John R. Zurbrick

6. REPORT DATE	7a. TOTAL NO. OF PAGES	7b. NO. OF REFS
1970 July 20	118	21

8a. CONTRACT OR GRANT NO.	9a. ORIGINATOR'S REPORT NUMBER(S)
N00156-69-C-0913 b. PROJECT NO.	AVSD-0331-70-RR
c.	9b. OTHER REPORT NO(S) (Any other numbers that may be assigned this report)
d.	

10. DISTRIBUTION STATEMENT

11. SUPPLEMENTARY NOTES	12. SPONSORING MILITARY ACTIVITY
	Advanced Research Projects Agency Naval Air Engineering Center Aero Materials Department Warminster, Pennsylvania 18974

13. ABSTRACT

The second annual period of research and development at Avco Systems Division into Nondestructive Tests for the Evaluation of Bonded Materials, sponsored by the Advanced Research Projects Agency, has continued the course of direction established by the first year's studies, namely development of NDT techniques for characterizing metallic substrate surfaces. Results of a Surface Condition Study on 6061-T6 aluminum alloy butt tensile, core shear, and single lap shear specimens of various roughnesses, bonded with an Epon 828/DETA formulation, have supported the creation of a practical equation for predicting bond adhesive strength (Zurbrick). Major controlling variables, i.e. substrate surface free energy, contact angle, and bondline thickness, are all potentially measurable nondestructively. A strong correlation between white light specular reflection values and values of aluminum substrate surface free energy calculated from experimental data was obtained, encouraging extensive investigation of this NDT technique. Exo-electron emission, ultrasonic gas-phase transmission, and electric field reflectometry techniques were also evaluated in continuing feasibility studies.

DD FORM 1 NOV 68 1473

UNCLASSIFIED

Security Classification

KEY WORDS	LINK A		LINK B		LINK C	
	ROLE	WT	ROLE	WT	ROLE	WT
Nondestructive Testing						
Adhesively bonded joints						
Bond Adhesive Strength						
bond strength prediction						
NDT technique development						
White light specular reflection						
Substrate surface free energy						
contact angle						
bondline thickness						
ultrasonic gas-phase transmission						
electric field reflectometry						
exo-electron emission						